CIVIL ENGINEERING STUDIES
Illinois Center for Transportation Series No. 17-002
UILU-ENG-2017-2002
ISSN: 0197-9191

MODELING THE PERFORMANCE PROPERTIES OF RAS AND RAP BLENDED ASPHALT MIXES USING CHEMICAL COMPOSITIONAL INFORMATION

Prepared By
Brajendra K. Sharma
Jing Ma
Bidhya Kunwar
Punit Singhvi
Hasan Ozer
N. Rajagopalan
University of Illinois at Urbana-Champaign

Research Report No. FHWA-ICT-17-001

A report of the findings of

ICT PROJECT R27-162
Chemical and Compositional Characterization of Recycled Binders

Illinois Center for Transportation

January 2017

TECHNICAL REPORT DOCUMENTATION PAGE

1. Report No. FHWA-ICT-17-001	**2. Government Accession No.** N/A	**3. Recipient's Catalog No.** N/A
4. Title and Subtitle Modeling the Performance Properties of RAS and RAP Blended Asphalt Mixes Using Chemical Compositional Information		**5. Report Date** January 2017 **6. Performing Organization Code** N/A
7. Author(s) Brajendra K. Sharma, Jing Ma, Bidhya Kunwar, Punit Singhvi, Hasan Ozer, and N. Rajagopalan		**8. Performing Organization Report No.** ICT-17-002 UILU-ENG-2017-2002
9. Performing Organization Name and Address Illinois Sustainable Technology Center Prairie Research Institute University of Illinois, Urbana-Champaign One East Hazelwood Drive Champaign, IL 61820-7465 and Illinois Center for Transportation Department of Civil and Environmental Engineering University of Illinois at Urbana-Champaign 205 North Mathews Avenue, MC-250 Urbana, IL 61801		**10. Work Unit No.** N/A **11. Contract or Grant No.** R27-162
12. Sponsoring Agency Name and Address Illinois Department of Transportation (SPR) Bureau of Materials and Physical Research 126 East Ash Street Springfield, IL 62704		**13. Type of Report and Period Covered** January 1, 2015, through January 31, 2017 **14. Sponsoring Agency Code** FHWA

15. Supplementary Notes
Conducted in cooperation with the U.S. Department of Transportation, Federal Highway Administration.

16. Abstract
Reclaimed asphalt pavement (RAP) and recycled asphalt shingles (RAS) can improve the sustainability of asphalt concrete (AC) due to cost savings and environmental factors, but it is necessary to ensure that pavement performance is not compromised. To study the effects of aging and increasing asphalt binder replacement levels, chemical characterization and rheological properties of binders from various sources were investigated. Binders from five ACs designed with varying ABR percentages (0% to 60%) were recovered using the standard Rotovap test procedure. The base binder used in the AC design and binders recovered from RAP and RAS were also tested. In addition to standard aging protocols, base binders were subjected to a second pressure aging vessel (PAV), whereas one PAV was applied for the extracted binders. Rheological parameters for low-temperature cracking susceptibility and block and fatigue cracking derived from dynamic shear rheometer (DSR) and bending beam rheometer (BBR) tests appeared to have consistent trends with aging and increasing ABR levels. These parameters are helpful in evaluating progression in brittleness of binders with ABR and aging. It was concluded that AC with ABR levels above 20% could suffer from short- and long-term cracking potential. Aging happens as a result of oxidation, which can be seen by an increase in carbonyl and sulfoxide components and larger molecular size components such as resins and asphaltenes. The difference in chemical composition of binders aged via rolling thin-film oven (RTFO) and PAV is small, but this gap increases on double PAV. It was also observed that the double-PAV binders have a chemical composition similar to those with a higher content of reclaimed binders. Asphalt concrete with high ABR content can be at an already critically aged condition immediately after production; moreover, aging progresses much faster in the binders of such mixes.

17. Key Words asphalt binder replacement, reclaimed asphalt shingles, recycled asphalt pavement, chemical composition, TLC-FID, SARA, FTIR, GPC, CHN analysis, correlation, rheology, performance properties	**18. Distribution Statement** No restrictions. This document is available through the National Technical Information Service, Springfield, VA 22161.

19. Security Classif. (of this report) Unclassified	**20. Security Classif. (of this page)** Unclassified	**21. No. of Pages** 65 pp. plus appendices	**22. Price** N/A

Form DOT F 1700.7 (8-72) **Reproduction of completed page authorized**

ACKNOWLEDGMENT, DISCLAIMER, MANUFACTURERS' NAMES

This publication is based on the results of **ICT-R27-162, Chemical and Compositional Characterization of Recycled Binders**. ICT-R27-162 was conducted in cooperation with the Illinois Center for Transportation; the Illinois Department of Transportation; and the U.S. Department of Transportation, Federal Highway Administration.

Members of the Technical Review panel were the following:

- Ron Price (TRP Chair), Illinois Department of Transportation
- Matt Mueller, Illinois Department of Transportation
- Vickie Prill, Illinois Department of Transportation
- James Trepanier, Illinois Department of Transportation
- Violet Goodman, Illinois Department of Transportation
- Dennis Oehmke, Illinois Department of Transportation
- Tom Zehr, Illinois Department of Transportation
- Brian Pfeifer, Federal Highway Administration

EXECUTIVE SUMMARY

Recycled materials such as reclaimed asphalt pavement (RAP) and recycled asphalt shingles (RAS) are among the most commonly used sustainable strategies for asphalt concrete (AC) due to initial cost savings and environmental benefits. However, the use of RAP and RAS poses some challenges in the production and performance stages of asphalt pavements. Specifically, as RAP and RAS content increases in pavement, its performance deteriorates as a result of increasing brittleness—making cold-season performance a challenge. Increased embrittlement is caused by the increased presence of aged and highly oxidized recycled binder and a reduction in virgin binder—even though total binder content remains the same. In addition, brittleness can be caused by partial blending of the recycled binder with the original binder.

The major cause of poor pavement performance is oxidation, which leads to aging. Extensive oxidation and polymerization cause the saturate, aromatic, resin, and asphaltene (SARA) component ratio to change over time. In addition, the molecular size of the components in the binders increases. Therefore, a thorough study of the oxidized components (carbonyl and sulfoxide), SARA, oxygen content, molecular size distribution, and topographic orientation in addition to rheological characterization was conducted on a variety of samples. The binders tested were categorized into three groups. The first group of binders was from five ACs designed with varying percentages (0% to 60%) of asphalt binder replacement (ABR) and various field cores; these binders were recovered using the standard Rotovap test procedure and tested as-is and after PAV. The second group was the base binders used in the AC designs of the first group. Base binder characterizations were conducted on the second group after RTFO aging, PAV aging, and double-PAV aging. The third group consisted of the binders recovered from RAS and RAP used in the AC designs.

For the study of chemical composition, Fourier transform infrared spectrometry (FTIR), gel permeation chromatography (GPC), thin-layer chromatography–flame ionization detector (TLC-FID), elemental analyzer, and atomic force microscopy (AFM) were used to investigate oxidized components (carbonyl and sulfoxide), molecular size distribution, SARA, oxygen content, and topographic orientation of the binders. Rheological characterization included dynamic shear rheometer (DSR) and bending beam rheometer (BBR) testing first to determine or verify PG grading and various other parameters that are indicators of brittleness and cracking resistance. These parameters were complex modulus, the Glover-Rowe parameter, R-value, and cross-over frequency from DSR testing and critical spread in low-temperature grades (also known as ΔT_c) from BBR testing.

The carbonyl index (ICO) and sulfoxide index (ISO) varied in the range of 0.01 to 0.05 and 0.05 to 0.09, respectively, for virgin binders. RTFO- and PAV-aged binders had ICOs as high as 0.06 and 0.09, respectively. RAS and RAP had ICOs between 0.10 and 0.12, whereas blends of reclaimed and virgin binders had ISOs and ICOs between those of the virgin and reclaimed binders. Aging and blending caused a decrease in aromatic content and an increase in resin, asphaltene, and insolubles in the binders. Longer-term-aged (i.e., double-PAV) or reclaimed binders were found to have aromatic contents lower than those of virgin binders and blends. Likewise, larger and medium molecular size (LMS and MMS) components in the binders increased with aging. Of all binders, reclaimed and double-PAV binders showed the highest LMS and MMS. Overall, as binder aging progresses from

RTFO to PAV conditions, small changes in chemical composition were observed, while under double-PAV conditions, a pronounced alteration in the chemical composition was observed. The results showed that double-PAV binders have a chemical composition similar to that of reclaimed binders such as RAS and RAP. The chemical compositional properties of ABR-blended binders began to approach those of the RAS and RAP as the ABR content increased in the samples.

Atomic force microscopy (AFM) images were used to identify the multiphase composition of binders with an objective of evaluating the homogeneity of distribution. Blends, virgin binders, and reclaimed binders showed a distinct difference, with pronounced periphase (the dark-colored phase around more polar structures; also known as bee structure) in the binders with the highest recycled component. In addition, repeatability of similar images in replicates of blends containing 10%, 20%, and 30% ABR was attributed to a good blending of virgin and reclaimed binders that provided a more homogeneous mixed binder. This repeatability was absent in the blend containing 60% ABR, which is attributed to the fact that homogeneity could be lost with an increase in reclaimed content in binders.

Additional PAV for original and extracted binders changed almost all of the rheological characteristics significantly. Most of the additional rheological parameters appeared to have consistent trends with aging and increasing ABR levels. As the ABR level increased, both the high- and low-temperature grades increased by one or two grades above their corresponding binder with an ABR content below 30%. Among the other parameters investigated, Glover-Rowe and ΔT_c parameters showed consistent trends with increasing aging and amount of recycled binder. The ΔT_c parameter increased with additional aging and increasing ABR levels. The proposed threshold of –5°C was exceeded by a considerable margin when PAV was applied to the extracted binder recovered from AC with an ABR greater than 20%. The values were in the range of –8°C to –21°C. Similarly, the effects of aging and ABR levels were observed in the Glover-Rowe parameter, especially after the additional PAV. All the base binders reached the critical threshold of 180 kPa only after the second PAV. The extracted binder from AC with 60% ABR had values exceeding the critical thresholds even before PAV aging.

The equivalency analysis using the ΔT_c and Glover-Rowe parameters showed that increased aging and ABR levels had similar effects on low- and intermediate-temperature cracking susceptibility. The analysis demonstrated that binders in AC with an ABR level less than 20% were at an aging level equivalent to their RTFO-aged base binders and after one PAV were nearly equivalent to the PAV condition of their base binders—indicating a similar magnitude and progression of aging with the base binder. However, when the extracted binders with ABR levels of 20% or more were tested as-is, their brittleness parameter values were higher than those of their corresponding PAV-aged base binders. It was also found that after PAV aging, they well exceeded the values of the second-PAV-aged base binders.

Correlations were evaluated between each parameter from the rheological and the chemistry and compositional tests to determine critical performance thresholds. In general, the parameters obtained from the FTIR tests (ICO and ISO) had the best correlation to the rheological parameters, followed by SMS obtained from the GPC test and SARA components. The correlation between the Glover-Rowe parameter and the rutting parameter with ICO, ISO, and SMS had the highest regression

coefficient. Preliminary thresholds to ensure good performance of binders are proposed in various combinations of rheology-chemistry space diagrams. The approach and thresholds are preliminary and need additional binder data for validation and fine-tuning. However, according to the initial results, the proposed thresholds are in agreement with the expectation and mixture-level performance data obtained from the binders recovered from N90 mixes. An implementation plan was recommended for detection of binders that could be at a critical state of brittleness after short- and long-term aging.

Based on the combined results of rheological characteristics, chemistry, and composition, it was concluded that AC prepared with high levels of ABR (more than 20%) using only RAS could have short- and long-term cracking potential because aging progresses much faster and their lifetime starts at an already critically aged condition. Asphalt concrete with high ABR content can be at an already critically aged condition immediately after production; moreover, aging progresses much faster in the binders of such mixes.

CONTENTS

LIST OF FIGURES

LIST OF TABLES

CHAPTER 1: INTRODUCTION

1.1 BACKGROUND AND MOTIVATION

It is widely accepted that using reclaimed asphalt pavement (RAP) and recycled asphalt shingles (RAS) can improve the sustainability of asphalt concrete (AC) due to cost savings and environmental factors when short- and long-term pavement performance is not compromised. Illinois has had many years of experience utilizing various reclaimed materials in highway construction. Past reports provide excellent background information on reclaimed and recycled materials used in Illinois highway construction (Liu et al. 2015; Rowden et al. 2012; Lippert et al. 2012). In recent years, RAS has been adopted for use in hot-mix asphalt (HMA) along with much higher amounts of RAP (Rowden et al. 2012).

Using RAP and RAS has numerous economic benefits because they replace petroleum-based asphalt binder. However, as the level of asphalt binder replacement (ABR) increases, production and in-service performance of pavements built with such mixes become a challenge. These reclaimed asphalt materials introduce aged and brittle asphalts into the pavement, which can make cold-season performance a challenge. To counter these hard asphalts, softer asphalts are incorporated into the HMA mix. The goal for the final mix is to have acceptable mix properties for the life of the pavement (Rowden et al. 2012; Lippert et al. 2012; Al-Qadi et al. 2012).

Many studies have investigated the effect of increasing levels of RAP and RAS on critical performance characteristics predominantly at the mixture level and some at the binder level. The primary concern with recycled mixes are thermal and fatigue cracking. Because the standard Superpave test methods, including volumetric measurements and indirect tensile strength tests, are not sufficient to capture cracking resistance in the performance of such mixes with RAP and RAS, alternative testing protocols have been developed and implemented, with two major goals. First is to gain a fundamental understanding of the mixes' behavior under different temperature and loading conditions. Second is to develop practical methods that can be adapted by agencies as a quality assurance and control measure to avoid premature failures and ensure long-term cracking performance. Recently, the Illinois Center for Transportation (ICT) completed a study to develop a practical semi-circular bending (SCB) fracture method known as the Illinois Flexibility Index Test (I-FIT) protocol (Al-Qadi et al. 2015). There are many other mixture-level test methods proposed for the same purposes.

Similarly, both chemical and rheological properties of asphalt binder have been shown to affect the performance of asphalt binder at the early stages of Strategic Highway Research Program (SHRP) resulting to the Superpave binder grading system (Robertson et al. 1991). Those properties can be adversely affected by the use of modifiers and recycled binder. To ease widespread implementation, the Superpave grading system ended up only using rheological characterization methods and had a relatively limited scope. However, it was also known that the final standard Superpave test method and grading system failed to capture performance characteristics of binders in recycled mixes or modified binders with various softeners commonly used in the marketplace. The limitations of the Superpave system were identified for polymer-modified binder soon after its adoption by manufacturers and agencies. Therefore, the first alternative testing protocol considering higher stress

levels and recovery characteristics of binder was the multiple stress creep recovery (MSCR) protocol (D'Angelo et al. 2007).

The next step is to achieve a better understanding of binders as they become more brittle and susceptible to cracking as a result of the addition of recycled materials and some modifiers. Some work is currently under way to develop test methods to fill this gap. However, our understanding of blending of virgin binder with recycled binder in RAP/RAS, long-term aging of recycled binders, and long-term effects of modifiers on the chemistry and performance of binders is still limited.

Therefore, there is a need to evaluate the structural and compositional information with recycled binders (RAP and RAS) existing in virgin binder, as they determine the final properties of the mix. Asphalt binders contain hundreds of thousands of unique molecular species that vary widely in polarity and molecular weight. This complex microstructure changes with the crude source, refining process, additives and modifiers, time (aging), and other loading and environmental conditions. Although it is challenging to do so, achieving a better understanding of a binder's chemistry and composition is as important as knowing its final physical and rheological characteristics. This is a critical step toward ensuring long-term performance of asphalt mixtures laid and compacted in pavement layers.

1.2 PROBLEM STATEMENT

Existing studies emphasize a need for reliable AC and binder performance test methods and criteria for AC containing high recycled content or binders. Existing Superpave binder tests and parameters cannot capture the short-term and long-term behavior of existing binders in the current marketplace in the presence of recycled materials and other modifiers such as the ones used to lower the grade of the binder.

Research efforts have recently been undertaken to update binder testing protocols to meet the needs of agencies and producers. However, most of these methods have not been fully implemented or are at the research and experimentation stage; therefore, agencies cope with performance challenges associated with recycled content by limiting the use of RAP and RAS in AC to levels that will not compromise pavement performance. The relationship between performance and the chemistry and composition of blended binders and asphalt concrete with recycled content after long-term aging is not clearly understood; therefore, limits were generally determined based on engineering judgment or plant production capacity rather than through a thorough experimental characterization supported with field results.

This report presents the results of an experimental program developed to characterize short- and long-term performance of binders with various levels of RAP and RAS content and changes in their chemistry and composition. In addition to advanced chemical and compositional characterization methods, standard and more recently developed binder rheology tests were used to evaluate the impact of various RAP and RAS blends at intermediate and high temperatures. Binder chemistry/composition and rheological tests were chosen in this study not only to complement the recently completed ICT study with mixture-level testing, but they also offer several advantages. Test

results on binders are more repeatable because of the relatively more homogenous microstructure of binders compared with that of AC. The effect of changes in the constituents (e.g., addition of recycled binder at different ratios or modifiers) can be directly observed in the results. A proven binder aging method exists to evaluate the long-term impact of recycled materials.

1.3 RESEARCH OBJECTIVES

The overall objective of this project was to study how chemical properties of binders with recycled content such as RAP and RAS affect the performance properties of the binders. Recently, the ICT study (R27-128, "Testing Protocols to Ensure Performance of High Asphalt Binder Replacement Mixes Using RAP and RAS") developed a mixture-testing protocol to predict cracking susceptibility of mixes (Al-Qadi et al. 2015). The current project provides additional support to the findings of the previous project by conducting binder-level characterization using the same materials.

The major objective of this project is to explain the effects of RAS and RAP blending on performance characteristics in roadways through chemical characterization and correlation of the chemical data to performance properties. The goal is to classify RAS and RAP asphalt binder blends based on chemical characterization in the similar way that they are distinguished by their performance characteristics. The three main objectives of this study are as follows:

- Evaluate chemical properties of virgin binders, aged binders, binders extracted from RAP and RAS, and binders containing recycled content, such as RAP and RAS
- Generate rheological data on these binders and support the existing ICT project to determine what levels of RAS and RAP are compatible without affecting performance
- Correlate composition data and rheological performance properties

This work was conducted in close consultation with Imad L. Al-Qadi and Hasan Ozer, Illinois Center for Transportation (ICT), to augment their current work on performance data on binders and mix samples with chemical data and to develop correlations between compositional and performance data. This information will provide additional guidance to IDOT on how much RAS and RAP material can be used without affecting long-term performance, which will be supported by engineering properties and composition of asphalts mixes.

An interdisciplinary team from the Illinois Sustainable Technology Center (ISTC) and ICT worked together to fill this gap in correlating structural information to performance properties.

1.4 REPORT ORGANIZATION

The scope of the research study included compositional and performance testing of various binder samples. Chapters are organized as follows:

- Chapter 2 of this report presents a brief literature background on the compositional and rheological performance of binders.

- Chapter 3 is a summary of the materials and experimental plan.
- Chapter 4 presents the rheological results of sample testing.
- Chapter 5 discusses the compositional data generated on from the results of sample testing.
- Chapter 6 explores the correlation between compositional and rheological data.
- Chapter 7 summarizes the primary and other findings of the study and provides recommendations for future work.

CHAPTER 2: RESEARCH BACKGROUND

With the increasing use of recycled materials in AC, a better understanding of AC and binder properties and the correlation between them is needed for AC that includes higher amounts of RAP and RAS. Binder existing in RAP and RAS can be oxidized and exhibit higher stiffness characteristics and lower load- and non-load-associated cracking resistance compared to original binders.

A number of studies evaluating the characteristics of mixes with recycled materials have been conducted at the binder and mixture levels. Binder-level characterization includes both rheological characterization, which may also include Superpave tests, and chemistry/compositional characterization. This chapter briefly summarizes the literature background for binder-level characterization. Additional details and a summary of studies conducted as part of the literature review for the current project can be found in Appendix A.

2.1 RHEOLOGICAL PROPERTIES AND STUDIES FOR RECYCLED MIXES

Many laboratory studies have recently been conducted to quantify the effects of using recycled materials, including RAP and RAS, on AC and binder performance characteristics (Al-Qadi et al. 2009; Cooper et al. 2015; Ozer et al. 2016). These studies focused mainly on the characterization of performance in the compacted mixture level.

A variety of challenges and performance risks are associated with the use of RAP and RAS. Recycled binder existing in RAP and RAS is generally considerably more aged than virgin binder. Increased stiffness with aging can pose premature and long-term cracking-related performance risks in the field, even though it may be considered an advantage in improving the rutting resistance of AC (Al-Qadi et al. 2009; Al-Qadi et al. 2012; Cooper et al. 2015). A second challenge is variability in aggregate and binder properties of recycled stockpiles. Finally, unknown or partial blending of recycled binder with the original binder can result in AC with insufficient total binder content. Partial blending can influence an AC's compaction behavior, which may hinder the achievement of target density in the field. Another consequence of partial blending is that it can result in heterogeneous distribution of recycled binder in the matrix of AC.

Many studies have investigated the effect of increasing levels of RAP and RAS on critical performance characteristics of AC and binders. A comprehensive and recent review of literature on the effects of RAP and RAS or ABR on AC performance characteristics was conducted by Al-Qadi et al. (2015) and Li and Gibson (2012). At the AC level, most of these studies concluded that low-temperature and fatigue-cracking performance of AC with high recycled content could be compromised as AC becomes more brittle. Depending on the test methods and quality of laboratory AC design preparation and specimen fabrication, the significance of the impact varied, and sometimes the results were inconsistent. However, the majority of the studies showed improvement in rutting resistance of AC with increasing recycled content. In most of the studies available in the literature, AC characterization with recycled content was limited to short-term-aged laboratory-produced and plant-produced AC.

Even though AC performance tests can have a direct relationship with field performance of pavements, binder characterization has also been considered when evaluating the effects of recycled binder, modifiers, and additives at the constituent level. Some of the standard binder tests included intermediate- and high-temperature tests conducted using the dynamic shear rheometer (DSR) and low-temperature tests using the bending beam rheometer (BBR).

A study by Colbert et al. (2012) evaluated virgin binder blended with 30%, 50%, 70%, and 100% RAP before aging and after aging via rolling thin-film oven (RTFO) and pressure aging vessel (PAV). The study found that binder with higher viscosity will blend with RAP content and that further aging produces a continuous increase in stiffness.

Generally speaking, Superpave tests, along with frequency sweep tests, were performed in the other studies—with a primary focus on characteristics of recycled binders. It was shown in these studies that standard Superpave tests and methods may not accurately and consistently capture the intermediate-temperature behavior of binders, especially when they are blended with modifiers or recycled content. Additional test methods and analysis approaches were proposed to characterize brittleness and cracking susceptibility in the presence of modifiers, additives, and recycled content under standard and extreme conditions. In addition to the Superpave standard tests, Gibson et al. (2012) used other test methods in comparing the fatigue-cracking susceptibility of various polymer modifiers with field-accelerated pavement test results. The results indicated that critical tip opening displacement (CTOD) and binder yield energy had more discrimination potential than the Superpave parameters did.

Recently, several other binder performance criteria have been developed. One of them, developed by Rowe (2014), can be used for predicting fatigue and block cracking susceptibility of binders at intermediate temperatures. The parameter is derived from DSR complex modulus tests and is known as the Glover-Rowe parameter. The R-value and crossover frequency are additional parameters that can be obtained from DSR temperature and frequency sweep tests.

As for low-temperature performance, a new parameter, ΔT_c, was defined as the difference between the critical temperature of stiffness and m-value, where stiffness threshold equals 300 MPa and m-value equals 0.300 (King et al. 2012). These parameters were recently used by Mogawer et al. (2016) to assess the impact of re-refined engine oil bottoms (ReOB) using two different binder grades and various aging durations. The parameters successfully showed the progression of brittleness with aging for the two ReOB sources, compared with control binders.

2.2 BINDER CHEMISTRY AND COMPOSITION

2.2.1 Binder Chemistry and Microstructure Theories

Asphalt binder is the residual product from the distillation of crude oil in petroleum refining. The vast majority of petroleum asphalt binders produced conform to the characteristics of materials described by CAS #8052-42-4, #64741-56-6, or #64742-93-4. Asphalt binder molecules consist primarily of carbon (80.2% to 84.3%) and hydrogen (9.8% to 10.2%) and also contain one or more heteroatoms, such as sulfur (0.9% to 6.6%), nitrogen (0.2% to 1.2%), and/or oxygen (0.4% to 1.0%). Chemically,

petroleum asphalt binder comprises the four major classes of compounds: saturates (5% to 20%), aromatics (30% to 60%), resins (15% to 55%), and asphaltenes (5% to 31%), as shown in Figure 2.1.

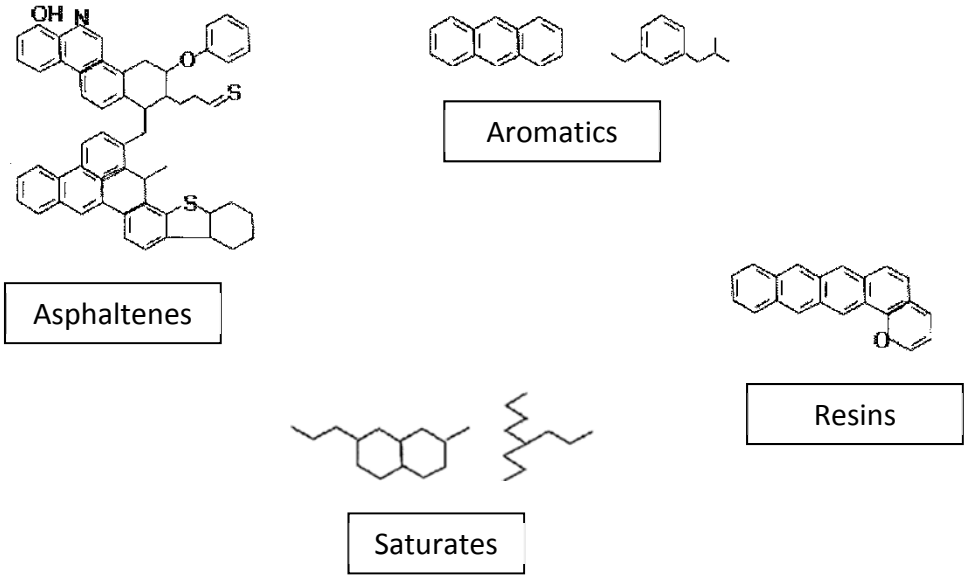

Figure 2.1 Typical molecular chains existing in an asphalt binder.

The physical and chemical properties of asphalt binder influence the interaction with the other materials in asphalt (aggregates, sand, gravel) in a complex, nonlinear manner. For example, controlling changes in viscosity/viscoelasticity of the binder with temperature is important in ensuring that the final product can withstand vehicle loadings across seasons. It is also important to emphasize that it is the chemical nature of asphalt binder that gives rise to the observed physical properties.

It is no accident that, given the complex nature of the product and the high economic costs of poorly performing materials, extensive physical and chemical characterization of bitumen products is demanded by customers. Ideal bitumen (Roberts et al. 2014) should possess both (1) high relative stiffness at high service temperatures (summer) to reduce rutting and shoving and (2) increased adhesion between bitumen and aggregate in the presence of moisture to reduce stripping.

A common explanation for asphalt microstructure stems from colloidal theory, in which polar groups form structured phases in a non-polar solution, as shown in Figure 2.2. The distinctive four phases describing this microstructure: catanaphase (bee structure), periphase (around catanaphase), paraphase (solvent regions), and salphase (high phase contrast spots) (Das et al. 2010). The phases are shown in an image taken by the atomic force microscopic (AFM) method are shown in Figure 2.2. Microstructural differences between different binders (virgin, aged, and recycled) can be studied using imaging with the AFM (Zhao et al. 2015; Allen et al. 2014).

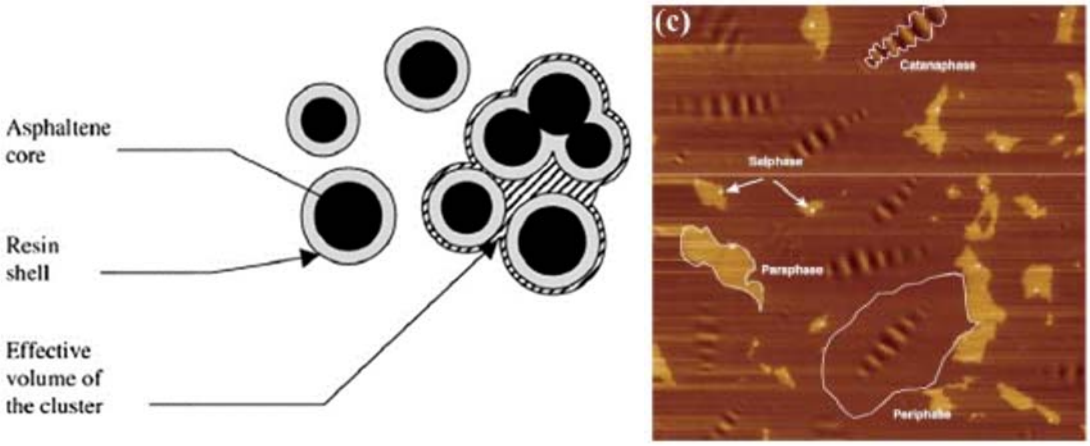

Figure 2.2 Assumed colloidal binder microstructure and the four phases of this microstructure (Yu et al. 2015).

The rippled microstructures several micrometers in diameter and tens of nanometers in height were reported and nicknamed bumblebees because of their black and yellow stripes; they are now commonly referred to as bee-shaped microstructures. Authors such as De Moraes et al. (2010), Wang et al. (2015), Schmets et al. (2010), and Pauli et al. (2011) have ascribed the bee structure resemblance to crystalline microstructures consisting primarily of paraffin waxes. Pauli et al. (2011) concluded that the interaction between paraffin waxes and the remaining asphalt fractions is responsible for the bee-like structure, which is referred to as wax-induced phase separation. Moya-Aguiar et al. (2015) studied the bee structure by separating the components in binders using various solvents; each component was investigated using AFM. Surprisingly, their results were contradictory to results obtained in other studies. Their results showed that the bee structure is caused by the presence of aromatics.

The study of relationships between chemical composition and physical performance properties of asphalt is significant for designing the needed compositional features to produce material with the desired properties (Robertson et al. 1991). Asphalt binder consists primarily of saturates, aromatics, resins, and asphaltenes. With time and weather effect, the composition of binder changes from aromatics to resins and resins to asphaltenes. The oxidation of binder increases the carbonyl and sulfoxide content in the binders. Carbonyl and sulfoxide group initiate polar bond forming aggregation or association. The hypotheses for the effects of each component on the asphalt performance are summarized in Table 2.1. It is important to note that binder microstructure is complex and is an area of ongoing research with the use of advanced microscopic and analytical techniques. Therefore, it is possible to see conflicting results in the literature to explain binder microstructure and chemical composition and effects on performance.

Table 2.1. Binder Components and Their Effects on Performance

Component	Effect	Reference
Saturates	• Crack initiator • Cracking at lower temperature/no water effect • High saturates content in non-aged asphalt can have an effect similar to oxidative aging on asphalt microstructure, chemical polarity, and asphalt physical properties • An increased bee structure	Allen et al. 2014
Resin	• Larger polyaromatic and polar compounds can form H-bond and polar bond, thereby increasing viscosity and stiffness	Redelius et al. 2015
Asphaltene	• Increase bee structure • Cause hardening and brittleness	Allen et al. 2014
Carbonyl and sulfoxide	• With an increase in carbonyl compounds and sulfoxides, the mechanical properties of aged binder become more solid and harden, as indicated by increased complex modulus and decreased phase angle	Lu et al. 2002

The composition of asphalt material changes with time, oxidation, temperature, and moisture. Generally, it can be expected that there are more polar materials in RAP and RAS) than in virgin binders.

Oxidation and low temperature make the asphalt material hard, brittle, and highly associated, leading to fatigue cracking and total loss of adhesion. Oxidation, which contributes additional polar material, has a significant influence on the organized structure. More linear aliphatic materials shrink with decreasing temperature. Oxidation imparts permanent hardening, while physical hardening due to exposure to low temperatures and molecular reorganization are reversible.

Zhao et al. (2015) described the possibility of interaction between RAP or RAS and virgin binder as follows:

- Assuming the RAP or RAS is black rock: there is no interaction between recycled material and virgin binder
- Mixing: the materials are homogeneously together
- Blending: the materials work together smoothly and inseparably, and perform a new material "phase" is formed

Binder microstructure depends on the chemical structure, which highly affects the asphalt binder performance (Wang et al. 2015). Molecular weight and chemical structure are two of the most fundamental chemical properties of any organic substance. Separating asphalts into distinct chemical fractions and into fractions of different molecular sizes is emphasized from the beginning of binder characterization and evaluation (Branthaver et al. 1993). There are molecular and intermolecular-

level forces in asphalt. Hydrogen bonds and other interactions between polar molecules are intermolecular forces, which hold asphalt molecular association together (Branthaver et al. 1993).

Both molecular- and intermolecular-level forces control the adhesion of asphalt components to aggregate. Functional groups (molecular types) and polarity, which separate charge within the organic molecules, promote attraction of polar asphalt components to the polar surface of aggregate, are two important aspects of asphalt. Field performance of asphalt binder has strong dependence on its polarity. Polar materials tend to associate strongly into a matrix that is dispersed in non-polar and less polar materials. Mechanical properties of asphalt are associated with the intermolecular structuring of polar components. To form a matrix within the non-polar continuous medium, the overall assemblage nature of a set of polar materials is more important than the exact nature of individual chemical species. Excessive structuring makes the binder more brittle. Materials with too little structuring exhibit large deformations under stress. Non-polar materials tend to be organized into rigid materials at very low temperature. The rigid material shrinks at low temperature.

The molecules slowly find the best orientation to reach the thermodynamic stable state/equilibrium. Oxidation and changing temperature lead to a changing of thermodynamic equilibrium. Heavy traffic loads tend to disorient molecular species. An organized structure can be rearranged/scrambled from physical stress or an increase in temperature. It will occur without changing the molecular composition (Rowden 2013). Oxidation, which contributes additional polar material, has a significant influence on the organized structure. A highly organized structure resists motion/deformation; that is, it is more like a spring, is more viscous, and is stiffer. An organized structure depends on the strengths of the attractions and the amount of sites where intermolecular attractions happen. The overall process of association of asphalt is slow because of the high viscosity. Less associated material disperses the polar materials as a solvent, which could reduce the association of the polars. The association of polars depends on their composition, thermal history, and the differing chemistry within the continuous neutral phase (Robertson et al. 1991).

2.2.2 Analytical Techniques for Binder Composition and Microstructure

The techniques commonly used in the literature to understand binder microstructure and chemical composition are given in Table 2.2. A detailed review of these techniques, along with some example use cases from the literature, is provided in Appendix A.

Table 2.2 Analytical Techniques for Binder Chemical Characterization

Technique	General Purpose	Test Parameter
Fourier transform infrared spectroscopy (FTIR)	Aging	Carbonyl compounds, sulfoxides, and amount of polymer (C=O, S=O, and SBS)
Elemental analysis	Aging, elemental composition	Carbon, sulfur, oxygen, hydrogen content
SARA analysis using the thin-layer chromatography–flame ionization detection Iatroscan system (TLC-FID)	Aging, chemical composition	SARA fractions (saturates, aromatics, resins, asphaltenes) and chemical composition colloidal index resulting from SARA fractions
AFM	Microstructures, study of mixing/blending of ABR with virgin binders	Topographic images and force/stiffness
GPC	Aging, molecular weight distribution	Low molecular weight (LMW), medium molecular weight (MMW), and high molecular weight (HMW) components

CHAPTER 3: MATERIAL AND EXPERIMENTAL PLAN

3.1 MATERIAL

Three binder sources were used in the study: original binders were used in the preparation of AC (as the control binder); binders were recovered from recycled constituents (RAP and RAS) used in the AC; and binders were recovered from laboratory-designed and -produced mixes with ABR content of varying percentages (0%, 10%, 20%, 30%, and 60%). Table 3.1 presents a complete list of binder sources.

Table 3.1 Binder Sources and AC Design Properties Used in the Experimental Program

Original Binders			
PG 58-28	*PG 64-22*	*PG 70-22*	
Extracted Binder from Recycled Constituents (RAP and RAS)			
Binder ID	*Source*	*Binder Content (%)*	
RAP1	District 5	5.5	
RAP2	District 5	3.9	
RAS1	Source 1	26.7	
RAS2	Source 1	27.4	
Extracted Binders from AC			
Binder ID	*Base binder of AC*	*RAP and RAS Source of AC*	*ABR*
N90-0[1]AS[2]	PG 64-22	0.0%	0.0%
N90-10	PG 64-22	2.5% RAS1	10.5%
N90-20	PG 58-28	5.0% RAS1	21.2%
N90-30	PG 58-28	7.0% RAS1	29.8%
N90-60AS	PG 52-34	7% RAS2 + 20% RAP1 + 20% RAP2	60.8%

[1] N90-0, N90-10, N90-20, N90-30, and N90-60 indicate N-design and ABR percentage

[2] AS: 1% of Pavegrip 550 anti-strip was added to the total binder weight for some of the AC to reduce stripping potential and meet the tensile strength minimums and ratio requirements

The laboratory-prepared asphalt mixtures (N90) were designed in the ICT R27-128 study to develop the most effective mixture-performance testing protocol to ensure cracking resistance (Al-Qadi et al. 2015). These ACs were chosen for the current study because they were designed using stringent volumetric criteria by changing the ABR level gradually, starting from a parent control AC design. In addition, complete mixture-performance test results exist for these ACs and can be used for correlation (Al-Qadi et al. 2015).

Control binders used in the mixes were PG 52-34, PG 58-28, and PG 64-22. In this study, PG 58-28 and PG 64-22 were investigated and compared with the results from extracted binders. Because PG 52-34 is not commonly available or used in AC in Illinois or elsewhere in the United States, it was excluded from the testing program. Two RAP and RAS sources were included in this study to evaluate source variability.

The experimental program included other materials including field cores and binders with various modifiers such as vegetable oil and re-refined engine oil bottoms. A list of these materials can be found in Appendix B.

3.2 TESTING METHODS AND EXPERIMENTAL PLAN

3.2.1 Extraction and Recovery Method

Binder extractions were performed on the laboratory-produced mixtures, plant-produced mixtures, and field cores. The standard Rotovap test procedure was used to extract asphalt binder from cores and mixes in accordance with AASHTO T391-15. Figure 3.1 shows a setup of the Rotovap device for extraction of asphalt binder from the mixes.

Following the specifications, the asphalt mixture was repeatedly washed and filtered with solvent (Entron n-propyl bromide was used in this study) in a filtration apparatus. Each filtration was then distilled under vacuum in a rotary evaporator with the asphalt remaining in the flask (Figure 2.1). The solvent was distilled at 100°C. After recovery of the final filtrate, the solution was concentrated to about 300 mL and centrifuged to remove the aggregate fines. At the final phase when the nitrogen gas is introduced, the distillation temperature was increased to 174°C.

Figure 3.1 Rotovap equipment.

3.2.2 Aging Methods

The characteristics of asphalt binder change with time. Two aging methods were used in this study to evaluate short-term and long-term binder performance: RTFO and PAV. In accordance with ASTM D6373 (Superpave PG grading), the DSR should be conducted with both RTFO-aged binder at high

temperature and PAV-aged binder at intermediate temperature, and the BBR test should use the PAV-aged binder.

Aging protocols applied to the samples include standard and non-standard extra-long-term aging procedures. The aging history for each sample is as follows:

- All samples were subjected to standard aging protocols for low- and high-temperature Superpave grading.
- Control binders were subjected to RTFO, PAV, and second PAV (2PAV) protocols in addition to testing without any aging.
- Extracted binders from mixtures were tested as-is and after one PAV.
- Extracted binders from RAP and RAS were tested as-is.

3.2.2.1 Rolling Thin-Film Oven (RTFO)

RTFO aging is a short-term aging method that represents aging performance during construction. In accordance with ASTM D2872, the asphalt material should be heated in the RTFO for 85 min at 163°C under air pressure. The machine can hold eight bottles at a time (Figure 3.2). The mass of the material in each bottle should be 35 ± 0.5 grams, and the mass change of each bottle after aging should be less than 1%. In this study, the RTFO-aged material was used in DSR Superpave high-temperature grading test and frequency sweep tests.

Figure 3.2 RTFO equipment.

3.2.2.2 Pressure Aging Vessel (PAV)

The PAV aging method simulates long-term aging conditions of asphalt binder. The material must first be RTFO aged and then subjected to the PAV process (Figure 3.3). The procedure starts with heating the RTFO-aged material then pouring it into the PAV pans. Each pan can contain 50 grams of material, and ten pans can be heated at one time. The aging process takes 20 hr under air pressure. In this study, the PAV-aged material was used in both DSR and BBR tests.

Figure 3.3 PAV equipment.

3.2.3 Rheological Testing Plan

The standard Rotovap test procedure was used to extract asphalt binder from the AC, and RAP/RAS were recovered in accordance with ASTM D6847. ASTM D2872 [Rolling Thin-Film Oven (RTFO)] and ASTM D6521 [Pressurized Aging Vessel (PAV)] were used to simulate the short-term and long-term aging of virgin binders, respectively. Aging protocols applied to the samples include standard and non-standard extra-long-term aging procedures. The aging history for each sample is as follows:

- Control binders analyzed as unaged were subjected to RTFO, PAV, and a second PAV (2PAV)
- Extracted binders from AC were tested as-is and after one PAV
- Extracted binders from RAP and RAS were tested as-is

3.2.3.1 Dynamic Shear Rheometer (DSR)

The DSR is used to characterize the viscous and elastic behavior of asphalt binders at intermediate and high temperatures (Figure 3.4). The basic DSR test uses a thin asphalt binder sample sandwiched between two circular parallel plates. The lower plate is fixed, while the upper plate oscillates back and forth across the sample to create a shearing action. Two important parameters can be obtained from the DSR test: G^* (complex modulus) and δ (phase angle).

$$G^* = \frac{\tau_{max}}{\gamma_{max}} \tag{3.1}$$

where δ is the lag between applied shear stress and the resulting shear strain. The phase angle presents the viscoelasticity of binder, and it can provide the asphalt with stress relaxation. For failure at the same stiffness level, a lower phase angle means less strain than a higher phase angle.

The DSR test in this study was used to calculate the following: Superpave binder grade, Superpave fatigue cracking and rutting threshold, complex modulus, Glover-Rowe parameter, R-value, and crossover frequency.

Figure 3.4 DSR equipment.

3.2.3.1.1 Superpave Low and High-Temperature Grading

Developed as part of the Strategic Highway Research Program, $G*/\sin\delta$ defined as a rutting factor is used to predict high-temperature binder behavior. A minimum limit is placed on the rutting parameter:

$$\text{Unaged binder } \frac{G^*}{\sin\delta} \geq 1.0 \text{ KPa} \quad (3.2)$$

$$\text{RTFO residue } \frac{G^*}{\sin\delta} \geq 2.2 \text{ KPa} \quad (3.3)$$

The DSR equipment can be used for measuring binder resistance to fatigue cracking. Based on the Superpave specification, the PAV-aged binder is used in fatigue testing to simulate pavement service life. G*sinδ is defined as the fatigue-cracking parameter with a maximum limit of 5,000 KPa measured at a strain amplitude of 1% and frequency of 10 rad/s. For each test, two replicates were used to obtain the final results.

3.2.3.1.2 Temperature-Frequency Sweep Test for Complex Modulus

Temperature-frequency sweep tests were conducted on the unaged and on the RTFO-, PAV-, and 2PAV-aged control binders (PG 58-28 and PG 64-22), as well as on the unaged extracted and PAV-aged extracted materials. All DSR data were obtained within the strain range from 0.05% to 5%, and the test was performed at a range of temperatures from 15°C to 64°C or 76°C (depending on material properties) at 12°C intervals. Test frequency was from 0.1 to 100 Hz at each temperature. Parallel plates of 8 mm diameter with a 2 mm gap were used at 15°C, 28° (sometimes at 40°C if the binder was too stiff). A 25 mm diameter plate with a 1 mm gap was used at temperatures greater than 28°C or greater than 40°C (depending on material properties). The master curves were constructed using the Christensen-Anderson model and shifted to a 28°C reference temperature (Christensen et al. 1992). Two replicates were used to determine the final master curve of each material.

The outcome of the temperature-frequency tests are master curves defining the complex modulus G^* and phase angle δ across a wide range of temperatures and frequencies. Additional parameters (Glover-Rowe, crossover frequency ω_c, and R-value) were calculated to characterize overall brittleness and cracking susceptibility. The methods used to calculate these additional parameters were as follows:

- The Glover-Rowe parameter was found using the expression $G * (\cos\delta)^2/\sin\delta$ measured at 15°C 0.005 rad/s. The criterion for onset damage was 180 kPa, and for significant cracking, it was 450 kPa (Rowe 2014).
- The crossover frequency was found using the master curve when loss and storage moduli were equal to each other—that is, when the phase angle became 45 degrees.
- The R-value was found to increase with asphalt aging. It is defined as the difference between the log of the glassy modulus and the log of the modulus at crossover frequency (Mogawer et al. 2016; Anderson et al. 2011).

The Glover-Rowe parameter can be used for predicting the cracking performance of a binder (Rowe 2014). According to this parameter, there is a relationship between cracking and $G'/(\frac{\eta'}{G'})$. The assumption was proved by Anderson et al. (2011), and after Rowe's analysis, the Glover-Rowe parameter becomes $G^*(\cos\delta)^2/\sin\delta$.

Because the frequency is constant, the Glover-Rowe parameter is a function of G and δ. At the limiting value of 9E-04 MPa/sec at 0.005 rad/s for the onset of cracking, the Glover-Rower parameter is 180 KPa. For the second value suggested by Anderson et al. (2011), which presents the development of significant cracking, the Glover-Rowe parameter is 450 KPa. The limiting values are as follows:

Damage onset: $$G * \frac{(\cos\delta)^2}{\sin\delta} = 180 \text{ KPa} \quad (3.4)$$

Significant cracking: $$G * \frac{(\cos\delta)^2}{\sin\delta} = 450 \text{ KPa} \quad (3.5)$$

Figure 3.5 is an example plot of the Glover-Rowe parameter. The Glover-Rowe parameter plotted in a black space diagram (the Y axis is complex modulus, and the X axis is phase angle) is a useful way to illustrate aging condition (Mogawer et al. 2016). The current study did not include any ABR binder, but it included highly aged material properties—and using recycled material can result in the mixes having an already aged condition. As shown in this figure, there were two types of binder (PG 76-22 and PG 64-22) and four aging conditions for each (RTFO, 20 hr PAV, 40 hr PAV, and 60 hr PAV). The two lines in the figure are the two criteria for the Glover-Rowe parameter. As the aging condition increases, the same trend can be observed for each material: the complex modulus increases, the phase angle decreases, and the points moved to the fail side.

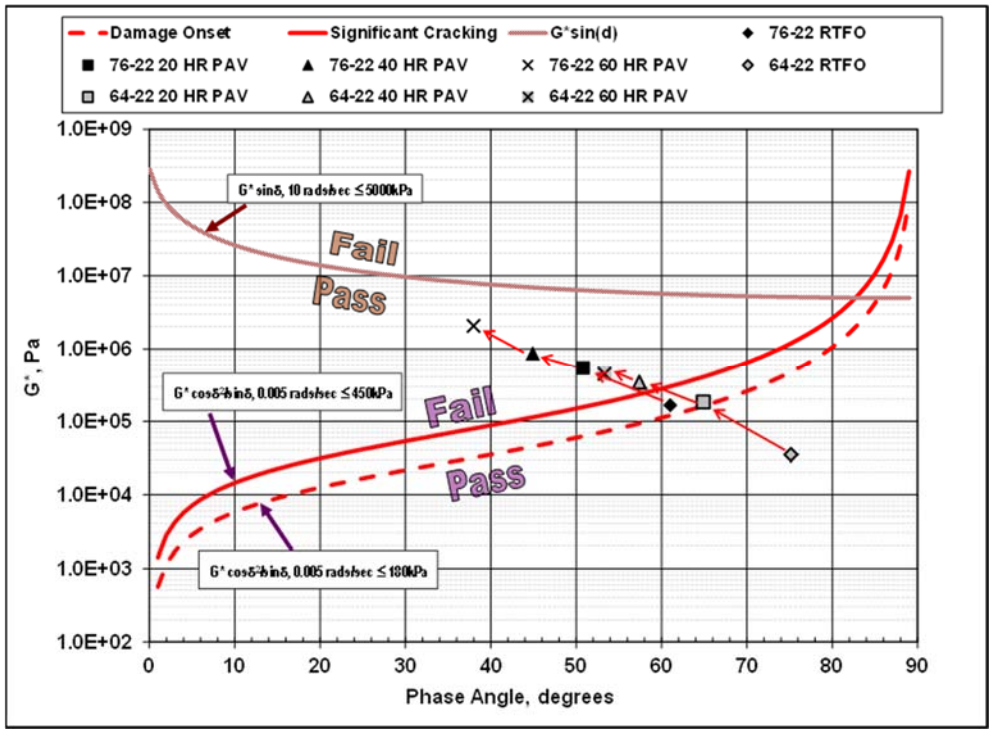

Figure 3.5 PAV-aged binders passing through the Glover-Rowe damage zone (Mogawer et al. 2015).

As previously discussed, the crossover frequency is the frequency at which the master curve phase angle equals 45 degrees (reference temperature 15°C), and the difference between the log of the glassy modulus and the log of the modulus at crossover frequency is defined as R-value. Figure 3.6 illustrates the determination of R-value and crossover frequency. Following the horizontal blue line starting at 45 degrees of phase angle, we can find the cross-over frequency, which is where the vertical blue line intersects with the x-axis. The upper bound of the complex modulus in this figure is the glassy modulus 10^9 Pa, so the difference between the glassy modulus and the crossing of the vertical blue line and complex modulus (marked as R in the figure) is used to determine the R-value.

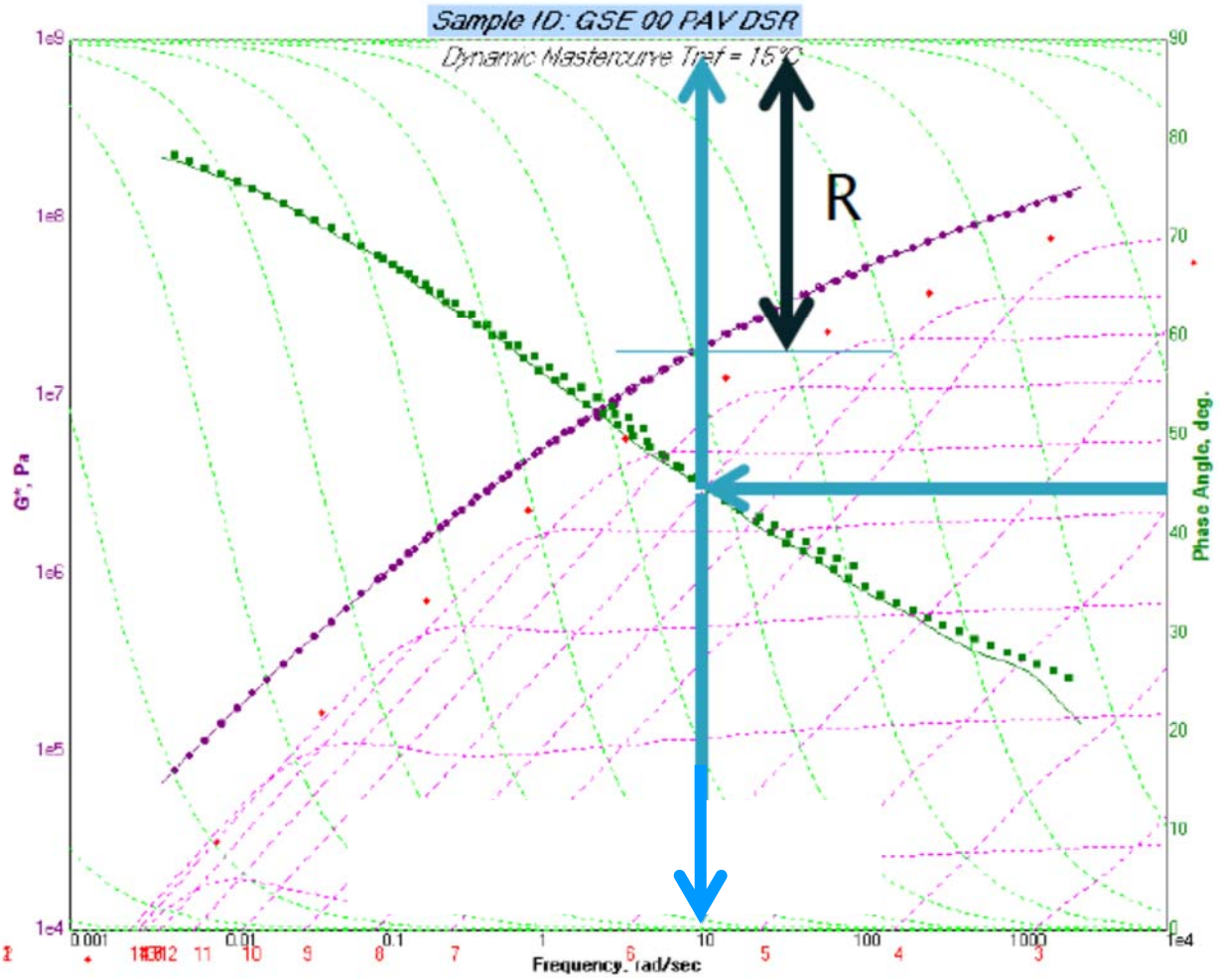

Figure 3.6 Crossover frequency and R-value (Rowe 2014).

3.2.3.2 Bending Beam Rheometer (BBR)

The BBR test is used to characterize the low-temperature performance of asphalt binder based on PAV-aged residue (Figure 3.7). Two parameters are obtained from this test: flexural creep stiffness, which is used to limit thermal stress build-up, and m-value, which indicates the binder's ability to relax stress and resist thermal cracking. AASHTO specifies a maximum measured stiffness of 300 MPa and a minimum m-value of 0.300.

In addition to Superpave results, another parameter to indicate low-temperature brittleness can be derived from the BBR tests results: ΔT_c. The ΔT_c parameter was shown to be a promising indicator of low-temperature cracking, which is the difference between PG stiffness temperature (stiffness exceeds 300 MPa) and PG m-value temperature (m-value goes below 0.300). It was shown that ΔT_c decreases with aging, which indicates an increase in brittleness. There are no specified criteria for this parameter—just an empirical threshold of –5°C used in this report based on personal communications of the authors. Because of excessive brittleness, testing could not be conducted for

RAS, even at intermediate temperature; therefore, the ΔT_c parameter was not calculated for RAS. This was found to be consistent with a study by Willis et al. (2016).

In the current study, four replicates were used for tests of PAV-aged control binders and extracted binders. Because of limited material, only two replicates were tested for the 2PAV control binders and PAV-aged extracted binders.

Figure 3.7 BBR equipment.

3.2.4 Chemistry Testing Plan

The following techniques were used for chemical characterization of various virgin and aged binders and extracted binders from RAP, RAS, and mixes. The typical results of each testing method are described here.

3.2.4.1 Fourier Transform Infrared (FTIR) Spectroscopy

An FTIR spectrometer was used to determine the functional characteristics of virgin, reclaimed, aged, and modified binders in wavenumbers ranging from 4000 to 600 cm^{-1}. Binders were heated at either 135°C (virgin and aged) or 165°C (reclaimed) and mixed thoroughly for analysis or were directly analyzed without heating. The carbonyl, sulfoxide, and poly(styrene-butadiene-styrene, or SBS) indices were calculated from spectra using Equations 3.6, 3.7, and 3.8 respectively.

$$\mathrm{ICO} = \frac{\text{Area around } 1700\mathrm{cm}^{-1}}{\text{Area around } 1460\mathrm{cm}^{-1} + \text{Area around } 1375\mathrm{cm}^{-1}} \tag{3.6}$$

$$\mathrm{ISO} = \frac{\text{Area around } 1030\mathrm{cm}^{-1}}{\text{Area around } 1460\mathrm{cm}^{-1} + \text{Area around } 1375\mathrm{cm}^{-1}} \tag{3.7}$$

The peaks that are used in these equations are shown in FTIR spectra of binders in Figure 3.8.

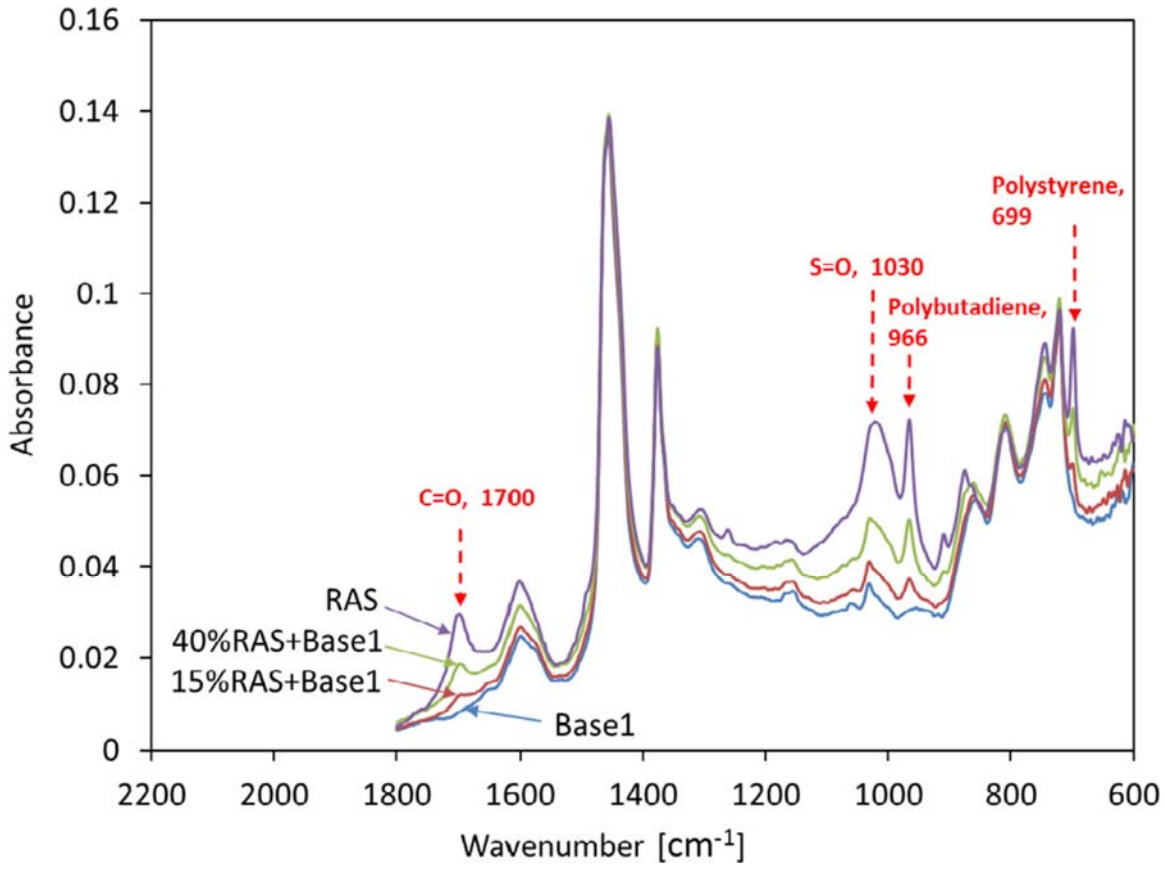

Figure 3.8. FTIR curves for RAS + base 1 binder group (Liu et al. 2015).

3.2.4.2 Elemental Analysis

Elemental analyses of the virgin, reclaimed, aged, and modified binders were conducted in duplicates in an Exeter Analytical (Chelmsford, MA) CE-440 elemental analyzer located at the University of Illinois Noyes Laboratory (Urbana, IL). This process was used to determine percentages of carbon, hydrogen, nitrogen, and sulfur (CHNS) elements. Percent oxygen was calculated by subtracting CHNS percentage from 100%.

3.2.4.3 Thin-Layer Chromatography–Flame Ionization Detection (TLC-FID) Analysis (SARA)

In the TLC-FID analyses, 2% (w/v) solutions of the virgin, reclaimed, aged, and modified binders were prepared in chloroform and filtered through a 0.45 µ syringe filter to remove any insoluble residue from the solution. The syringe filter was weighed before and after drying to constant weight to calculate percent residue. The sample solution (1 µl) was spotted on Chromarods coated with a thin film of silica gel, using a microsyringe. The separation of bitumen into four generic fractions (saturates, aromatics, resins, and asphaltenes) was performed in a three-stage development process using n-heptane, toluene, and tetrahydrofuran. During this three-stage development, the Chromarods were dried for 10 min and humidified in $NaNO_2$ for 10 min between each development. The Chromarods were scanned with an Iatroscan MK-5 analyzer (Iatron Laboratories Inc., Tokyo, Japan) with an FID detector, which provided chromatograms with peaks for saturates, aromatics, resins, and asphaltenes as shown in Figure 3.9.

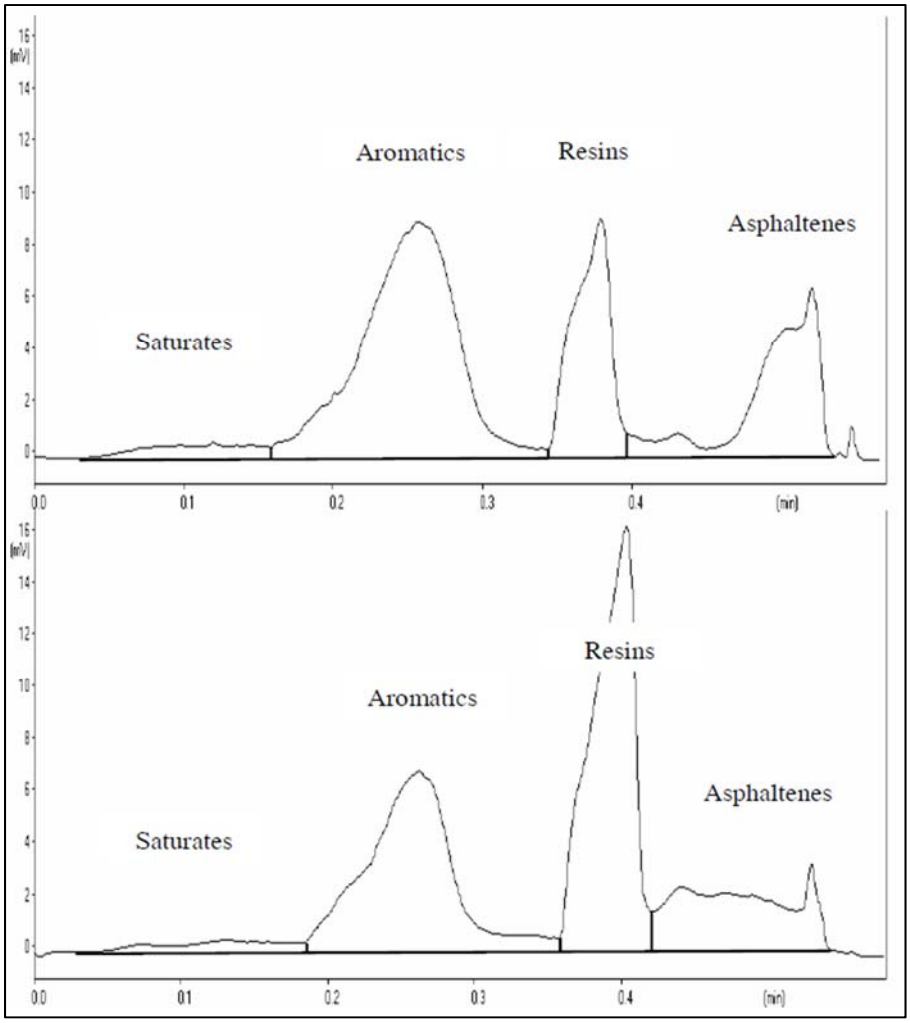

Figure 3.9 Typical chromatograms of plain bitumen B 50/70 original (top) and after RTFOT+PAV aging (bottom) (Stangl et al. 2006).

3.2.4.4 Atomic Force Microscopy (AFM) Imaging

Virgin, reclaimed, aged, and modified binders were melted at approximately 100°C. The melted binder was poured onto a glass slide, and a blade was used to create a thin film. In AFM imaging, a cantilever with an extremely sharp tip (nominal tip radius of 8 nm) located on its free end is scanned over the sample surface using a piezoelectric scanner. The changes in tip-sample interactions result in deflection of the cantilever, which is measured by an optical-lever detection system. Tapping-mode AFM was used to characterize all the binders. In tapping mode, the probe is modulated near its first resonant frequency while it is scanned across the sample. Thus, the tip maintains an intermittent contact over the sample surface, keeping the tapping force low and the lateral forces negligible. This moderate force exerted on the surface leads to scanning in a non-invasive manner, which is ideal for soft material surfaces such as bitumen.

A common explanation for asphalt microstructure stems from colloidal theory, in which polar groups form structured phases in a non-polar solution. The four distinctive phases describing this

microstructure are catanaphase (bee structure), periphase (around catanaphase), paraphase (solvent regions), and salphase (high phase contrast spots) (Das et al. 2010) and were shown in an image taken via the AFM method (see Figure 2.2 in this report).

3.2.4.5 Molecular Weight Distribution Using Gel Permeation Chromatography (GPC)

GPC analysis was conducted in triplicate on all binder samples for weight-average molecular weight (M_w), number-average molecular weight (M_n), polydispersity index (PDI), and molecular size distribution. Binder samples were prepared as 3% (w/w) in tetrahydrofuran (THF) and filtered through a 0.45 µ syringe filter to remove any insoluble residue. The size exclusion chromatography (SEC) instrument was equipped with a Waters (Milford, MA) Styragel HR1 SEC column (7.8 mm × 300 mm) and a Waters 2414 RI detector. THF was used in a mobile phase (1.0 mL/min) for this study. The resulting chromatographic data (retention time-signal intensity) shown in Figure 3.10 was converted into molecular weight distribution (molecular weight-signal intensity) using a calibration curve of polystyrene standards in MATLAB. The total peak area was then divided into three groups based on the molecular size distribution: larger molecular size (LMS), medium molecular size (MMS), and smaller molecular size (SMS). The GPC peak in the chromatogram was divided into 13 slices (slices 1–5 for LMS, slices 6–9 for MM), and slices 10–13 for SMS) for analysis. The section that elutes first is traditionally referred to as the large molecular size fraction, the second fraction as the intermediate or medium molecular size fraction, and the last fraction as the small molecular size fraction.

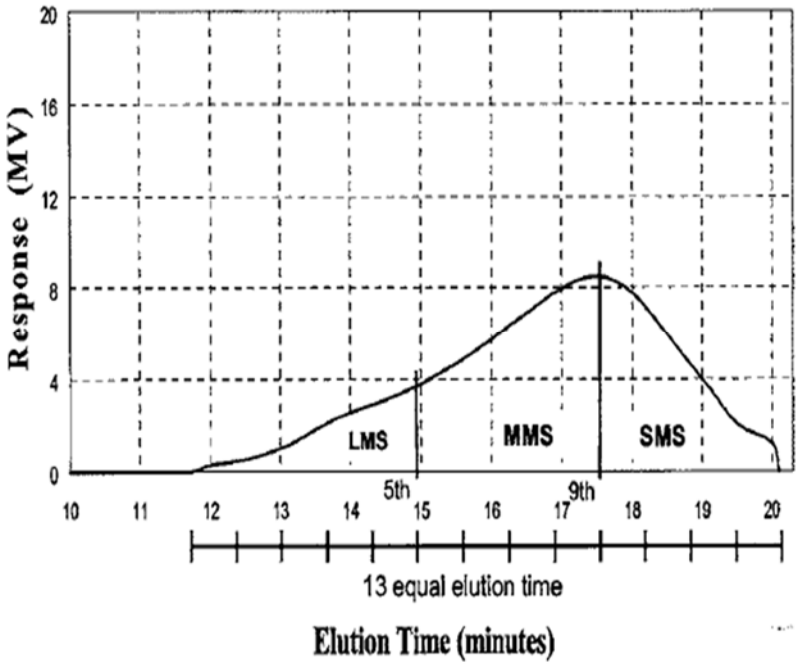

Figure 3.10 GPC chromatograms for asphalt binders containing RAS (Abbas et al. 2013).

CHAPTER 4: RHEOLOGY RESULTS

4.1 SUPERPAVE GRADING RESULTS

Table 4.1 shows the Superpave grading results of all binders at various short- and long-term aging conditions. All the unaged control binders were graded based on the Superpave specification that $G^*/\sin\delta > 1.0$ kPa. RTFO-aged and unaged extracted binders were graded based on $G^*/\sin\delta > 2.2$ kPa. The results in Table 4.1 show that all the virgin and RTFO-aged control binders met the Superpave specifications.

Table 4.1 Superpave Grading Results for Control and Extracted Binders

Binder Type	S(t) (MPa)	m —	$G^*/sin\delta$ @ un-aged (kPa)	$G^*/sin\delta$ @ RTFO (kPa)	$G^*sin\delta$ @ PAV (kPa)	Base Binder	Resultant Continuous Grade (°C)	Resultant Performance Grade
Original Binder								
PG 58-28	220	0.31	1.91	5.76	2155	—	CG 63.4-29.2	PG 58-28
PG 64-22	239	0.301	1.89	4.65	1737	—	CG 69.5-23.6	PG 64-22
Extracted Binder								
N90-0AS	219	0.302	—	2.39	3155	PG 64-22	CG 70.7-22.3	PG 70-22
N90-10	90	0.35	—	4.58	3168	PG 64-22	CG 69.7-21.0	PG 64-16
N90-20	78	0.326	—	2.70	1575	PG 58-28	CG 77.9-18.9	PG 76-16
N90-30	61	0.352	—	3.24	1259	PG 58-28	CG 79.3-15.9	PG 76-10
N90-60AS	53	0.303	—	2.27	880	PG 52-34	CG 88.2-10.7	PG 88-10
Extracted Constituents								
RAP1	107	0.349	—	2.84	1380	—	CG 90.1-14.0	PG 88-10
RAP2	159	0.316	—	2.66	1731	—	CG 77.6-24.4	PG 76-22
RAS1	—	—	—	256.77	—	—	CG 156.7-	—
RAS2	—	—	—	182.30	—	—	CG 150.1-	—

The high-temperature grades of RAS1 and RAS2 were above 150°C—much higher than those of other binders. The results showed that RAP1 was stiffer than RAP2 at high temperature, which was graded as 88°C; the average true grade of RAP1 was 90.1°C, and RAP2 was 77.6°C. For the extracted N90 binders, the high-temperature grade generally increased with ABR content regardless of base binder grade. The true grades of N90-0AS and N90-10 with a base binder of PG 64-22 were 70.7°C and 69.7°C, respectively. This finding indicated that after adding 2.5% RAS, the high-temperature grade changed very little. However, when the ABR content changed to 20% (N90-20), even with a softer binder of PG 58-28, the true grade increased to 77.9°C; for 30% ABR, it increased to 79.3°C. The true grade of N90-60AS with the softest base binder of PG 52-34 was 88.2°C.

The low-temperature grade shows that the PAV-aged PG 58-28 and PG 64-22 were graded as –28°C and –22°C, respectively, which met the Superpave specifications. The RAP1 was graded as –10°C and

RAP2 as –22°C. For the extracted N90 binders (except N90-0AS), their low-temperature grade increased compared with that of their base binders. The N90-0AS with base binder of PG 64-22 was still graded as –22°C, but after its ABR content was increased to 10% (N90-10), it was graded as –15.9°C; the low-temperature grade increased by 6°C. For the N90-20 and the N90-30 with a base binder of PG 58-28, the low-temperature grade of the former increased by 12°C (to –15.9°C), and for the latter, by 18°C (to –10°C). PAV-aged N90-60AS was graded as –10°C with the softest base binder PG 52-34; after approximately 60% recycled binder was added, its low-temperature grade increased by 24°C compared with the base binder. The results showed an increasing trend (warming) of low-temperature grade with ABR content regardless of base binder type, and the difference in low-temperature grades between the PAV-aged N90 series and their base binders increased as ABR content increased.

4.2 COMPLEX MODULUS MASTER CURVES

This section presents the constructed master curves with 28°C as a reference temperature. Figure 4.1 is an overall plot of all evaluated ABR binders, and Figure 4.2 shows the results for various combinations of extracted binders and control binders. The results are presented in each combination as follows:

- **Figure 4.2(a)** presents original binders only, at various aging conditions (unaged, RTFO, PAV, and 2PAV) to evaluate aging impact on base binders used in the AC as well as extracted constituents. Binder modulus consistently increased with aging, as expected.
- **Figure 4.2(b)** presents the results of RAP1 and RAP2 compared with 2PAV- and PAV-aged original binders. The RAP1 is stiffer than RAP2 and approaches the modulus values of the 2PAV-aged PG 64-22.
- **Figure 4.2(c)** presents recovered binders from low ABR mixes and with their corresponding base binders (binders recovered from N90-0AS and N90-10 with PG 64-22 at all aging conditions). As shown in Figure 4.2(c), there may be an equivalency of modulus between RTFO of virgin binder and extracted binder prior to PAV. When extracted binder was subjected to PAV, the same equivalency could be observed with the RTFO and PAV of the corresponding base binder. None of the recovered binders before and after PAV could obtain the values attained by 2PAV base binder.
- **Figure 4.2(d)** presents recovered binders from high ABR mixes and with their corresponding base binders (binders recovered from N90-20 and N90-30 with PG 58-28; N90-60AS with its RAP sources at all aging conditions). The equivalency noted in the previous curve (Figure 4.2(c)) no longer exists. RTFO and RTFO + PAV of base binder fell short of extracted binder prior to PAV. The modulus curve of extracted binder is somewhere between the first and second PAV of base binders. When extracted binder was subjected to PAV aging, the modulus of N90-20 and 30 reached the stiffness of 2PAV PG 58-28.
- **Figure 4.2(e)** presents N90-60AS with its RAP sources. Extracted binder from N90-60AS had the softest base binder (PG 52-34), but because of the presence of 7% RAS2, the modulus curve was between its RAP sources before aging. One PAV increased the moduli significantly,

to much higher than its RAP sources. These results indicate that the binder present in high ABR AC is already at a severely aged state immediately after production.

- **Figure 4.2(f)** presents recovered binders from AC with five different ABR levels (immediately after recovery and after PAV) to evaluate ABR level in the AC. Binders recovered from AC with 60% ABR mixes (N90-60AS) had significantly higher moduli than the others, even though this AC had the softest base binder (PG 52-34). One PAV shifted up the modulus curves by almost the same amount for all binders. It was also noted that there may be an equivalency between binders obtained from higher ABR mixes (such as N90-20 and N90-30) and PAV of binders recovered from zero or low ABR mixes (N90-0AS and N90-10).

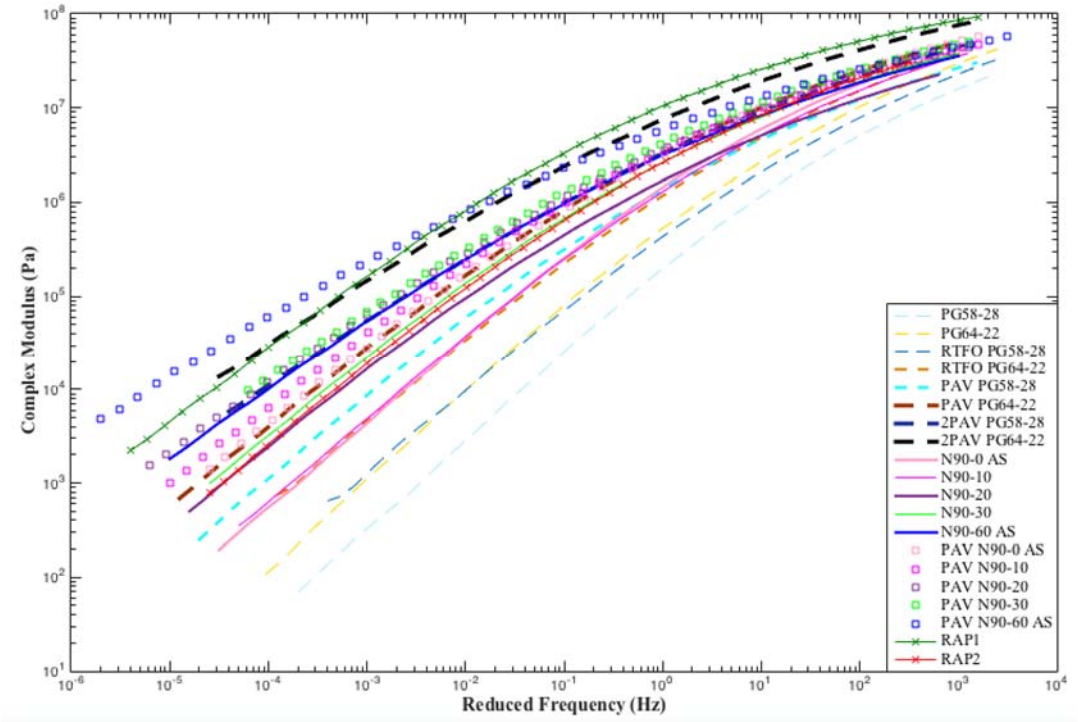

Figure 4.1 Complex modulus master curves for all evaluated ABR binders.

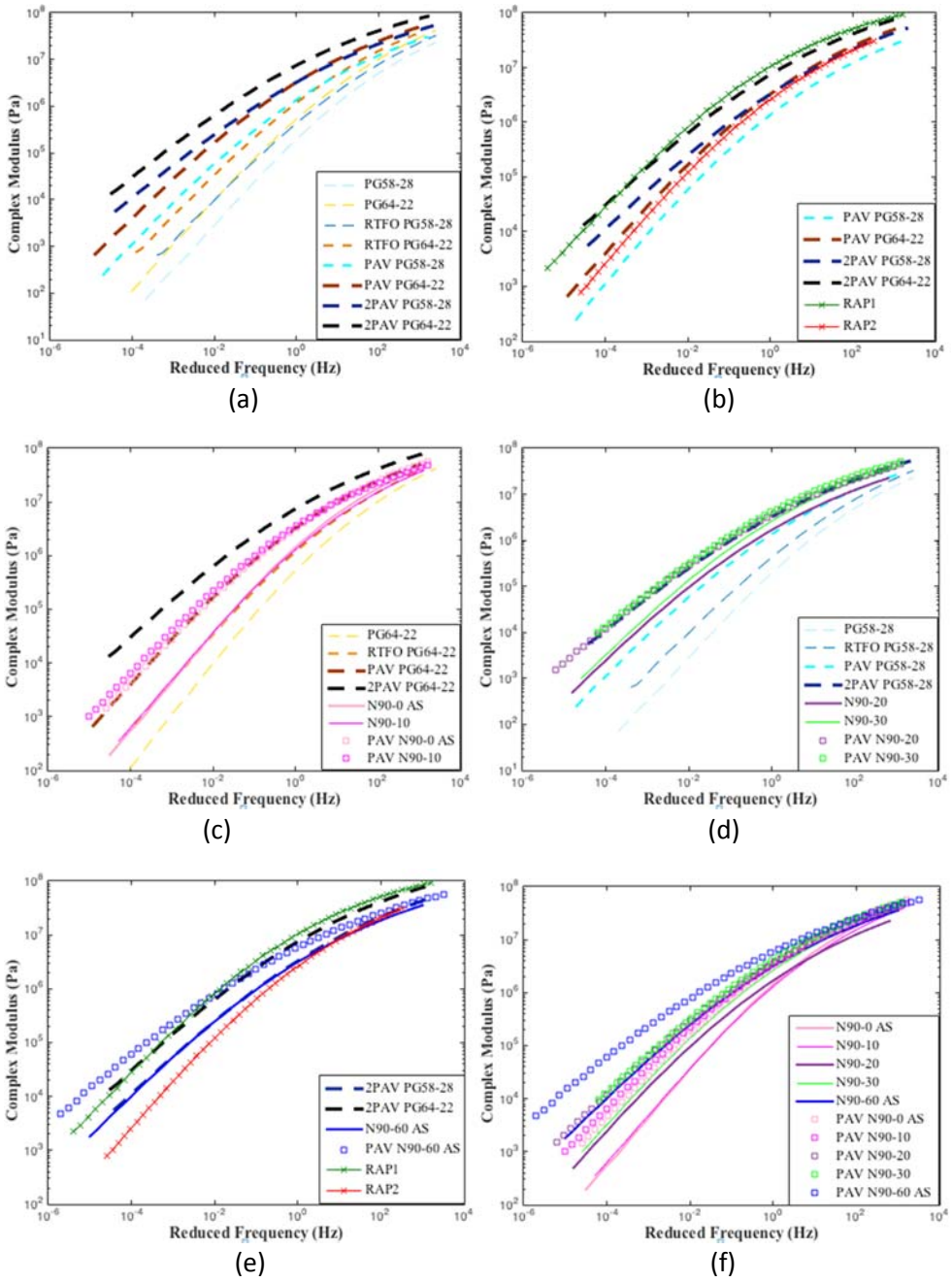

Figure 4.2 Subplot of complex modulus at reference temperature of 28°C (a) unaged, RTFO-, PAV-, and 2PAV-aged control binders; (b) RAP with 2PAV- and PAV-aged control binders; (c) N90-0AS and N90-10 binders of two aging conditions compared with their base binder, PG 64-22, under four aging conditions; (d) N90-20 and N90-30 binders of two aging conditions compared with their base binder, PG 58-28, under four aging conditions; (e) N90-60AS with two aging conditions compared with its RAP source and 2PAV-aged control binders; (f) PAV-aged and unaged extracted binders from AC.

4.3 DERIVED RHEOLOGICAL PARAMETERS

As previously discussed, additional parameters were used to obtain a better understanding of ABR levels and aging on a binder's brittleness. These parameters were ΔT_c obtained from low-temperature BBR, the Glover-Rowe parameter, R-value, and crossover frequency from the DSR complex modulus tests. A summary of the additional rheological parameters is presented in Table 4.2. Each of these parameters will be discussed separately.

Table 4.2 Results of Rutting, Glover-Rowe Parameter, Crossover Frequency, R-value, and ΔT_c

Virgin Binder	Aging Status	Rutting (kPa) 50°C; 10 rad/s	Glover-Rowe (kPa) 15°C; 0.005 rad/s	w_c (Hz) 15°C	R-value 15°C	ΔT_c
PG 58-28	—	6.34	0.07	12,728	0.593	—
PG 58-28	RTFO	22.83	0.92	9,392	0.854	—
PG 58-28	PAV	79.09	23.65	312	1.733	0.39
PG 58-28	2PAV	231.59	207.69	28	1.866	–7.73
PG 64-22	—	13.35	0.66	11,488	0.466	—
PG 64-22	RTFO	41.22	6.77	2,403	1.210	—
PG 64-22	PAV	183.41	106.90	123	1.576	–0.26
PG 64-22	2PAV	536.55	757.65	8	1.740	–5.97
Extracted Binder						
RAP1		693.40	875.53	16	1.525	–5.37
RAP2		124.46	73.98	218	1.568	–2.44
ABR Binder	**Base Binder**	**ABR Content**	**Rutting (kPa)**	**Glover-Rowe (kPa)**	**w_c (Hz)**	**R-value**	**ΔT_c**
N90-0AS	PG 64-22	0.0%	49.97	8.67	1,168	1.363	2.22
N90-10	PG 64-22	10.5%	44.67	10.10	899	1.464	1.45
N90-20	PG 58-28	21.2%	93.38	93.49	323	1.736	–4.12
N90-30	PG 58-28	29.8%	167.27	90.20	168	1.643	0.35
N90-60AS	PG 52-34	60.8%	266.75	284.05	17	1.995	–8.69
N90-0AS PAV	PG 64-22	0.0%	158.47	116.03	192	1.507	–1.27
N90-10 PAV	PG 64-22	10.5%	227.15	187.12	78	1.680	–3.41
N90-20 PAV	PG 58-28	21.2%	378.24	243.69	14	1.964	–17.71
N90-30 PAV	PG 58-28	29.8%	342.12	280.88	21	1.823	–8.37
N90-60AS PAV	PG 52-34	60.8%	736.60	1269.90	1	2.336	–21.60

4.3.1 Rutting Parameter

The rutting parameter was derived using $G^*sin\delta$ at 50°C for each binder and aging condition. Results are shown in Figure 4.3. A higher value of rutting parameter indicates a higher resistance to rutting. The results showed that rutting parameter increased with aging as well as with ABR content. The rutting resistances observed for unaged N90-0AS and N90-10, RTFO-aged PG 64-22, and PAV-aged N90-0AS were still close to those of the PAV-aged PG 64-22, while the rutting resistance for PAV-aged N90-10 was higher than for PAV-aged PG 64-22 and PAV-aged N90-0AS. When ABR contents

increased to 20 and 30, compared with their base binder PG 58-28, rutting resistance increased significantly for unaged or PAV-aged status. The rutting parameter of unaged N90-60AS was higher than that of PAV-aged PG 64-22, even though the base binder was PG 52-34 in this mix. After PAV aging, the rutting resistance of N90-60AS became nearly as high as that of RAP1.

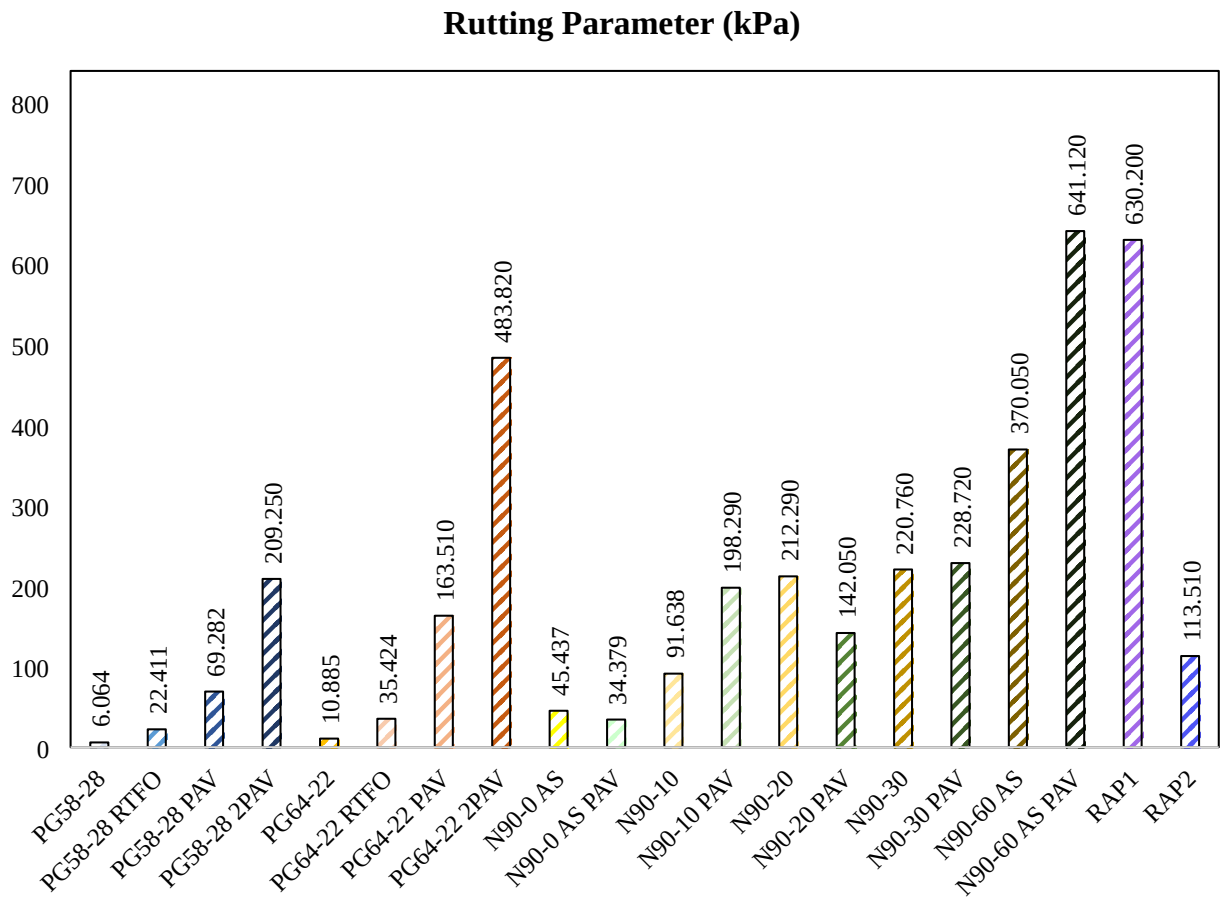

Figure 4.3 Bar chart of rutting parameters for all ABR binders.

4.3.2 ΔT_c Parameter

As shown in Table 4.2, PG 58-28 and PG 64-22 had a relatively small ΔT_c , warmer than –1°C under PAV conditions. After 2PAV aging, the absolute value of ΔT_c for each binder decreased dramatically, to –7.73°C and –5.97°C for PG 58-28 and PG 64-22, respectively. Other constituents used in the AC design of the N90 series (RAP1 and RAP) had ΔT_c values around –5°C. Because of excessive brittleness, testing could not be conducted for RAS, even at intermediate temperature; therefore, the ΔT_c parameter was not calculated for RAS.

A consistent trend was observed with the ΔT_c for all extracted binders with increasing ABR and PAV. In general, the ΔT_c parameters were greater than –5°C, except for the binder with 60% ABR (N90-60AS), which had a value of –8.69°C. After PAV aging, a dramatic decrease (as high as approximately –20°C) was consistently observed for all of the extracted binders starting from 20% ABR (with RAS

only). Considering the empirical preliminary threshold of –5°C proposed for low-temperature susceptibility of binders, the AC with 60% ABR could suffer from brittleness in both the short and long terms.

4.3.3 Glover-Rowe Parameter

Figure 4.4 presents the Glover-Rowe parameter values in the black space diagram presented by complex modulus and phase angle. The solid line indicates onset damage, and the dashed line indicates the point at which significant fatigue damage occurs. In general, the expected behavior resulted: binders moved from the lower right quadrant (high phase angle and lower modulus) to the upper right quadrant (lower phase angles and higher modulus, indicating a decrease in viscous components). Figure 4.4(a) is the plot of two control binders under all aging conditions. As aging increased, the values moved to the upper right quadrant, approaching the potential failure zones. The 2PAV PG 64-22 passed the significant damage line. As shown in Figures 4.4(b) and (c), before PAV aging only the N90-60AS passed the onset damage. On the other hand, all binders except the N90-0AS passed the onset damage line or significant failure zone after PAV.

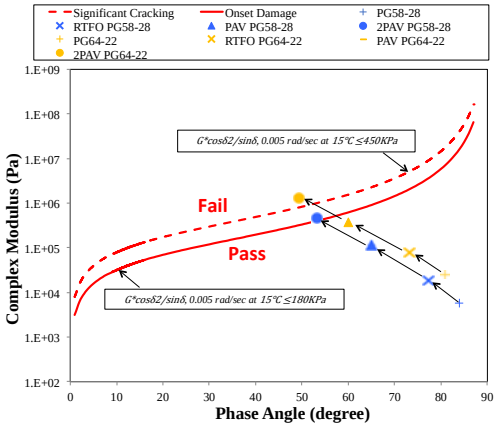

(a)

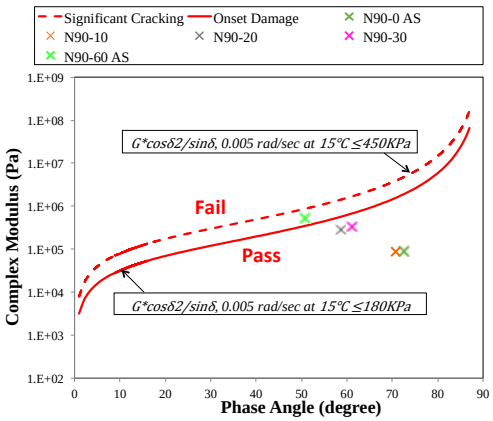

(b)

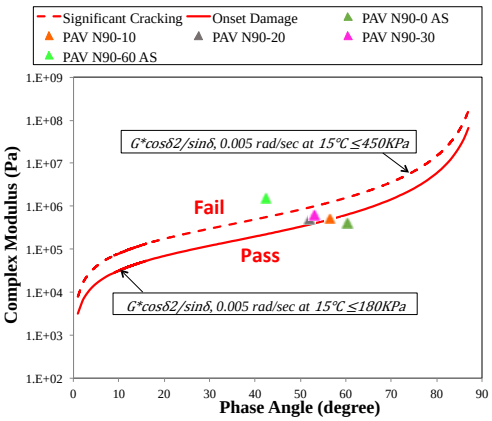

(c)

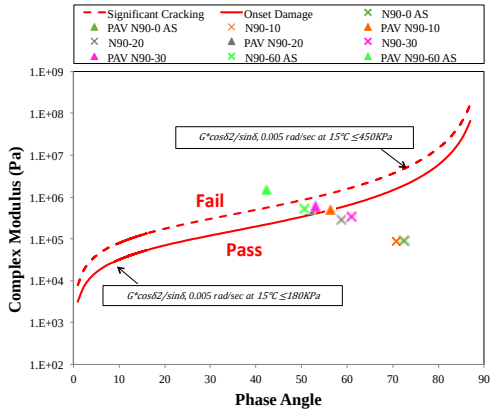

(d)

Figure 4.4 (a) Black space diagram of all aging conditions of PG 64-22 and PG 58-28 at 15°C and 0.005 rad/s; (b) black space diagram of unaged extracted N90 series at 15°C and 0.005 rad/s; (c) black space diagram of PAV-aged extracted N90 series at 15°C and 0.005 rad/s; (d) combined diagram of (b) and (c).

4.3.4 R-Value and Crossover Frequency

Figure 4.5 presents the plots of the crossover frequency and R-value results obtained by shifting the master curves to a reference temperature of 15°C. The crossover frequency is a measure of overall binder hardness, which should generally decrease with binder aging and is usually higher for oxidized binder (Rowe 2014; Ozer et al. 2016). Figure 4.5(a) shows the results of control binders under all aging conditions as well as for the RAP. Consistent with previous studies, the crossover frequency decreased, and the R-value increased with aging. The R-value versus crossover frequency for the N90 series is shown in Figure 4.4(b)—generally, as the ABR content increased, the crossover frequency decreased, and the R-value increased at each aging condition.

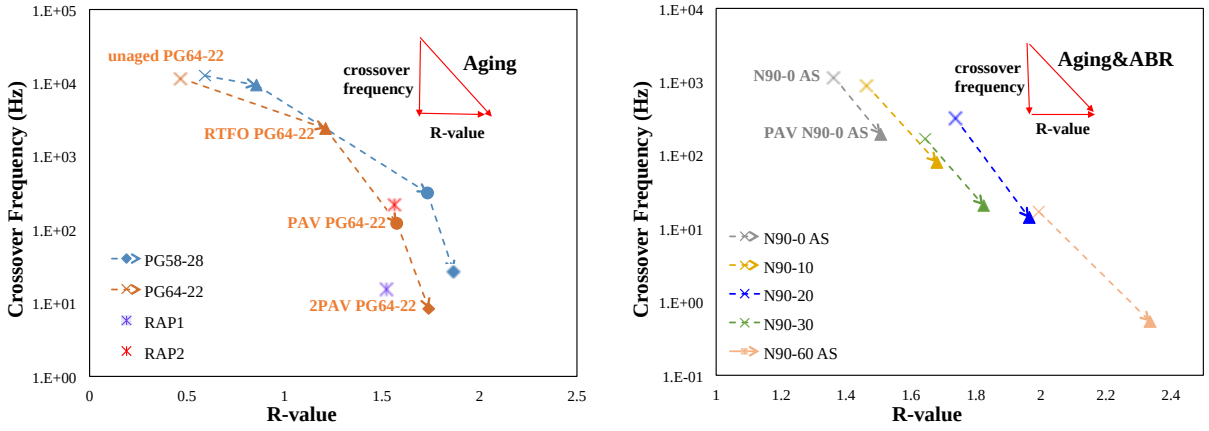

(a) (b)

Figure 4.5 (a) Crossover frequency versus R-value of control binders and RAP at a reference temperature of 15°C; (b) crossover frequency versus R-value of extracted binders at a reference temperature of 15°C.

4.4 EQUIVALENCY OF AGING AND ABR LEVELS FOR BRITTLENESS OF BINDERS

There was a consistent trend with an increase in the ABR level; that trend can be helpful in evaluating brittleness of binders that would otherwise be masked within the Superpave grade changes. This section presents an evaluation of the additional rheological parameters used to determine critical ABR levels in AC.

Figure 4.6 illustrates the change in the ΔT_c parameter with aging of the original binders [Figure 4.6(a)] and ABR level of extracted binders [Figure 4.6(b)]. It is clear from the original binder data that the critical threshold of –5°C is exceeded only with the second PAV. An equivalency, not shown in Figure 4.6 (b), could be established between extracted binder as-is and one-PAV-aged base binders for the ΔT_c parameter only for low ABR content mixes. However, the ΔT_c parameter for extracted binders progresses much more rapidly when ABR level increases to 20% and higher. Even before PAV was applied, AC with higher ABR levels (more than 20%, with the exception of 30% ABR) had ΔT_c values around critical thresholds. After one PAV application, the binders recovered from the high ABR mixes (20%, 30%, and 60% ABR) exhibited values well beyond the critical threshold of –5°C and beyond that

of the 2PAV corresponding binders (PG 58-28 and PG 52-34). It is important to note that the low and medium ABR mixes were prepared with RAS only (i.e., no RAP). The situation may not be as critical for AC with ABR 20% or 30% with RAP only or RAP and RAS because RAP binder exhibited moderate values of brittleness. It was also noted that when ABR level was high, the PAV-aged extracted binders can have much more critical values of ΔT_c than the second PAV of their corresponding base binders.

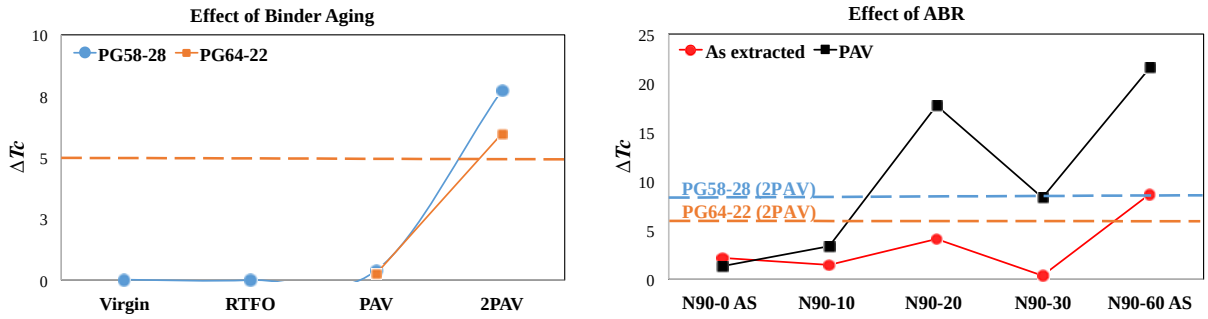

(a) (b)

Figure 4.6 (a) Comparison of the ΔT_c parameter with changing aging levels of control binders; (b) comparison of the ΔT_c parameter with changing ABR and aging levels of extracted N90 binders.

Two performance issues can be inferred from this equivalency analysis. The first is that the binder in high ABR AC can be relatively more brittle immediately after production than its counterparts with no or low ABR. This finding indicates that these ACs can have some short-term low-temperature cracking performance issues. A second, and more important, observation is what happens to these ACs when they are aged. Laboratory environment PAV of extracted binders for high ABR AC indicates that these AC will age much faster than the binder in the AC with no or low ABR. Accordingly, it was concluded that the critical ABR level for AC with only RAS should be below 20%, which corresponds to below 5% RAS.

A similar analysis was conducted for the Glover-Rowe parameter as an indication of block and fatigue cracking. Figures 4.7(a) and (b) show the results for the Glover-Rowe parameter with aging of the original binders as well as the ABR levels for the extracted binders. A clear and similar trend of an increase in the Glover-Rowe parameter with aging and ABR level was observed. Both base binders reached the critical threshold proposed for cracking (180 kPa) after the second PAV. For the extracted binders, the Glover-Rowe parameter consistently increased with increasing ABR, but a much higher rate of increase was observed for binders with higher ABR levels. The critical threshold of 180 kPa was reached for the binder with 10% ABR after PAV. As ABR increased to 60%, even before PAV, extracted binder exceeded the critical threshold.

Similar to the ΔT_c comparision for low ABR mixes, the Glover-Rowe values of extracted binder from low ABR mixes are equivalent to one PAV of their corresponding base binder; after PAV aging, it increased slightly, compared with 2PAV of the base binder. When ABR levels are greater than or equal to 20%, a single PAV of the extracted binders exhibited much higher values of the Glover-Rowe parameter as the second PAV of their corresponding base binders. The gap between the parameters calculated from PAV of extracted binder and a 2PAV of the base binder grew at the highest ABR level.

According to the progression in the Glover-Rowe parameters, the AC with high ABR content could suffer from short- and long-term brittleness that affects development of block cracking or fatigue cracking. In addition, AC with high ABR could age much faster than its counterpart AC with low or no ABR—reaching a state of severe brittleness.

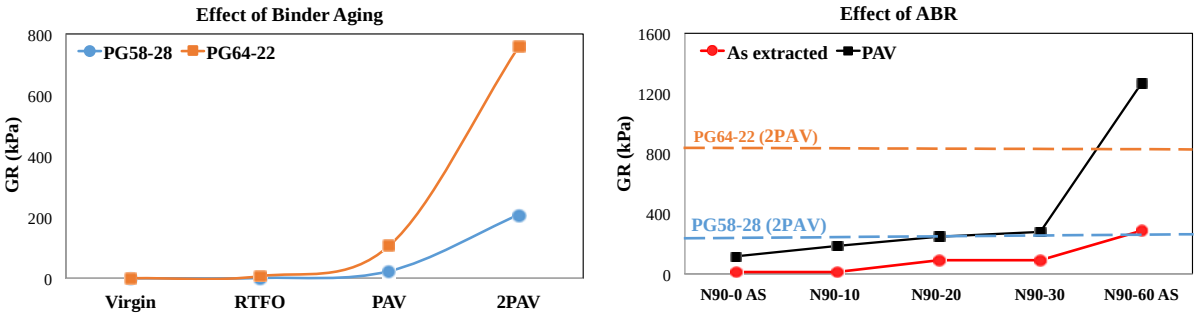

(a) (b)

Figure 4.7 (a) Comparison of the Glover-Rowe parameter with changing aging levels of control binders; (b) comparison of the Glover-Rowe parameter with changing ABR and aging levels.

4.5 CORRELATION TO MIXTURE PERFORMANCE

The flexibility index (FI) was developed as a parameter to characterize the damage resistance of an asphalt mixture, and it produces a good correlation with field performance (Al-Qadi et al. 2015). Generally speaking, good-performing mixtures had an FI value greater than 10, while the worse-performing ones had an FI lower than 4 (Al-Qadi et al. 2015). As shown in Figures 4.8(a) and (b), which show the correlation between FI and the as-extracted N90 binders, the Glover-Rower value and ΔT_c generally increased as FI decreased, which indicates that these two parameters provide failure trends similar to those of the FI. The same trend can be observed in the results of PAV-aged extracted N90 binders (Figure 4.8 (c) and (d)).

The FI showed that when ABR content increased to 30%, the mixture exposed to poor performance and the mix with 60% ABR could suffer from extreme lack of flexibility to release stress. Before PAV aging, except with N90-60AS, the Glover-Rowe parameters of the extracted N90 binders are generally below 100 kPa and ΔT_c are below 5, which means those binders still possess good stress- and crack-resisting properties at intermediate and low temperatures, and the FIs of their corresponding mixtures were higher than 4. After PAV aging, the Glover-Rowe parameter showed that when ABR reached 10%, it was already exposed to onset failure and the 20% and 30% ABR in the range between onset damage and significant cracking. A similar trend was observed in the relationship between the ΔT_c and FI; that is, except for N90-0AS and N90-10, the ΔT_c of other binders were much higher than 5, meaning that they are extremely brittle at low temperature.

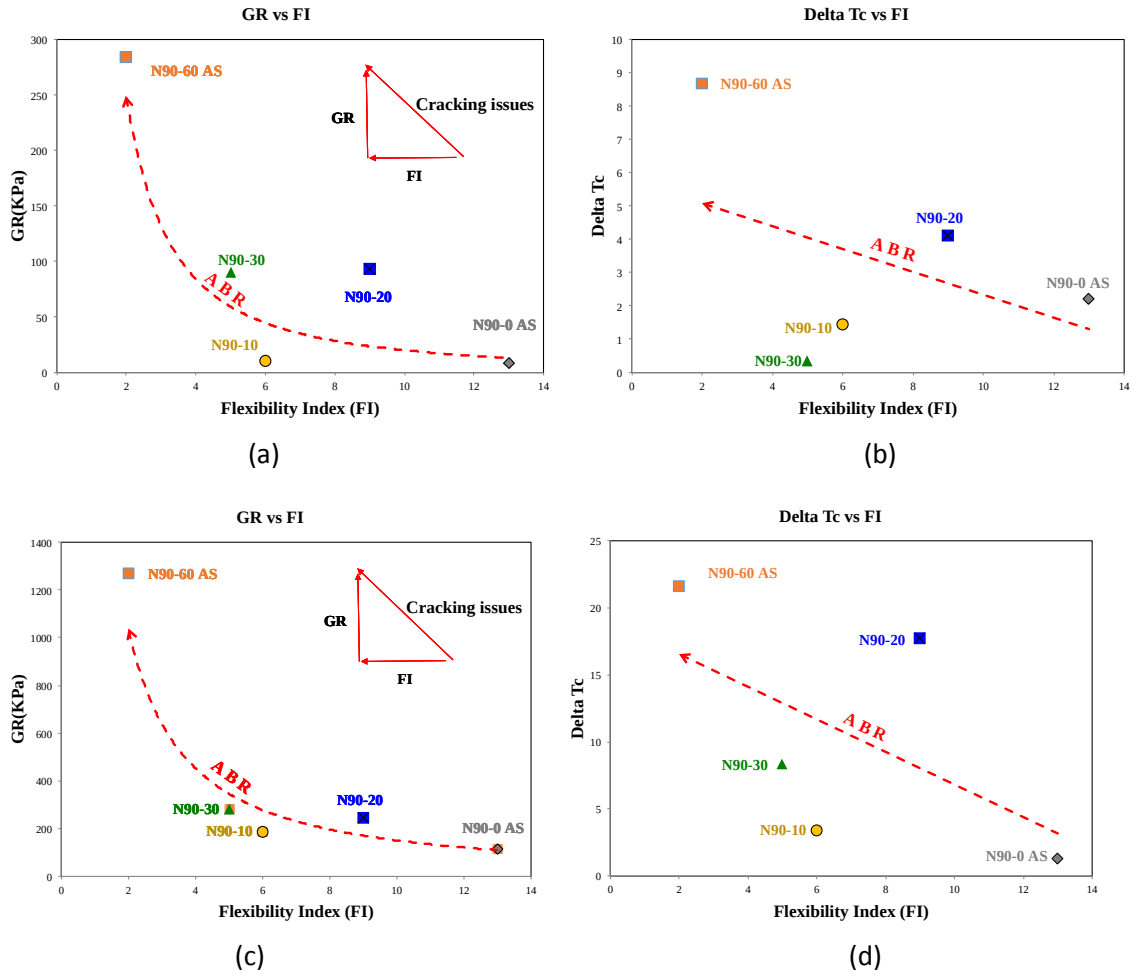

Figure 4.8 (a) Correlation between Glover-Rowe of as-extracted N90 binder and flexibility index; (b) correlation between ΔT_c of as-extracted N90 and flexibility index; (c) correlation between Glover-Rowe of PAV-aged N90 binder and flexibility index; (d) correlation between ΔT_c of PAV-aged N90 binder and flexibility index.

4.6 SUMMARY AND REMARKS

This chapter presented an experimental evaluation of the rheological properties of binders from various sources to investigate the effects of aging and increasing ABR levels. In addition to the standard Superpave grading parameters, the additional rheological parameters for low-temperature cracking susceptibility and block and fatigue cracking were derived from various DSR and BBR tests. Binders from five AC mixes designed with varying ABR percentages (0% to 60%) were recovered using the standard Rotovap test procedure. The base binder used in the AC design and binders recovered from RAP and RAS were also tested. In addition to standard aging protocols, base binders were subjected to a second PAV, whereas one PAV was applied for the extracted binders.

Almost all additional rheological parameters appeared to have consistent trends with aging and increasing ABR levels. The parameters under consideration were shown to be helpful in evaluating

progression in brittleness of binders with ABR and aging. Based on the outcome of the experimental program, it was concluded that AC with ABR levels above 20% could suffer from short- and long-term cracking potential. Asphalt concrete with high ABR content can be at an already critically aged condition right after production and, in addition to that, aging progresses much faster in the binders of such mixes.

On the basis of the experimental results and calculated parameters, the following conclusions can be drawn:

- As the ABR level increased, both the high- and low-temperature grades increased. Both the high and low-temperature grades of extracted binder generally increased one or two grades higher than its corresponding binder when ABR content was below 30%. In the case of the highest ABR level (60%), the high-temperature grade increased by six grades (from 52 to 88) and the low-temperature grade increased by four (from –34 to –10).
- Additional PAV for original and extracted binders changed almost all of the rheological characteristics significantly.
- Complex modulus values across a wide range of temperatures and frequencies clearly increased with higher aging level and ABR content, regardless of the base binder properties.
- The ΔT_c parameter increased with additional aging and increasing ABR levels. The proposed threshold of –5°C was exceeded by a great margin when PAV was applied to the extracted binder recovered from AC with ABR above 20%. The values were in the range of –8°C to –21°C.
- Similarly, the effects of aging and ABR levels were observed in the Glover-Rowe parameter, especially after the additional PAV. All the base binders reached the critical threshold of 180 kPa only after the second PAV. The extracted binder from AC with 60% ABR had values exceeding the critical thresholds even before aging. The designed AC (except 60% ABR) contained RAS only and no RAP. The effect of ABR with RAP could be expected to differ from that of the AC with RAS only—resulting in more moderate changes in the progression of brittleness for AC with RAP only.
- The crossover frequency decreased, and the R-value increased with aging level and increasing ABR for all the evaluated binders.
- It was shown with the equivalency analysis that increased aging and ABR levels had similar effects on the low- and intermediate-temperature cracking susceptibility evaluated using the ΔT_c and Glover-Rowe parameters. The analysis demonstrated that binders in AC with ABR levels less than 20% were at an aging level equivalent to their RTFO-aged base binder and after one PAV were nearly equivalent to the PAV condition of their base binder. When the extracted binders with ABR of 20% or more were tested as-is, their brittleness parameter values were higher than their PAV-aged base binder, and after aging with PAV, they well exceeded the values of the second-PAV-aged base binders.

- Results indicate that AC prepared with high levels of ABR and only RAS could have short- and long-term cracking potential because aging progresses much faster, and their performance lifetime starts at an already critically aged condition.

CHAPTER 5: CHEMICAL AND COMPOSITIONAL CHARACTERIZATION

5.1 FTIR ANALYSIS

The FTIR results showed that the virgin binders have a carbonyl index value between 0.01 and 0.05and a sulfoxide index value between 0.05 and 0.09. Similarly, aged samples using PAV and RTFO were also analyzed using the FTIR technique (Figure 5.1). The result showed that the oxidation of binders increased with aging. The virgin binders had a negligible amount of oxygen content, while the binders aged with the long-term aging method (PAV) had the highest oxygen content. The ICO value increased up to 0.06 by RTFO aging and 0.09 by the PAV aging technique. The result showed that the ICO index increased relatively in samples aged using the PAV method compared with RTFO methods. Double-PAV aging produced the highest carbonyl and sulfoxide content. There was a prominent increase in ICO and ISO in most of the samples as the aging went from PAV to double PAV. Similar trends were observed in the ISO index. These results indicated that samples with PAV aging were oxidized more than samples aged with RTFO methods. However, the content of sulfoxide depends on the initial sulfur content in the sample. Extra-long aging (2PAV) caused a large increase in both ICO and ISO values.

Similarly, the oxidation of RAS, RAP, and the N90 series was also studied. RAP and RAS had higher ICO values, between 0.10 to 0.12, whereas the N90 series had an ICO between that of RAS1 and virgin binder, as expected. The blends had a higher ISO index than the virgin binders (Figures 5.1 and 5.2). Both indices increased with an increase in ABR content in the sample. PAV-aged samples had higher carbonyl and sulfoxide values compared with their corresponding unaged samples. The result was as expected: as the binder is exposed to the changing environment, it ages faster with time due to oxidation.

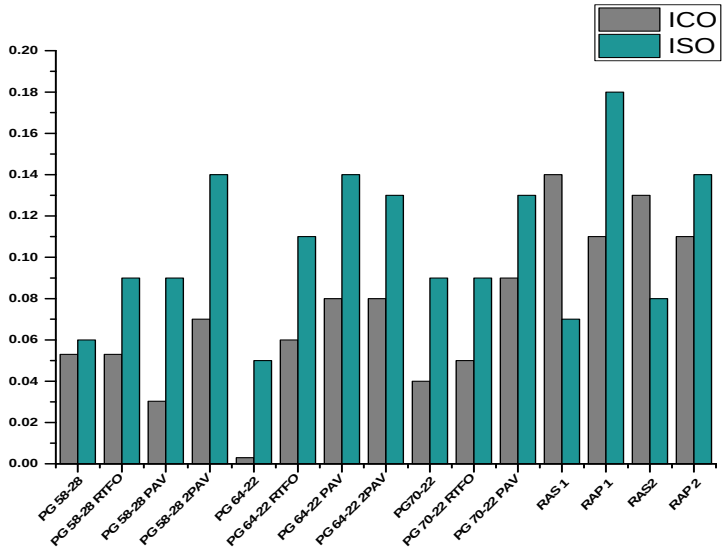

Figure 5.1 Carbonyl and sulfoxide indices calculated from FTIR spectra of virgin, RTFO- and PAV-aged binders, RAS, and RAP.

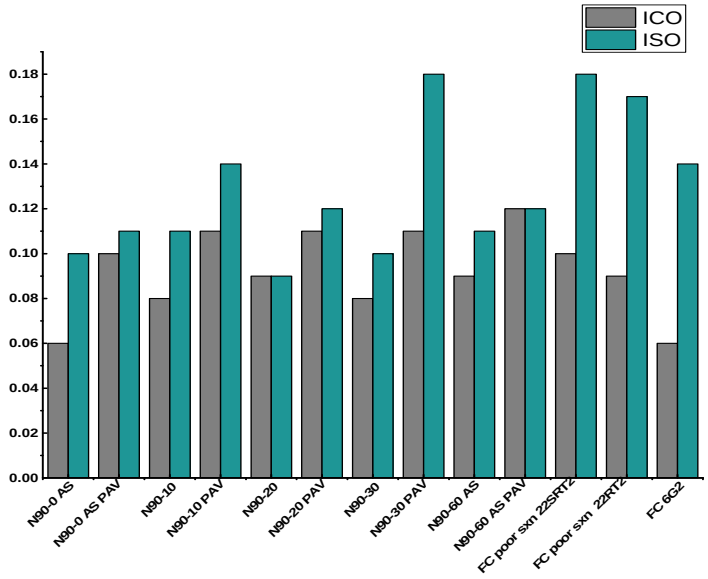

Figure 5.2 Carbonyl and sulfoxide indices calculated from FTIR spectra of binders with various percentages of ABR content, their PAV binders, and field core binders.

5.2 ELEMENTAL ANALYSIS

The elemental composition report was in agreement with the FTIR results. The oxygen/sulfur content of aged samples was higher than that of the virgin samples, as shown in Table 5.1. The oxygen/sulfur content is higher in samples that were aged using long-term aging (i.e., PAV) compared with short-term aging (i.e., RTFO). The oxygen/sulfur content was highest in all the double-PAV samples. The oxygen/sulfur content was lowest in virgin, RTFO-, and PAV-aged samples compared with reclaimed samples and samples containing ABR. PAV samples with ABR content had higher oxygen content compared to their unaged samples.

Table 5.1. Oxygen and Sulfur Content in Binders

Sample	S+O%	Sample	S+O%
PG 58-28	5.4	N90-0AS	6.8
PG 58-28 RTFO	5.5	N90-0AS PAV	7.2
PG 58-28 PAV	5	N90-10	6.8
PG 58-28 PAV+PAV	6.3	N90-10 PAV	7.2
PG 64-22	4.6	N90-20	7.1
PG 64-22 RTFO	4.9	N90-20 PAV	7.7
PG 64-22 PAV	5.6	N90-30	6.8
PG 64-22 PAV+PAV	6.3	N90-30 PAV	7.2
PG 70-22	5.5	N90-60AS	7.5
PG 70-22 RTFO	4.9	N90-60AS PAV	8.5
PG 70-22 PAV	5		
RAP2	8.6		
RAP1	8.2		
RAS2	4.7		
RAS1	4.1		

5.3 AFM ANALYSIS

Binder microstructure was evaluated using AFM images with an objective of understanding the blending between RAS and RAP binders. The virgin, aged, RAP, RAS, and blends were prepared with the heat-cast method and studied with the AFM technique. The following samples were prepared with the heat-cast method, which was believed to preserve the solid-state morphology better:

- Base binder at virgin, RTFO-, and PAV-aged state
- Binders recovered from N90 mix series
- Binders recovered from RAS and RAP constituents
- Forced blends with RAP and RAS with a base binder

Interpretation of AFM images is commonly done by identifying the multiphase composition. The three distinct phases observed in the AFM images are called catana, periphase, and paraphase (Das et al. 2016). The bee-like structures are called catana phase. Immediately around the catana phase is a dark-colored phase called periphase, which are separated from each other by another phase of a lighter shade called paraphase. There are various theories about which SARA component or binder content these phases correspond to and how it affects performance. Our objective in this study was to study these images to evaluate the effects of blending.

The three aforementioned phases can be observed in Figure 5.3, which presents the results from base binder PG 58-28 at various aging conditions. The characteristic bee-shaped microstructural feature was observed in most of the binders in this study. The size of the bee-shaped microstructure varied from binder to binder. However, the PG 58-28 topography looks very different from its aged binders, as well as from PG 64-22 and PG 70-22, as shown in Figures 5.3 and 5.4. The periphase is missing in the PG 58-28 virgin binder. The periphase became visible and pronounced by aging with the RTFO or PAV method. The topography of higher-grade binders (PG 64-22 and PG 70-22) was similar to RTFO- and PAV-aged PG 58-28. Because periphase became visible with aging, this finding may be attributed to the fact that periphase is commonly associated with resin or asphaltene.

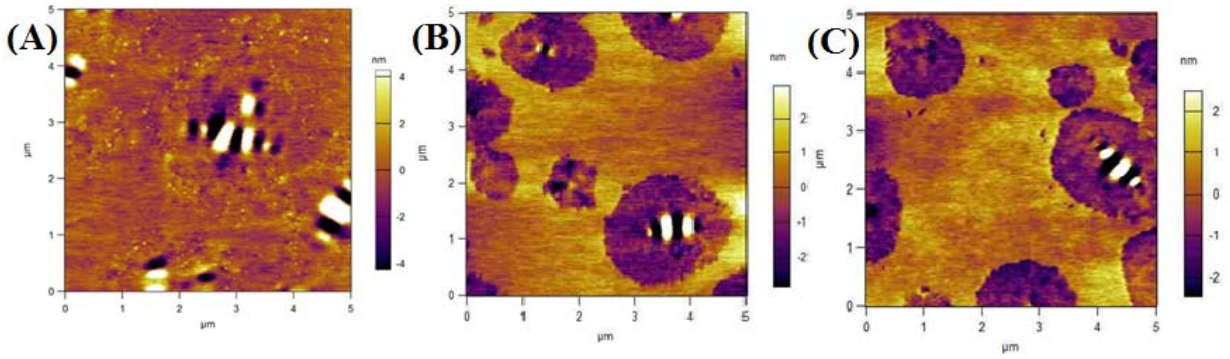

Figure 5.3 AFM images of (a) PG 58-28, (b) RTFO, and (c) PAV.

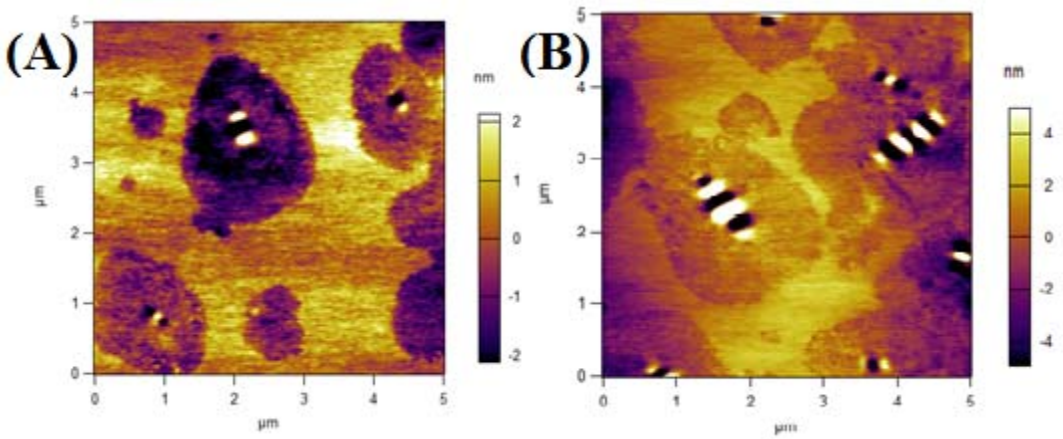

Figure 5.4 AFM images of (a) PG 64-22 and (b) PG 70-22.

Figure 5.5 shows the AFM images of RAS and RAP binder in addition to the forced blends prepared with a base binder. RAP2 shows larger catana phase compared with virgin binders. The periphase covered most of the binders with a very small portion of paraphase. However, no “bees” were found in the RAS2. The topography of RAS2 looks very different from all other binders. This observation is attributed to the fact that the topography of RAS2 was significantly rougher than that of the virgin binders, as shown in Figure 5.5. These changes in topography may be attributed to either the polymer modifier added during the production of shingles or to significant aging during the air-blowing process and/or environmental impact on the material after many years of service.

Figure 5.5 also shows the forced blends. Forced blends were prepared by adding 50% RAS or RAP to PG 58-28. An interesting observation is that the force blend sample obtained from PG 58-28 and RAS or RAP showed the presence of the typical bee-shaped, peri- and paraphases. The topography of the blended binders was found to be between that of the reclaimed binders and virgin ones, which was similar to PAV- and RTFO-aged binders, as shown in Figure 5.5. This indicates that these blended binders appeared as a transition from virgin binder to reclaimed binders. This observation supports the assumption that the microstructural changes, for the most part, resulted from aging.

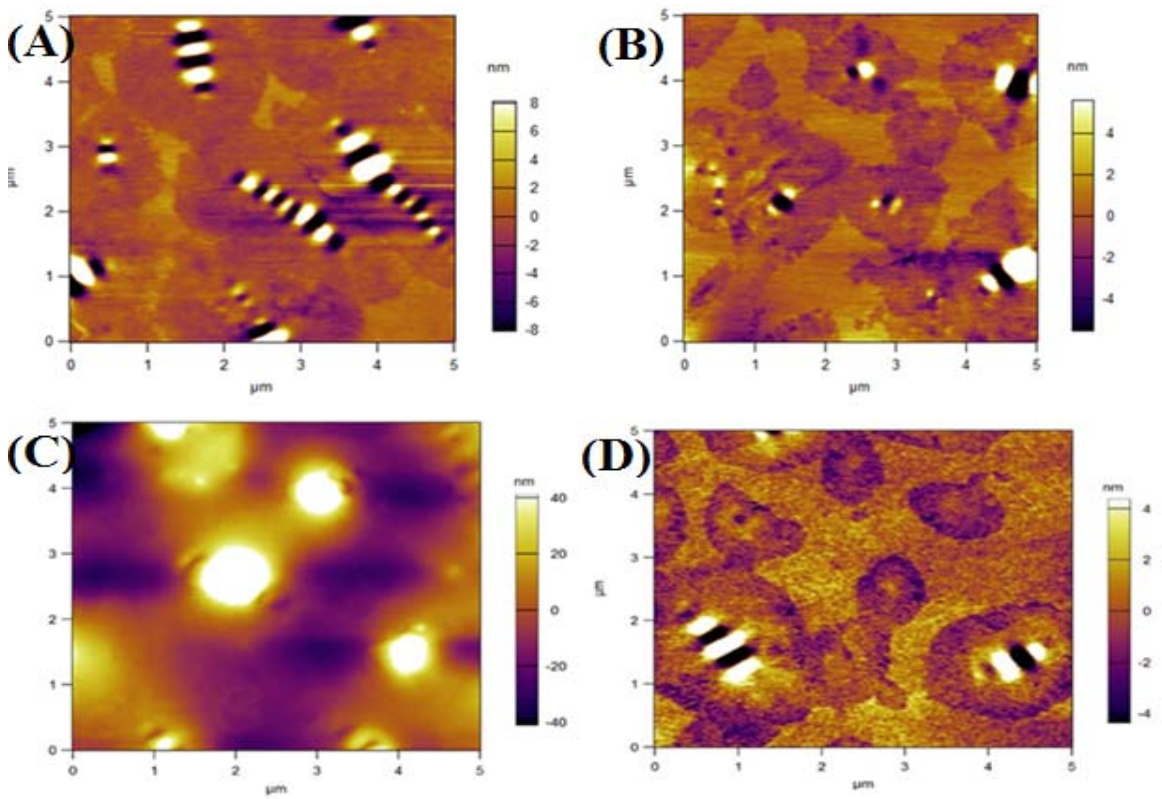

Figure 5.5 AFM images of (a) RAP, (b) blend of RAP and PG 58-28, (c) RAS, and (d) blend of RAS and PG 58-28.

The binders N90-0, N90-10, and N90-0AS had a topography very similar to virgin binders, while images observed for N90-20, N90-30, and N90-60AS differed, having hump-like periphase domains, which were very different from the topography of the virgin binders. These domains were either round or elliptical “humps” dispersed onto the surface of a homogeneous matrix. These hump-like phases were attributed to resin or asphaltenes. However, the bee-like shaped catana phase was very small or absent in these periphases, as shown in Figure 5.6. These observations validate the feasibility of using AFM to differentiate virgin, aged, reclaimed, and blender binder through direct observation in the solid state. The topographic images were repeatable for N90-10, N90-20 and N90-30 binders, which may be attributed to the good distribution of recycled binder after recovery. However, N90-60AS did not show repeatable images, such as shown in Figure 5.7. This might be due to the complexity of the mixture and that the sample with such a high ABR content remained heterogeneous, which means that high ABR content is not compatible enough to make a homogeneous binder. However, it is recommended that this observation be investigated thoroughly in future studies.

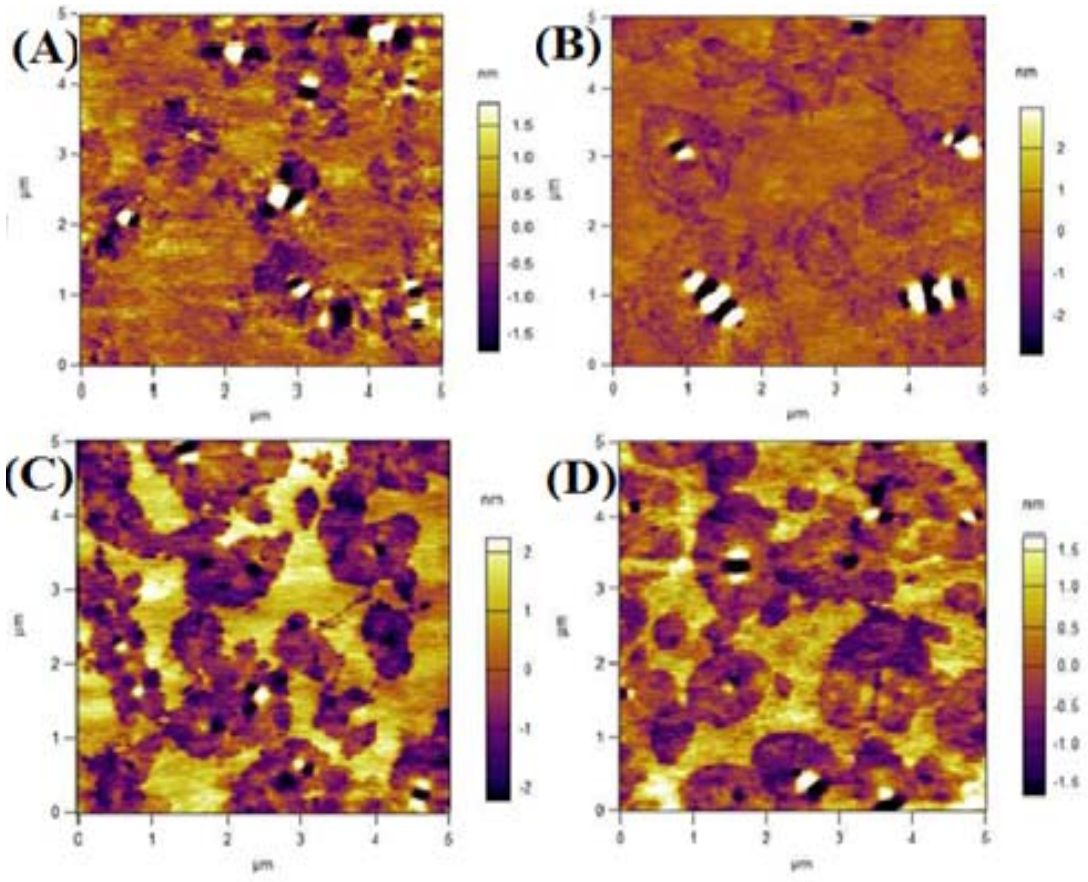

Figure 5.6 AFM images of virgin binder with various percentages of ABR content: (a) N90-0AS, (b) N90-10, (c) N90-20, and (d) N90-30.

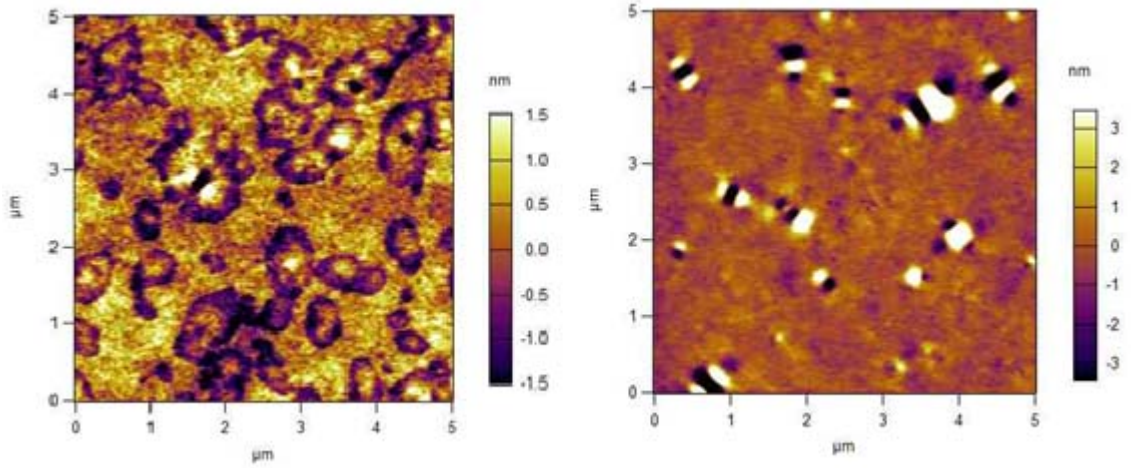

Figure 5.7 AFM images showing heterogeneity of complex blend N90-60AS.

5.4 SARA ANALYSIS

The SARA components and residue percentages were obtained using the TLC-FID technique. The results are presented with saturate, aromatic, resin, asphaltene, and residue percentages (Table 5.2). The SARA component percentages were calculated considering the residue as part of total binder weight. Alternatively, percentages were also presented after separating residue from the total binder weight. In the literature, the residue has not been commonly separated from the SARA components and most likely has been reported with asphaltene percentages. This study was able to separate residue from the SARA components because it may have a different composition.

As shown in Table 5.2, the asphaltene content was lower, as expected, because these virgin samples were not subjected to aging. Mixed results were observed in the earlier N90 series, RAS, RAP, and virgin binders. However, aromatics were higher in the virgin binders and N90-0 series. This result was expected because aromatics undergo a transition to resins and resins are converted to asphaltenes.

The aromatic content was higher in virgin binders and was expected to decrease with aging. As the binders age, resin content increases and aromatic content decrease. The asphaltene content was lower in virgin samples corresponding to its RTFO and PAV samples. The resin content increased by aging using RTFO followed by the PAV method, as shown in Table 5.2.

RAS binders had the highest resins content among all the binders. This result was in agreement with AFM result in which RAS had a completely different topographical image than RAP and any other binders. The N90-series binders had a resin content between that of the virgin and reclaimed binders as expected, as shown in Table 5.3. The resin content increased with an increase in ABR content and due to PAV aging. Even though the resin content increased in aged and reclaimed binders (as shown in Tables 5.2 and 5.3), there was no change in asphaltene content, which was unexpected. This might be due to the presence of a higher amount of insolubles in reclaimed and blended binders. Because of the extensive aging, asphaltene further converted to a higher molecular weight component, which was separated as insoluble before SARA analysis. Therefore, the percentage of insolubles was higher in aged, reclaimed, and blended binders compared with virgin binders.

Table 5.2 SARA Composition in Virgin and Its RTFO, PAV, and Double-PAV Binders, and RAS and RAP

Sample	Saturates	Aromatics	Resins	Asphaltenes	Residue
VIRGIN & AGED					
PG 58-28	7.7	35.2	45.3	11.3	3.6
PG 58-28 RTFO	6.7	38.4	45.4	9.5	4.9
PG 58-28 PAV	6.4	31.6	54.5	7.5	6.7
PG 58-28 PAV+PAV	5.9	29.7	60.5	4.0	6.5
PG 64-22	6.2	45.4	37.3	11.1	5.0
PG 64-22 RTFO	6.0	41.4	40.8	11.7	7.1
PG 64-22 PAV	5.0	39.3	50.4	5.3	7.7
PG 64-22 PAV+PAV	4.8	30.7	60.0	4.6	7.4
PG 70-22	7.2	41.1	48.8	2.9	1.9
PG 70-22 RTFO	3.5	42.4	53.0	1.2	5.8
PG 70-22 PAV	5.4	37.0	50.2	7.5	8.1
RAP & RAS					
RAS2	12.5	22.4	62.9	2.3	15.8
RAS1	8.3	24.0	64.7	3.0	11.7
RAP1	1.10	45.2	50.2	3.5	12.6
RAP2	7.8	38.6	50.1	3.5	29.3

Table 5.3 SARA Composition in Binders with 10%, 20%, 30%, and 60% ABR Content, Corresponding Aged Binders, and Field Core Samples

Samples	Saturates	Aromatics	Resins	Asphaltenes	Residues
MIXTURES					
N90-0AS (L3)	5.4	38.7	44.7	10.4	12.0
N90-0AS PAV	5.3	33.0	55.7	6.1	12.5
N90-10 (L8)	5.6	36.6	55.4	5.7	10.7
N90-10 PAV	6.0	32.0	57.4	4.7	11.1
N90-20	8.5	31.1	54.8	5.6	21.1
N90-20 PAV	11.0	27.4	56.0	5.7	13.7
N90-30 (L6)	6.3	30.3	57.1	6.2	16.9
N90-30 PAV	5.8	23	65.1	5.7	7.3
N90-60AS (L10)	10.4	29.3	54.2	6.1	20.0
N90-60AS PAV	24.9	18.0	54.4	2.8	41.3

5.5 MOLECULAR SIZE ANALYSIS

Molecular size analysis was conducted using the GPC technique. The results were grouped into three different bins with increasing molecular size: smaller molecular size (SMS), medium molecular size (MMS), and larger molecular size (LMS). The results are shown in Table 5.4. The SMS content was higher in virgin binders and was expected to decrease with aging. RTFO and PAV aging increased either the LMS or MMS content in the binders and decreased the SMS. The MMS and LMS did not increase prominently when the binders were RTFO- or single PAV-aged, whereas a pronounced increased in LMS and MMS was observed when binders were aged using the double-PAV method. Double-PAV binder LMS, MMS, and SMS were similar to those of the RAS and RAP, binders as shown in Table 5.4. This increase in MMS and LMS was attributed to the increase in resin content of the binders with aging. Molecular distribution results of the binder complemented the SARA results and showed that resin content increased with aging.

SMS ➡ MMS ➡ LMS

RAS, RAP, and field core binders had the highest LMS and MMS and lowest SMS among all the binders except the double-PAV binders. RAS had higher LMS content than RAP, as shown in Table 5.4. This result was in agreement with the AFM result in which RAS had a completely different topographical image than the RAP and any other binders, and with the SARA results, in which the resin content was highest in RAS. A similar trend of increasing MMS and LMS and decreasing SMS was observed in the N90-series binders with increasing ABR content and due to PAV aging, as shown in Table 5.5.

Table 5.4 Larger, Medium, and Smaller Molecular Size Distribution of Virgin, Aged Binders, RAS and RAP

Sample	LMS	MMS	SMS
VIRGIN & AGED			
PG 58-28	0.52	0.35	0.13
PG 58-28 RTFO	0.49	0.44	0.10
PG 58-28 PAV	0.52	0.38	0.10
PG 58-28 PAV+PAV	0.61	0.32	0.07
PG 64-22	0.44	0.43	0.13
PG 64-22 RTFO	0.42	0.46	0.12
PG 64-22 PAV	0.42	0.50	0.07
PG 64-22 PAV+PAV	0.45	0.53	0.02
PG 70-22	0.29	0.59	0.12
PG 70-22 RTFO	0.35	0.57	0.08
PG 70-22 PAV	0.53	0.41	0.06
RAP & RAS			
RAS2	0.54	0.44	0.02
RAS1	0.52	0.42	0.06
RAP1	0.44	0.54	0.01
RAP2	0.36	0.56	0.08

Table 5.5 Larger, Medium, and Smaller Molecular Size Distribution of Binders with 10%, 20%, 30%, and 60% ABR Content, Their Corresponding Aged Binders, and Field Core Samples

Sample	LMS	MMS	SMS
MIXTURES			
N90-0AS (L11)	0.36	0.53	0.10
N90-0AS PAV	0.48	0.51	0.01
N90-10	0.35	0.55	0.11
N90-10 PAV	0.44	0.49	0.07
N90-20	0.40	0.56	0.04
N90-20 PAV	0.48	0.49	0.03
N90-30	0.40	0.52	0.08
N90-30 PAV	0.44	0.52	0.04
N90-60AS	0.54	0.42	0.04
N90-60AS PAV	0.27	0.69	0.04

5.6 SUMMARY AND REMARKS

This chapter presented a chemical characterization of various binders (virgin, aged to different severities; binders extracted from RAP and RAS and ones with different ABR content) to investigate the effects of aging and increasing ABR levels on structural parameters. Analytical techniques such as FTIR, GPC, TLC-FID, elemental analysis, and AFM were used to study the compositional details and deduce important structural parameters.

Binder aging due to the oxidation of samples resulted in an increase in carbonyl and sulfoxide components and to larger molecular size components such as resins and asphaltenes. As aging of a binder progressed from RTFO to PAV conditions, small changes in chemical composition were observed; while under double-PAV conditions, a pronounced alteration in the chemical composition was observed. The results showed that double-PAV binders have a chemical composition similar to that of reclaimed binders such as RAS and RAP. The chemical compositional properties of ABR-blended binders began to approach those of the RAS and RAP as the ABR content increased in the samples.

On the basis of the experimental results and calculated parameters, the following conclusions can be drawn:

- RAS and RAP binders were found to have the highest resin and residue content.
- Aging increased resin and residue content in the binder.
- Aging increased LMS or MMS fractions in the binder.
- A large decrease in SMS was observed with aging.
- RAS and RAP binders were found to have the lowest SMS and highest LMS and MMS.

- Carbonyl and sulfoxide indices increased with aging.
- RAS and RAP binders were found to have ICO and ISO higher than 0.10.
- Extra aging caused a tremendous change in molecular size, SARA content, ICO, and ISO.
- Extra-aged samples were found to have similar chemical properties as reclaimed and blended samples.

CHAPTER 6: CORRELATION RESULTS

The previous chapters discussed rheological and chemical parameters of the asphalt binder. This chapter focuses on deriving meaningful correlations of the rheological parameters to those of the chemical parameters. The parameters evaluated from rheological characterization used for correlation were Glover-Rowe, crossover frequency, R-value, ΔT_c critical, and rutting parameter, whereas parameters for chemical characterization were SARA (saturates, aromatics, resins, and asphaltenes) components excluding residue, molecular size distribution (large, medium, and small), ICO and ISO indexes, and elements such as sulfur and oxygen.

6.1 INITIAL SCREENING OF CORRELATION PARAMETERS

Each of the rheological parameters was plotted against the parameters obtained from chemical characterization, and preliminary trends were developed as shown in Figure 6.1. The correlated parameters are summarized in Table 6.1. It was also noted that parameters showed different strengths of correlation, ranging from good to poor. In Table 6.1, good correlation is indicated in green, fair in yellow, and poor in red. Only a limited number of parameters were used for further evaluation.

The preliminary correlation showed that the Glover-Rowe parameter has good correlation with small molecular size, ICO and ISO index, and fair correlations with resins, asphaltenes, residue, sulfur, and oxygen contents. The rutting parameter from rheological characterization showed the opposite trends to that of Glover-Rowe parameter, but the strength of correlation was similar to Glover-Rowe. The ΔT_c had fair correlations while the least correlation was shown with the R-value. It is important to note the R-value calculations require accurate measurement of instantaneous (glassy) modulus, which was not in the scope of the experimental plan.

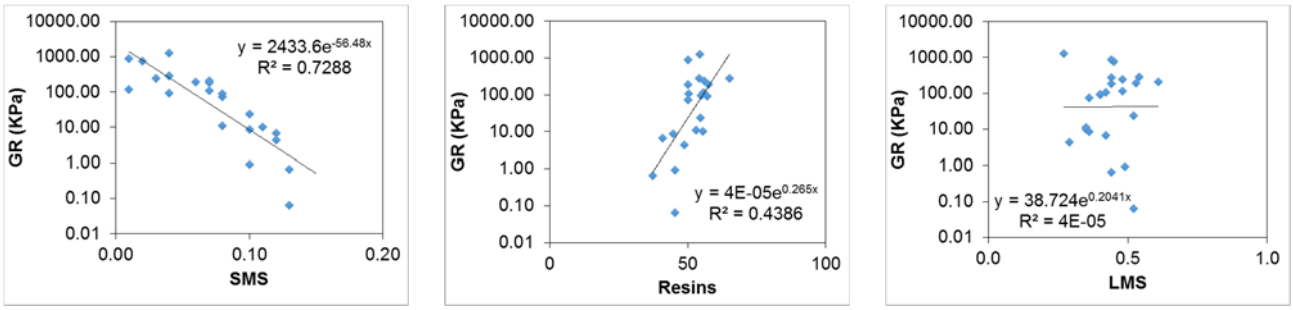

(a) (b) (c)

Figure 6.1 Correlation of rheological parameters to chemical parameters: (a) good, (b) fair, and (c) poor.

Table 6.1 Correlation Trends and Strength for Various Rheological and Chemical Parameters

Chemical Parameters		Rheological Parameters				
		Gr	Wc	R-Value	Delta T	Rutting
TLC FID	Saturates	Direct	No	Direct	Inverse	Direct
		8.6%	0.8%	6.8%	49.3%	9.7%
	Aromatics	Inverse	Direct	Inverse	Direct	Inverse
		24.8%	33.5%	14.1%	47.9%	28.8%
	Resins	Direct	Inverse	Direct	Inverse	Direct
		43.9%	40.8%	33.7%	9.2%	42.2%
	Asphaltenes	Inverse	Direct	Inverse	Direct	Inverse
		38.1%	47.5%	54.0%	26.2%	31.4%
	Residue	Direct	Inverse	Direct	Inverse	Direct
		34.8%	33.6%	10.6%	33.7%	34.2%
GPC	Large Molecular Size (LMS)	No	No	Inverse	No	No
		0.0%	0.3%	3.5%	0.6%	0.3%
	Medium Molecular Size (MMS)	Direct	Inverse	Direct	Inverse	Direct
		11.9%	13.1%	14.0%	9.6%	9.4%
	Smalll Molecular Size (SMS)	Inverse	Direct	Inverse	Direct	Inverse
		72.9%	59.4%	22.8%	27.0%	74.8%
FTIR	ICO	Direct	Inverse	Direct	Inverse	Direct
		60.1%	49.4%	20.5%	33.8%	62.7%
	ISO	Direct	Inverse	Direct	Inverse	Direct
		58.5%	43.3%	16.5%	6.5%	62.5%
Elemental Analysis	Sulfur	Inverse	Direct	Inverse	Direct	Inverse
		8.6%	8.7%	9.7%	6.3%	7.9%
	Oxygen	Direct	Inverse	Direct	Inverse	Direct
		33.9%	44.3%	51.3%	12.2%	23.8%
	Sulfur + Oxygen	Direct	Inverse	Direct	Inverse	Direct
		29.6%	43.3%	41.8%	16.1%	20.3%

6.2 DEVELOPMENT OF THRESHOLDS

Preliminary thresholds were developed for different rheological parameters using the strongly correlated chemical parameters. The thresholds were derived using the results from most severe aging conditions, namely, PAV (binders with recycled materials were excluded). Once the initial thresholds were established, different samples with varying characteristics were included in the matrix to validate the thresholds. Figure 6.2 is a flowchart showing the selection of preliminary thresholds. The following sections present a discussion of the selection of thresholds for different chemical parameters developed for various rheological parameters.

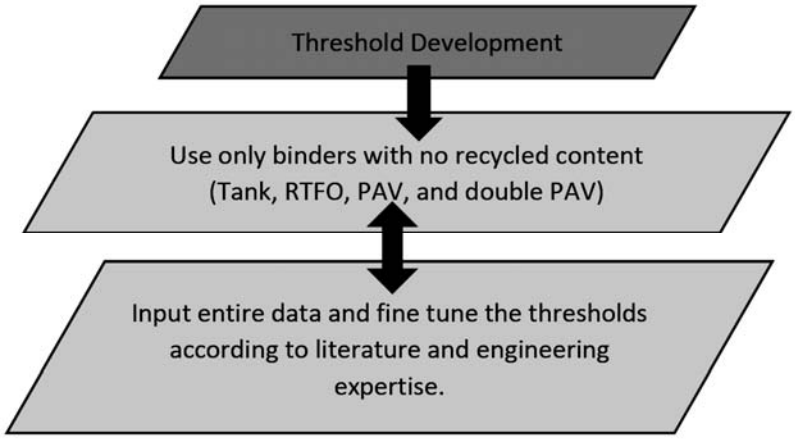

Figure 6.2 Flow diagram for threshold development.

6.2.1 Thresholds for Chemical Parameters Using Rheological Parameters

An illustration of the selection of thresholds is presented in Figure 6.3. Four aging conditions (tank, RTFO, PAV, and aging more severe than PAV) of binders with no recycled materials were used to develop the thresholds, as shown in Figure 6.3(a). According to the correlation and thresholding, it appears that binder with an ICO higher than 0.10 and a Glover-Rowe parameter higher than 200 kPa may be severely aged and brittle.

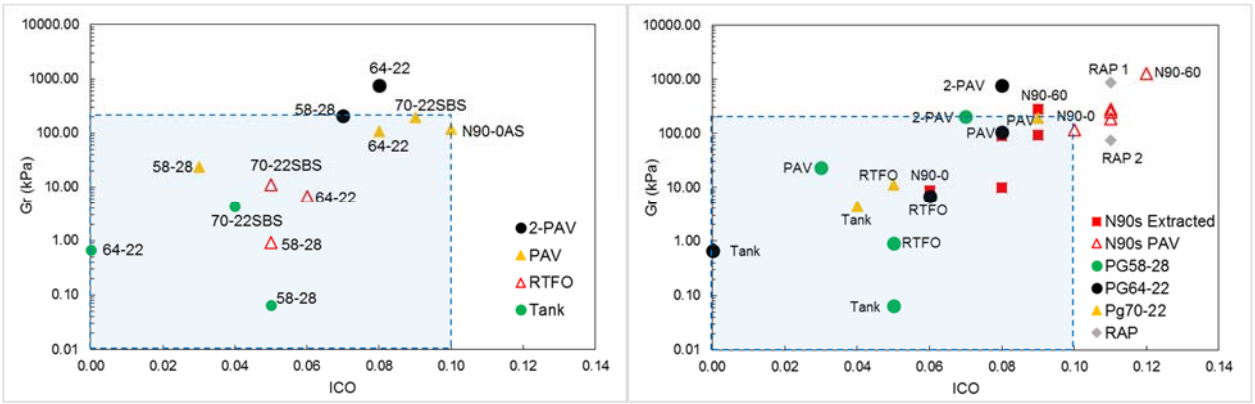

(a) (b)

Figure 6.3 (a) Conceptual presentation of threshold selection, (b) validation of thresholds with entire dataset.

The example shown in Figure 6.3 was used for threshold selection. The value of the Glover-Rowe parameter was selected for representing the limits for different aging conditions and correspondingly for the ICO index as well. The selected thresholds were used to validate the rest of the samples tested

in this study. Figure 6.3 shows all the binder samples plotted with the selected thresholds. A similar exercise was performed for the rest of the parameters evaluated.

6.2.1.1 Glover-Rowe (GR) Parameter

The ICO, ISO, and SMS showed a strong correlation to the Glover-Rowe parameter. The Glover-Rowe parameter represents the extent of cracking: the higher the Glover-Rowe, the higher the cracking potential. The correlation clearly showed that an increase in the Glover-Rowe parameter increased the ICO and ISO index, which represents oxidation potential of the asphalt binder. The preliminary threshold appears to be 0.15 for ISO. In contrast, Glover-Rowe decreased with an increase in SMS, which is a finding similar to what was observed in the literature, indicating that the conversion of small molecular weight size chains to more structured and polar to medium and higher molecular weight chains. When the SMS is less than 0.04, the binder may exhibit excessive aging and brittleness.

A summary of the selected preliminary thresholds is shown in Table 6.2 (see Section 6.2.2 later in this chapter)

Figure 6.3(a) shows the thresholds, while Figure 6.3(b) shows the validation of the thresholds. The results show that the N90 mixes with PAV and 30% ABR or more remained outside the threshold, indicating a higher potential for cracking. Hence, by restricting the ICO index, cracking resistance can be improved. It is also interesting to note that one of the RAP binders (RAP1) remained outside the boundaries, while the RAP2 binder appeared to be within the threshold.

Similar thresholds were developed and validated for the good correlating parameters such as ISO and SMS (Figure 6.4).

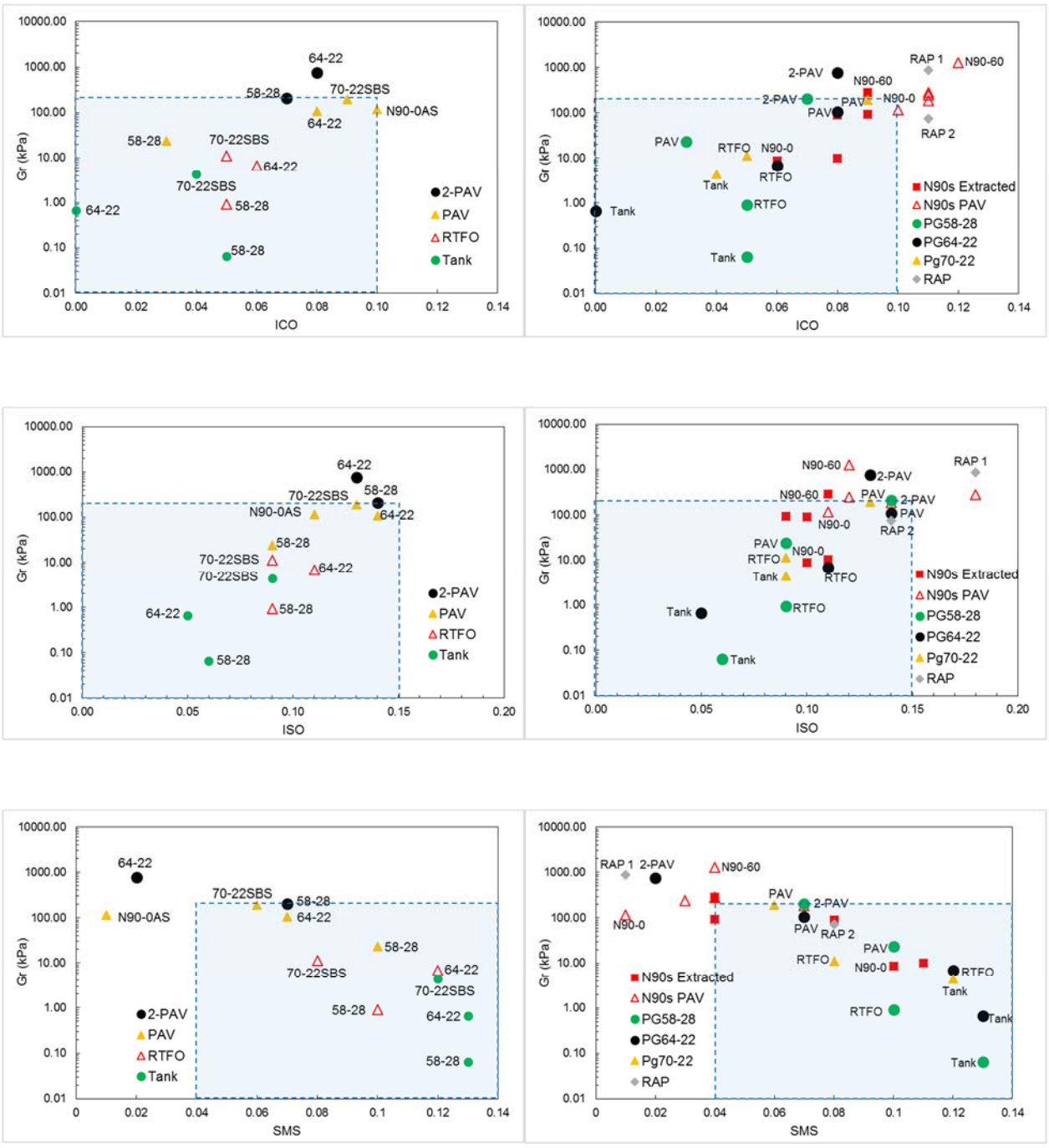

Figure 6.4 Thresholds for ICO, ISO, and SMS for the Glover-Rowe parameter.

Apart from ICO, ISO, and SMS, a few of the SARA components also showed fair correlations to the Glover-Rower parameter. Among them were resins, asphaltenes, and residue. An interesting observation was made in the analysis of SARA components. According to the literature, it is believed that an increase in asphaltenes represents the state of aged asphalt. However, the results from this study showed that an increase in asphaltenes is inversely correlated to the aging of asphalt. It should be noted, however, that residue was separated from asphaltenes in the current study, which may

have caused the results that contradict the literature. Separating asphaltene and residue resulted in a better correlation to the Glover-Rowe parameter. The selected thresholds for correlating parameters are shown in Table 6.2 (see Section 6.2.2 of this chapter). Figure 6.5 shows that deviation from the prescribed SARA components can lead to higher cracking susceptibility. Also, an excess of residue content can be a reason for cracking-related distresses.

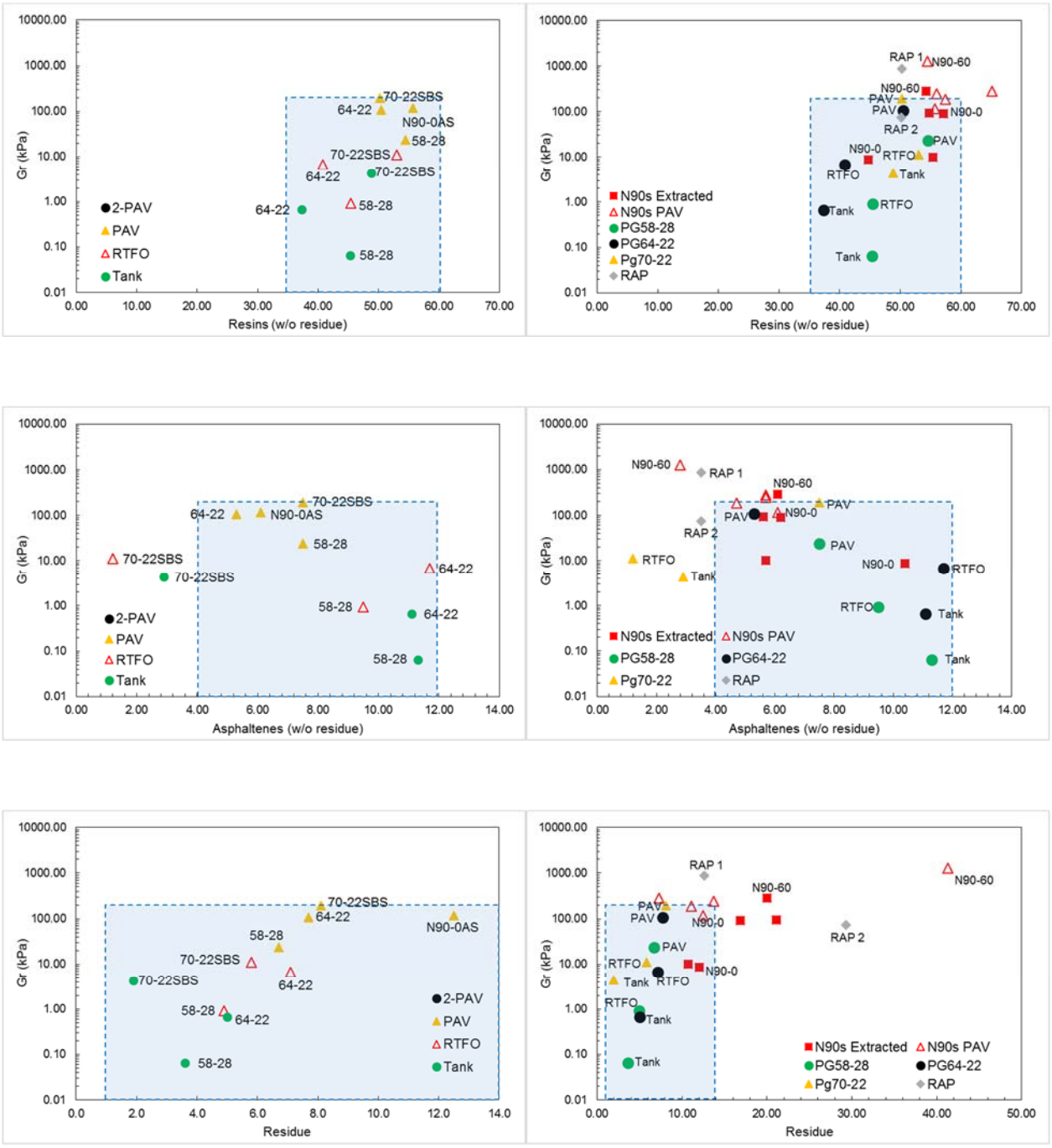

Figure 6.5 Thresholds for resins, asphaltenes, and residue for the Glover-Rowe parameter.

6.2.1.2 Crossover Frequency (w_c)

The crossover frequency is a measure of overall binder hardness, which should generally decrease with binder aging and is usually higher for oxidized binder (Rowe 2014; Ozer et al. 2016). It is obtained by shifting the master curves to a reference temperature of 15°C. The most highly correlated chemical parameters were ICO, ISO, and SMS, which are presented in Figure 6.6. Table 6.2 summarizes the thresholds for w_c parameter.

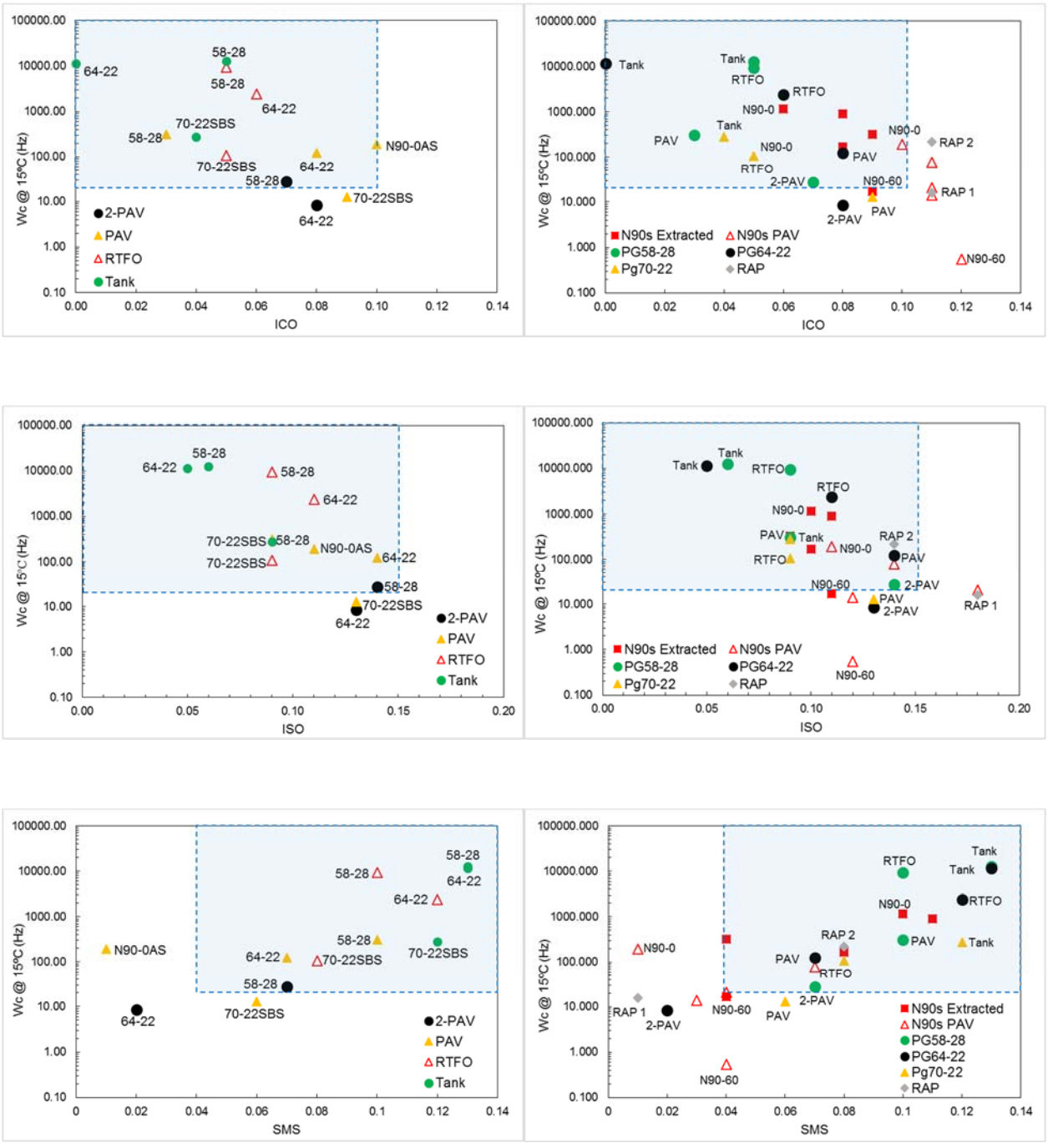

Figure 6.6 Thresholds for ICO, ISO, and SMS for the w_c parameter.

6.2.1.3 Critical Low Temperature (ΔT_c)

$\Delta T_c$is a parameter obtained from the standard BBR test. This parameter has shown good correlation to field data and engineering intuition in identifying brittleness of binders. A value of less than –5°C is considered to indicate susceptibility to cracking or the brittleness threshold for binders. The correlation with chemistry and composition parameters was fair. The samples with high ABR and double-PAV aging clearly followed the ΔT_c parameter. The chemical parameters ICO, ISO, and SMS were used to develop the threshold and are presented in Figure 6.7.

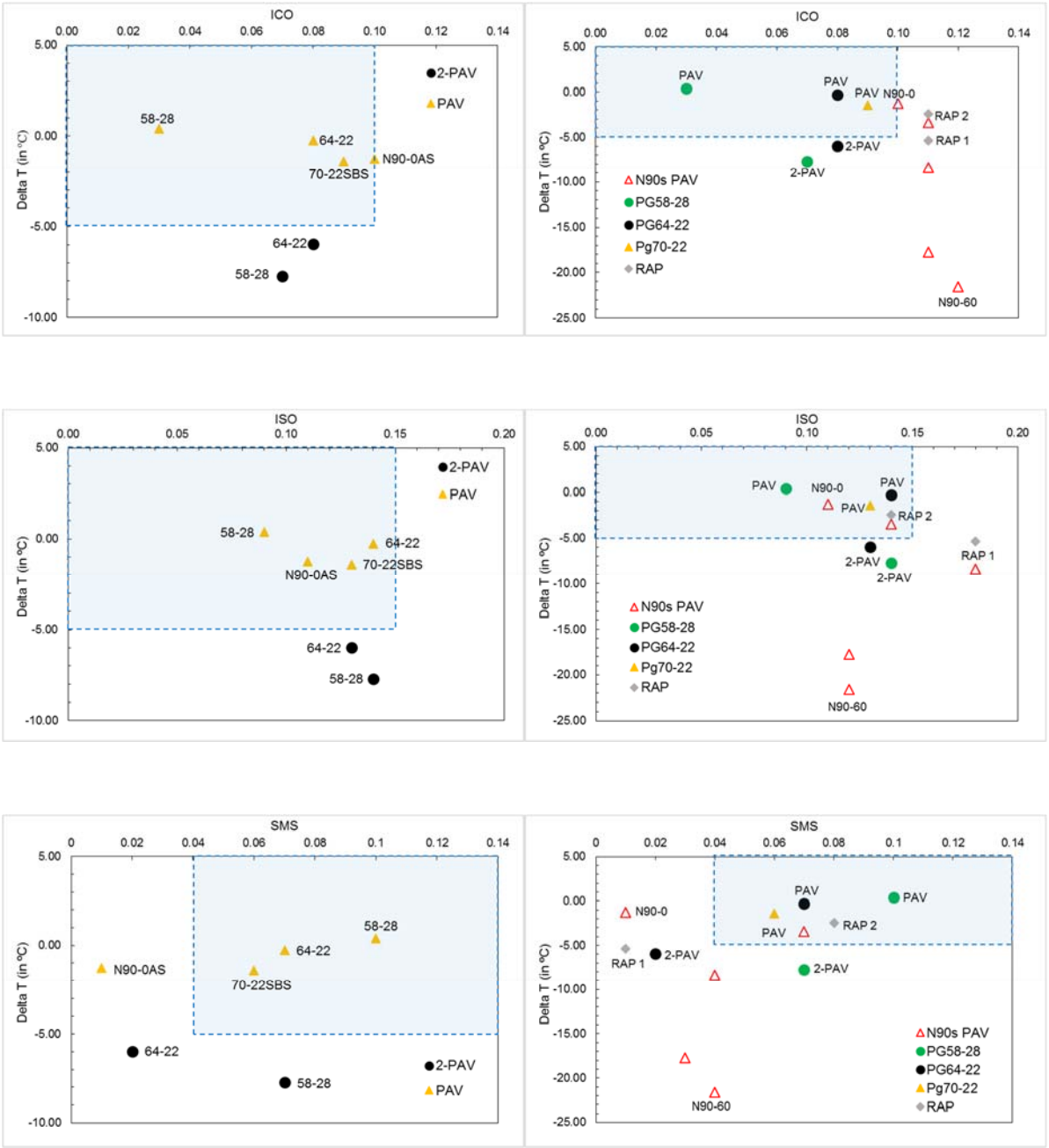

Figure 6.7 Thresholds for ICO, ISO, and SMS for the ΔT_c parameter.

6.2.1.4 Rutting Parameter

A higher value of the rutting parameter indicates higher resistance to rutting. A correlation of the rutting parameter to the chemical parameters ICO, ISO, and SMS was performed to develop the thresholds; the results are presented in Figure 6.8.

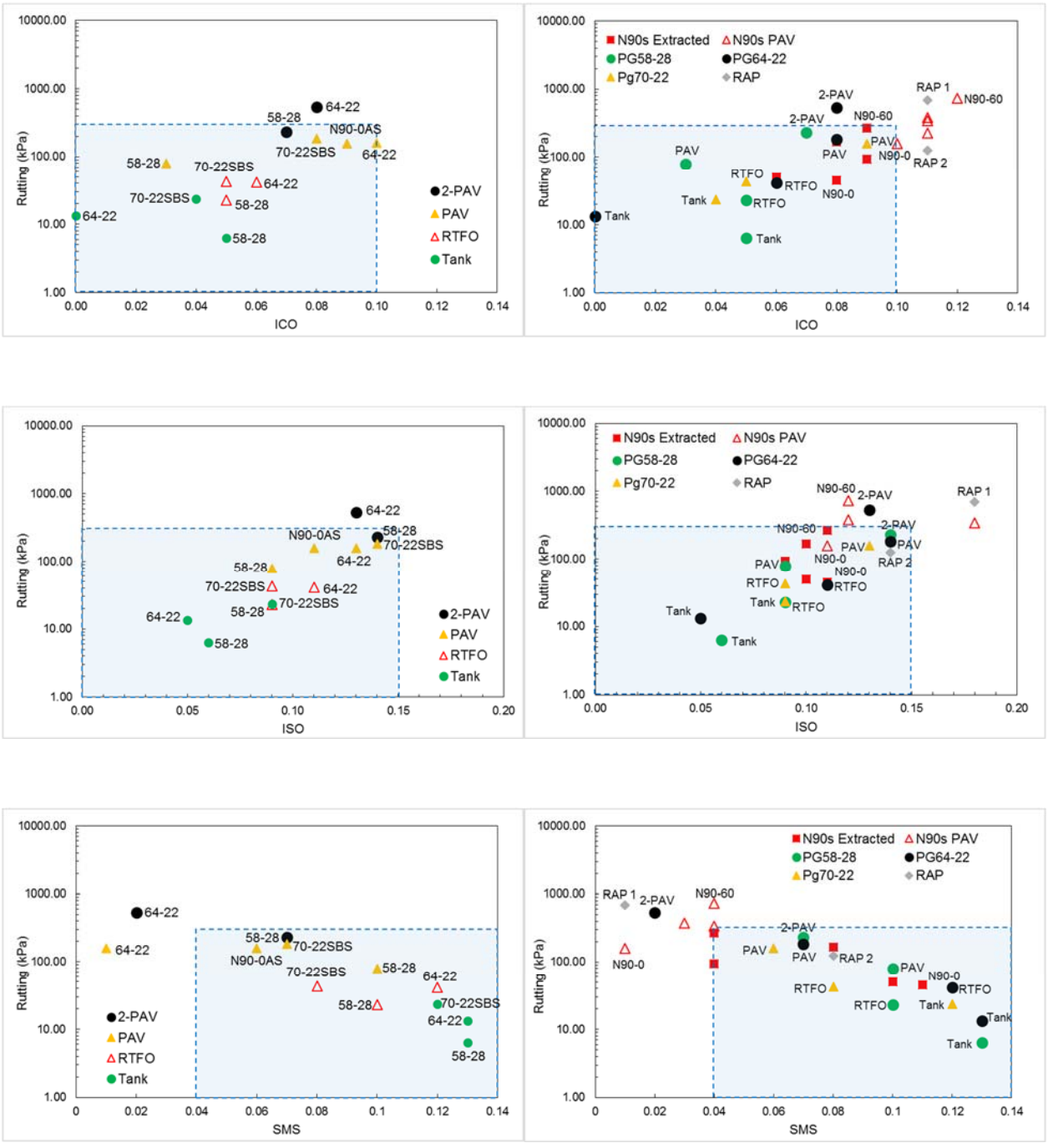

Figure 6.8 Thresholds for ICO, ISO, and SMS for the rutting parameter.

6.2.2 Thresholds Summary

A summary of preliminary thresholds determined by combining rheological parameters with chemistry- and composition-related parameters is shown in Table 6.2.

Table 6.2 Preliminary Thresholds for Rheological and Chemical Parameters

Chemical Parameters	**Rheological Parameters**			
	Glover-Rowe	w_c	Rutting	ΔT_c
Thresholds	**< 200 kPa**	**>20 Hz**	**< 300 kPa**	**> –5°C**
ICO	0–0.10			
ISO	0–0.15			
SMS	0.04–0.14			
Resins	35%–60 %			
Asphaltenes	4%–12 %			
Residue	1%–14%			

6.3 SUMMARY AND REMARKS

This chapter presented a discussion of the efforts to combine and correlate the data obtained from rheological and chemistry/compositional tests as discussed in Chapters 4 and 5. Correlations were evaluated between each parameter from rheological tests and from the chemistry and compositional tests. The procedure consisted of checking and screening each combination for the existence (based on regression) and nature of correlation (inverse or direct). That task was followed by proposing some values that could be used as thresholds to bracket the performance of asphalt binders. An initial check on the threshold was done using the extracted binders from N90 mixes containing various levels of ABR and extra-aged base binder. It was assumed that the extracted binder recovered from the N90 mix with 30% or more ABR would be more brittle and susceptible to cracking. The worst scenario (representing long-term conditions) was the case when the extracted binder was PAV aged.

On the basis of the correlation results, the following conclusions can be drawn:

- In general, the parameters obtained from the FTIR tests (ICO and ISO) had the best correlation to the rheological parameters, followed by SMS obtained from the GPC test and SARA components.
- The Glover-Rowe parameter, crossover frequency (w_c), critical low temperature (ΔT_c), and rutting parameters were found to have a fair or better correlation to ICO, ISO, SMS, and some of the SARA components (resins and asphaltenes).
- The correlation between the Glover-Rowe parameter and the rutting parameter with ICO, ISO, and SMS had the highest regression coefficient.
- The approach and thresholds presented in this chapter are preliminary and need additional data and research for validation and fine-tuning. According to the initial results, the proposed thresholds are in agreement with the expectation and mixture-level performance data obtained from the binders recovered from N90 mixes.

CHAPTER 7: CONCLUSIONS

This report presented the results of an experimental evaluation of the rheological and chemistry/compositional characteristics of binders from various sources: base binders used in designed AC, recovered binders from the AC with increasing ABR, and recovered constituents in the AC (RAP and RAS). The objective of the project was to find chemical and rheological footprints of brittleness in asphalt pavements that may result from the use of stiffer aged binder in RAP and RAS, poor or incomplete blending, or excessive aging in the field.

The key conclusions from this project are presented separately, as follows.

7.1 RHEOLOGY CONCLUSIONS

The experimental program included determination of standard Superpave grading and additional rheological parameters derived from various BBR and DSR tests: ΔT_c (for low-temperature cracking susceptibility), Glover-Rowe parameter, R-value, and crossover frequency (the last three parameters indicate block and fatigue-cracking performance). These parameters can aid in the assessment of the brittleness of binders that would otherwise be masked within the changes in the Superpave grade, unless the changes were highly significant. On the basis of the experimental results and calculated parameters, the following key conclusions can be drawn:

- The Superpave grade reflected changes in the ABR to a certain degree. In general, as the ABR level increased, both the high- and low-temperature grades increased. The range of grade change was between one to two grades for low to medium ABR to as high as four grades (for high ABR).
- Additional PAV for original and extracted binders significantly changed all of the rheological characteristics.
- The additional tests or parameters used in the study (Glover-Rowe, w_c, and ΔT_c) were found to be very useful for identifying brittleness in binders. The results obtained from these parameters were consistent with the literature and engineering intuition in capturing the factors that may affect aging and brittleness.
- It was shown with the equivalency analysis that increased aging and ABR levels had similar effects on the low- and intermediate-temperature cracking susceptibility evaluated by the ΔT_c and Glover-Rowe parameters. According to this analysis, it was concluded that the mixes with an ABR level of 20% (with RAS) could have high cracking potential in both short- and long-term aging conditions. Binders recovered from these mixes were already at an aged state equivalent to (or worse than) the corresponding base binder.
- The results are consistent with mixture-performance data obtained in the ICT R27-128 project using the flexibility index.

7.2 CHEMISTRY AND COMPOSITION CONCLUSIONS

A complete chemical and compositional characterization of a variety of asphalt binders was performed. Materials were chosen from the companion ICT study (R27-128), with a focus on mixture characterization. Therefore, the results obtained in this study will allow a correlation of compositional characteristics with ultimate mixture properties. In addition, the results of this study will assist in the development of a database of binder properties for future referencing.

The key conclusions from the chemical characterization work are as follows:

- Different techniques were used to perform compositional and elemental analysis of binder. Among them, FTIR was found to be a very promising technique to investigate the aging of asphalt binders due to oxidation. There was a clear increment in the carbonyl and sulfoxide indices in aged samples. The N90-0 and N90-60 had sulfoxide and carbonyl indices between those of the virgin and reclaimed binders, as expected. The virgin samples had an ICO < 0.04, and reclaimed samples had an ICO > 0.10. However, the ICO for the blends was between 0.04 and 0.10.
- The elemental analysis showed that with aging, the oxygen content increased in the asphalt binders.
- Both FTIR and elemental analysis techniques are very reliable for studying the aging and chemical composition of asphalt binders.
- Method development is key for SARA analysis using TLC-FID. Our investigation method of SARA components using TLC-FID included separation of residue from asphaltenes. This resulted in repeatable results. However, there are additional methods in the literature that can be investigated for further comparison.
- Double-PAV-aged binders showed signs of excessive aging. The chemical composition of double-PAV-aged binders was similar to that of RAS and RAP.
- The chemical and compositional indicators manifested the effect of aging in the binder.
- The AFM tests alone were not sufficient for making decisions in this study; however, along with other tests and additional information, the AFM test can be very valuable. For the current project, the specific objective of using AFM was to evaluate blending and heterogeneity with increasing RAP and RAS content in the binder.

7.3 GENERAL CONCLUSIONS AND RECOMMENDATIONS

Correlations were sought between rheological properties and chemical and compositional parameters. The objective of correlation was to find meaningful relationships between different methods of characterization and interpret increasing brittleness better by understanding the chemical and compositional makeup of binders. This exercise also allowed us to develop combined preliminary thresholds that can be used to screen binders that may have performance issues caused by excessive aging and brittleness.

The data from rheological and chemistry/compositional tests were used to seek correlations. Correlations were evaluated between each parameter from rheological tests and from chemical/compositional tests. It was assumed that the extracted binder recovered from the N90 mix with 30% or more ABR would be more brittle and susceptible to cracking. The worst scenario (representing long-term conditions) was the case when the extracted binder was PAV aged. The following key conclusions can be drawn in general from this study and the correlations:

- Structural parameters obtained using FTIR tests (ICO and ISO) were found to provide the best correlation to the rheological parameters, followed by SMS obtained using GPC data and SARA components.
- The Glover-Rowe parameter, crossover frequency (w_c), critical low temperature (ΔT_c), and rutting parameters were found to have a fair or better correlation to ICO, ISO, SMS, and some of the SARA components (resins and asphaltenes).
- The correlation between the Glover-Rowe parameter and the rutting parameter with ICO, ISO, and SMS had the highest regression coefficient.

According to the initial results, the proposed thresholds were in agreement with expectations and the mixture-level performance data obtained from the binders recovered from N90 mixes. The approach and thresholds presented in this report are preliminary and require additional data and research for validation and fine-tuning. To strengthen these correlations for eventual implementation by IDOT, additional data must be generated on binders of the same grades but from different sources, and the investigation should focus only on parameters that provide the highest regression values. This additional data would also be used for validation purposes to test these correlations. The ultimate aim is to use these correlations to flag binders with potential problems.

The proposed implementation plan is shown in Figures 7.1 and 7.2. Modified binders would be subjected to RTFO, PAV, and double-PAV conditions, and five rheological parameters would be determined using DSR and BBR (Figure 7.1). If a binder fails at least two of three parameters, then additional rheological analysis would be necessary, such as obtaining a master curve, followed by compositional analysis leading to stage 2 (Figure 7.2). In Stage 2, a detailed analysis would be conducted using various analytical techniques to generate structural parameters. As shown in Figure 7.2, if a binder fails at least two parameters in each category, then the next step would be to determine whether it is a source issue or severely oxidized, in which case the binder can be rejected or required to be reformulated.

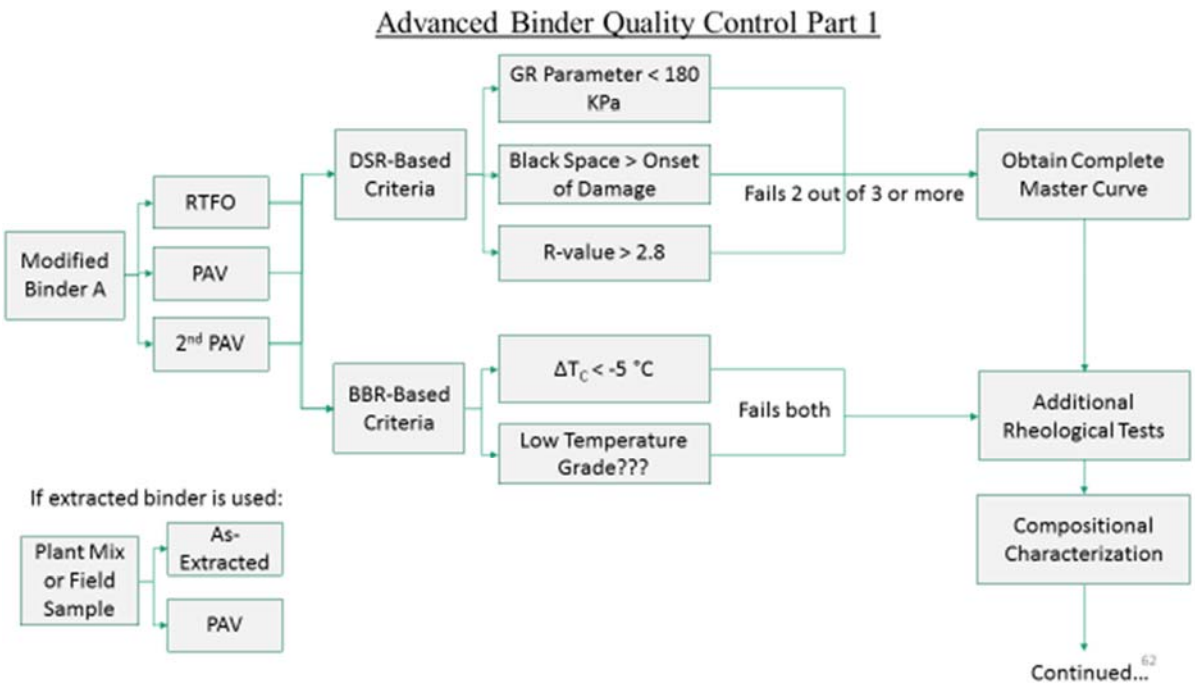

Figure 7.1 Stage 1 of advanced binder quality control.

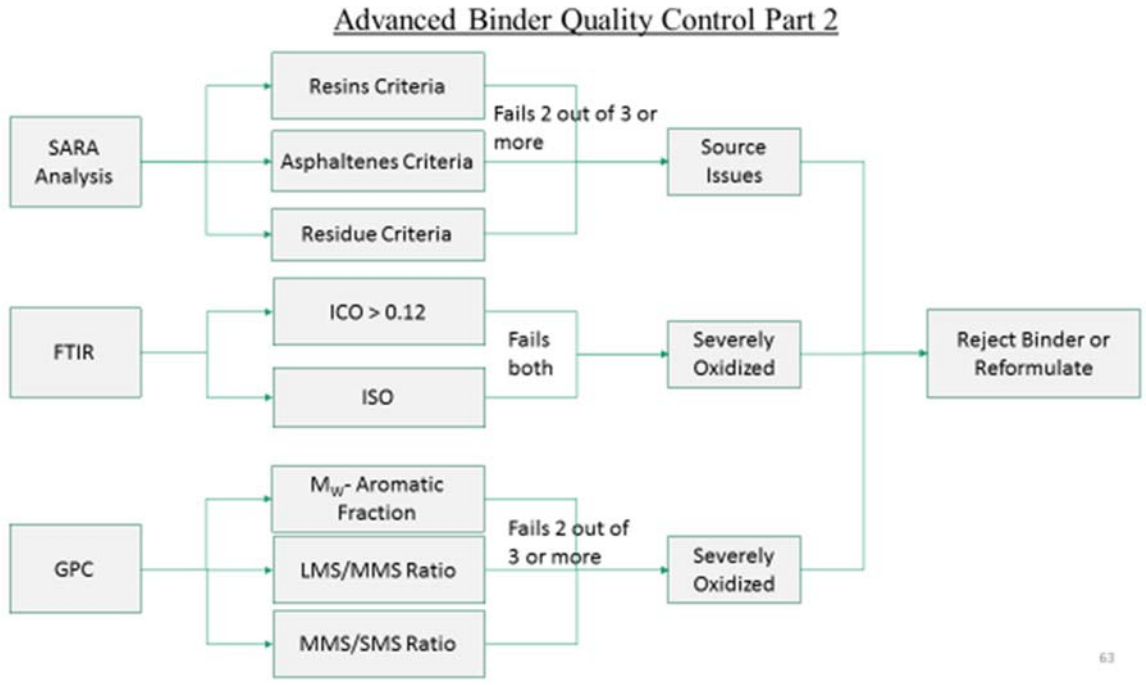

Figure 7.2 Stage 2 of advanced binder quality control.

REFERENCES

Abbas, A.R., U.A. Mannan, and S. Dessouky. 2013. “Effect of recycled asphalt shingles on physical and chemical properties of virgin asphalt binders.” *Construction and Building Materials* 45: 162-172.

Aguiar-Moya, J.P., et al. 2015. “Morphological analysis of bitumen phases using atomic force microscopy.” *Road Materials and Pavement Design* 16(sup1): 138-152.

Allen, R.G., et al. 2014. “The effects of chemical composition on asphalt microstructure and their association to pavement performance.” *International Journal of Pavement Engineering* 15(1): 9-22.

Al-Qadi, I.L., et al. 2015. *Testing Protocols to Ensure Performance of High Asphalt Binder Replacement Mixes Using RAP and RAS*. Rantoul, IL: Illinois Center for Transportation.

Al-Qadi, I.L., Q. Aurangzeb, S.H. Carpenter, W.J. Pine, and J. Trepanier. 2012. *Impact of High RAP Contents on Structural and Performance Properties of Asphalt Mixtures*. Rantoul, IL: Illinois Center for Transportation.

Al-Qadi, I.L., S.H. Carpenter, G. Roberts, H. Ozer, Q. Aurangzeb, M. Elseifi, and J. Trepanier. 2009. *Determination of Usable Residual Asphalt Binder in RAP*. Rantoul, IL: Illinois Center for Transportation.

Anderson, R.M., G.N. King, D.I. Hanson, and P.B. Blankenship. 2011. “Evaluation of the relationship between asphalt binder properties and non-load related cracking.” *Journal of the Association of Asphalt Paving Technologists* 80.

Branthaver, J.F., et al. 1993. *Binder Characterization and Evaluation, Volume 2: Chemistry*. Report No. SHRP-A-368. Washington, DC: Strategic Highway Research Program.

Celauro, C., C. Bernardo, and B. Gabriele. 2010. “Production of innovative, recycled and high-performance asphalt for road pavements.” *Resources, Conservation and Recycling* 54: 337-347.

Chollar, B.H., et al. 1985. “Chemical and physical characterization of binder materials.” *Public Roads* 49(1): 7-12.

Christensen, D., and D. Anderson. 1992. “Interpretation of dynamic mechanical test data for paving grade asphalt.” *Journal of the Association of Asphalt Paving Technologists* 61: 67-116.

Colbert, B., and Z. You. 2012. “The properties of asphalt binder blended with variable quantities of recycled asphalt using short term and long term aging simulations.” *Construction and Building Materials* 26(1): 552-557.

De Moraes, M., et al. 2010. “High temperature AFM study of CAP 30/45 pen grade bitumen.” *Journal of Microscopy* 239(1): 46-53.

Das, P. K., et al. 2016. “Atomic force microscopy to investigate asphalt binders: A state-of-the-art review.” *Road Materials and Pavement Design* 17(3): 693-718.

Gibson, N., X. Qi, A. Shenoy, G. Al-Khateeb, M.E. Kutay, A. Andriescu, and T. Harman. 2012. *Performance Testing for Superpave and Structural Validation*. Report No. FHWA-HRT-11-045. Washington, DC: Federal Highway Administration Research and Technology.

Gong, M., J. Yang, J. Zhang, H. Zhu, and T. Tong. 2016. “Physical-chemical properties of aged asphalt rejuvenated by bio-oil derived from biodiesel residue.” *Construction and Building Materials* 105: 35-45.

Huang, S.-C., et al. 2014. “Ageing characteristics of RAP binder blends—What types of RAP binders are suitable for multiple recycling?” *Road Materials and Pavement Design* 15(sup1): 113-145.

Khosla, N.P., et al. 2012. “Effect of reclaimed asphalt and virgin binder on rheological properties of binder blends.” *International Journal of Pavement Research and Technology* 5(5): 317.

Lippert, D., and M. Brownlee. 2012. *Use of Reclaimed Asphalt Shingles in Illinois*. Springfield, IL: Illinois Department of Transportation, Bureau of Materials and Physical Research.

Liu, G., et al. 2015. “Influence of soft bitumens on the chemical and rheological properties of reclaimed polymer-modified binders from the old surface-layer asphalt.” *Construction and Building Materials* 79: 129-135.

Lu, X., and U. Isacsson. 2002. “Effect of ageing on bitumen chemistry and rheology.” *Construction and Building Materials* 16(1): 15-22.

Mogawer, W.S., A. Austerman, I.L. Al-Qadi, W. Buttlar, H. Ozer, and B. Hill. 2016. “Using binder and mixture space diagrams to evaluate the effect of REOB on binders and mixtures after aging.” In AAPT 91st Annual Meeting Compendium of Papers. Indianapolis, IN: Association of Asphalt Paving Technologists.

Nahar, S.N., et al. 2013. “Temperature and thermal history dependence of the microstructure in bituminous materials.” *European Polymer Journal* 49(8): 1964-1974.

Nahar, S., M. Mohajeri, A. Schmets, A. Scarpas, M. Van De Ven, and G. Schitter. 2013. “First observation of blending-zone morphology at interface of reclaimed asphalt binder and virgin bitumen.” *Transportation Research Record: Journal of the Transportation Research Board* 2370(1): 1-9.

Pauli, A.T., et al. 2011. “Morphology of asphalts, asphalt fractions and model wax-doped asphalts studied by atomic force microscopy.” *International Journal of Pavement Engineering* 12(4): 291-309.

Poulikakos, L.D., S. dos Santos, M. Bueno, S. Kuentzel, M. Hugener, and M.N. Partl. 2014. “Influence of short and long term aging on chemical, microstructural and macro-mechanical properties of recycled asphalt mixtures.” *Construction and Building Materials* 51: 414-423.

Redelius, P., and H. Soenen. 2015. “Relation between bitumen chemistry and performance.” Fuel 140: 34-43.

Robertson, R. E., J. Branthaver, H. Plancher, J. Duvall, E. Ensley, P. Harnsberger, and J. Petersen. 1991. *Chemical Properties of Asphalts and Their Relationship to Pavement Performance*. Washington, DC: Strategic Highway Research Program.

Rowden, L. 2013. *Utilization of Recycled and Reclaimed Materials in Illinois Highway Construction in 2012*. Springfield, IL: Illinois Department of Transportation, Bureau of Materials and Physical Research.

Rowe, G. 2014. “Analysis of SHRP core asphalts—New 2013/14 test results.” Presentation to the Binder Expert Task Group Meeting, San Antonio, TX.

Sa-da-Costa, M., et al. 2010. “Chemical and thermal characterization of road bitumen ageing.” *Materials Science Forum* 636: 273-279.

Schmets, A., et al. 2010. “On the existence of wax-induced phase separation in bitumen.” *International Journal of Pavement Engineering* 11(6): 555-563.

Shen, J., S.N. Amirkhanian, and S.-J. Lee. 2007. “HP-GPC characterization of rejuvenated aged CRM binders.” *Journal of Materials in Civil Engineering* 19(6): 515-522.

Stangl, K., A. Jäger, and R. Lackner. 2006. “Microstructure-based identification of bitumen performance.” *Road Materials and Pavement Design* 7(sup1): 111-142.

Stimilli, A., et al. 2014. “Chemical and rheological analysis of modified bitumens blended with an artificial reclaimed bitumen.” *Construction and Building Materials* 63: 1-10.

Sun, Z., J. Yi, Y. Huang, D. Feng, and C. Guo. 2016. “Properties of asphalt binder modified by bio-oil derived from waste cooking oil.” *Construction and Building Materials* 102: 496-504.

Wang, P., et al. 2015. “Investigating the interactions of the saturate, aromatic, resin, and asphaltene four fractions in asphalt binders by molecular simulations.” *Energy & Fuels* 29(1): 112-121.

Willis, J.R., and P. Turner. 2016*. Characterization of Asphalt Binder Extracted from Reclaimed Asphalt Shingles*. Auburn, AL: National Center for Asphalt Technology.

Xiang, L., J. Cheng, and S. Kang. 2015. “Thermal oxidative aging mechanism of crumb rubber/SBS composite modified asphalt.” *Construction and Building Materials* 75: 169-175.

Yu, X., et al. 2014. “Rheological, microscopic, and chemical characterization of the rejuvenating effect on asphalt binders.” *Fuel* 135: 162-171.

Zhao, S., et al. 2015. “Investigation on the microstructure of recycled asphalt shingle binder and its blending with virgin bitumen.” *Road Materials and Pavement Design* 16(S1): 21-38.

Zhou, F., et al. 2013. “Recycled asphalt shingle binder characterization and blending with virgin binders.” *Transportation Research Record: Journal of the Transportation Research* Board 2370: 33-43.

APPENDIX A: DETAILED LITERATURE REVIEW

A.1 RHEOLOGY

This section summarizes the results of recent studies investigating how pavement performance is affected by the use of reclaimed asphalt pavement (RAP) and recycled asphalt shingles (RAS) at the binder level or mixture level. Generally, most studies have concluded that using RAP or RAS can increase rutting resistance and that the low-temperature grade increases and becomes more sensitive to moisture damage, depending on the type and amount of RAP or RAS.

Most state highway agencies allow contractors to use less than 5% RAS in hot-mix asphalt (HMA; Abbas et al. 2013), and most allow 10% to 20% RAP for medium and heavy traffic for the surface course. A softer binder was suggested for use with RAP mixtures to improve the workability (Al-Qadi et al. 2009).

The purpose of the study by Al-Qadi et al. (2009) was to characterize the mixing efficiency of different percentages of RAP with virgin asphalt binder. Some performance tests showed that the amount of RAP caused an increase in the mixture stiffness of HMA, that brittle HMA might lead to low-temperature cracking, and that HMA with RAP had the potential to reduce stripping, perhaps because of the strong binder–aggregate bonds of RAP. The study recommended that more extensive performance testing be implemented to investigate the rutting, fatigue, and low-temperature performance of mixes containing high percentages of RAP.

In a study by Colbert et al. (2012), the authors evaluated a virgin binder blended with 30%, 50%, 70%, and 100% RAP before aging, rolling thin-film oven (RTFO) aging, and pressure aging vessel (PAV) aging. The study found that the higher viscosity of binder blends with RAP content, and further aging results in a continuous increase in stiffness.

Abbas et al. (2013) concluded that with additional RAS (0%, 5%, 7%, and 10%), the asphalt binder would become stiffer and harder to mix and handle, and they suggested that a softer base binder should be used for RAS-containing mixtures. The results of that study showed an increase in G^* and a decrease in δ at high service temperatures, which indicated a higher rutting resistance with additional RAS (Figures A.1 and A.2). At intermediate temperatures, however, there was no difference in $G^*\sin(\delta)$ with the addition of RAS (Figure A.3), which was inconsistent with previous studies that reported a decrease in the fatigue resistance of mixtures containing RAS. They also concluded that the fatigue parameter $G^*\sin(\delta)$ of Superpave might not be sufficient to characterize the fatigue behavior of asphalt binder at intermediate temperatures.

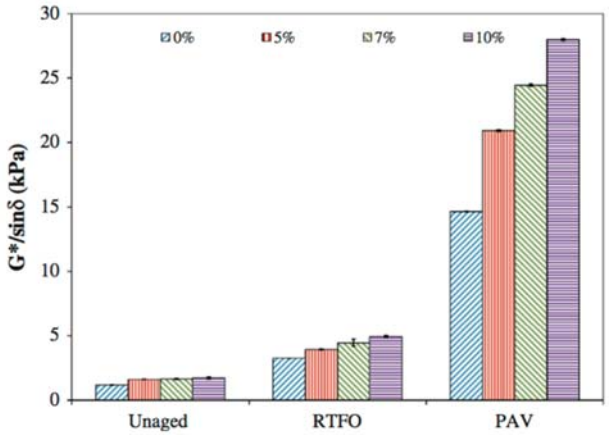

Figure A.1 Effect of the addition of RAS on *G/sin (*δ*) for unaged, RTFO- and PAV-aged binders, measured at 58℃ and 10 rad/s (Abbas et al. 2013).**

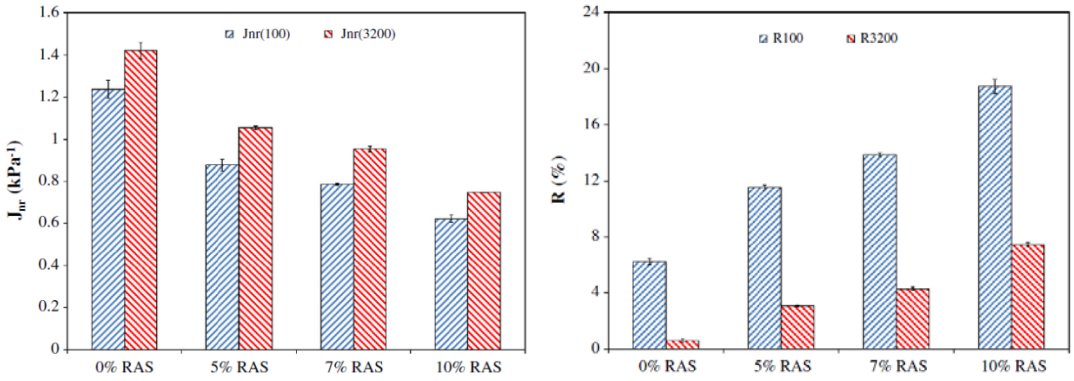

Figure A.2 Effect of RAS on the binder's non-recoverable creep compliance (Jnr) and percent recovery (R), measured using the MCSR test, for RTFO-aged binders at 58°C (Abbas et al. 2013).

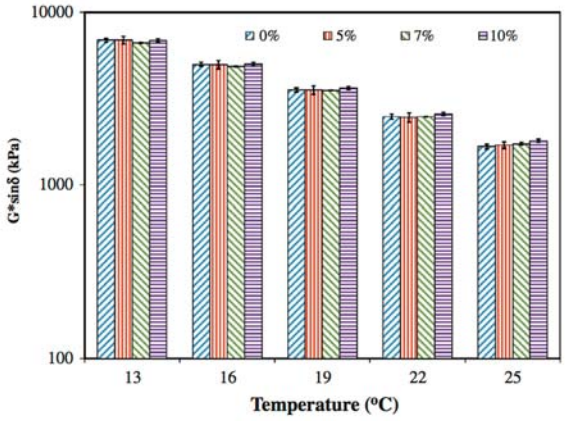

Figure A.3 Fatigue parameter comparison for binders containing different RAS levels (Abbas et al. 2013).

Frequency sweep tests conducted with a dynamic shear rheometer (DSR) can be used to construct a master curve. The master curve is a promising tool for detecting the overall performance of a binder. It can determine the fundamental properties of a binder (complex modulus, phase angle) over a large range of frequencies by conducting tests at different temperatures and then shifting the test data at different temperatures to the same reference temperature. The sample size to use for testing varies, depending on the material hardness and test temperature. Generally, a 25 × 1 mm sample has been used for high-temperature tests (40°C to 90°C), and an 8 × 2 mm sample has been used for low- and intermediate-temperature tests (–5°C to 40°C; Huang et al. 2014).

Huang et al. (2014) tested four binder sources and shifted them to a 20°C reference temperature; the results are shown in Figure A.4. Data were obtained at the region of frequency from 0.1 to 100 rad/s under controlled 1% strain loading conditions with temperatures of –20°C, 0°C, 20°C, 40°C, 60°C, and 80°C. According to the results, the two fresh binders (AAA-1 and AAC-1) showed similar rheological characteristics for either the high- or low-temperature range. The young RAP from Manitoba was much stiffer than the two fresh binders but softer than the old RAP. The old RAP from South Carolina had the highest complex modulus and the lowest phase angle; these behaviors are typical of highly oxidized aged binders. Figure A.5 shows the control binder blended with different percentages of RAP and the master curve shifted to 13°C. The results clearly show that the complex modulus increased with increasing RAP content (Zhou et al. 2013).

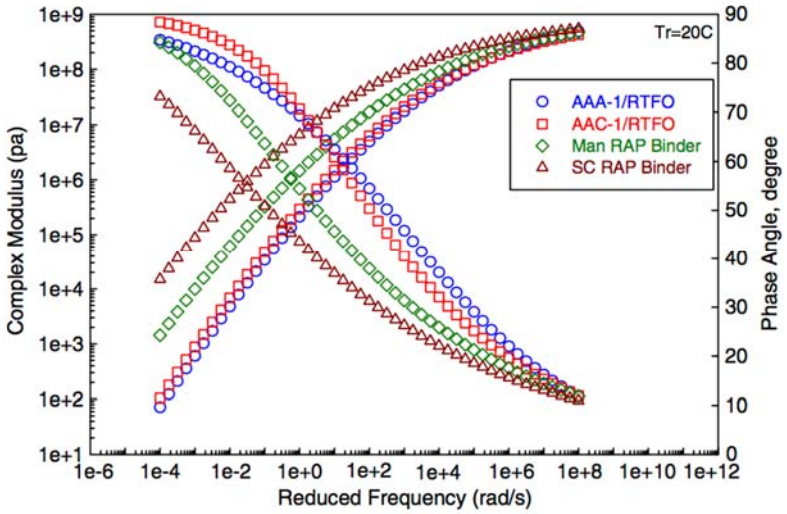

Figure A.4 Complex modulus and phase angle for four materials (Huang et al. 2014): SHRP asphalt AAA-1 and AAC-1, Man RAP (young RAP), and SC RAP (old RAP).

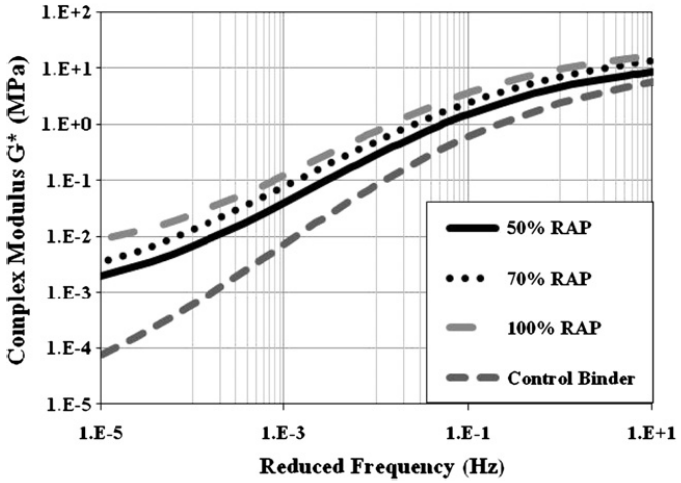

Figure A.5 Master curve shift to 13°C for binders containing varying amounts of RAP (Zhou et al. 2013).

The bending beam rheometer (BBR) test is used to characterize the low-temperature performance of an asphalt binder based on the PAV-aged residue. Two parameters are determined during this test: flexural creep stiffness, which indicates the thermal stress, and m-value, which indicates the ability of the binder to relax stresses and resist thermal cracking (Abbas et al. 2013). Results from BBR testing, shown in Figure A.6, indicate a clear increase in creep stiffness and a decrease in the m-value as RAS content increases. It was concluded that additional RAS will result in worse low-temperature behavior, even if the RAS content is less than 10% (Abbas et al. 2013). Similar results are shown in Figure A.7 for RAP contents from 0% to 100%: stiffness increased and the m-value decreased as RAP content increased (Khosla et al. 2012).

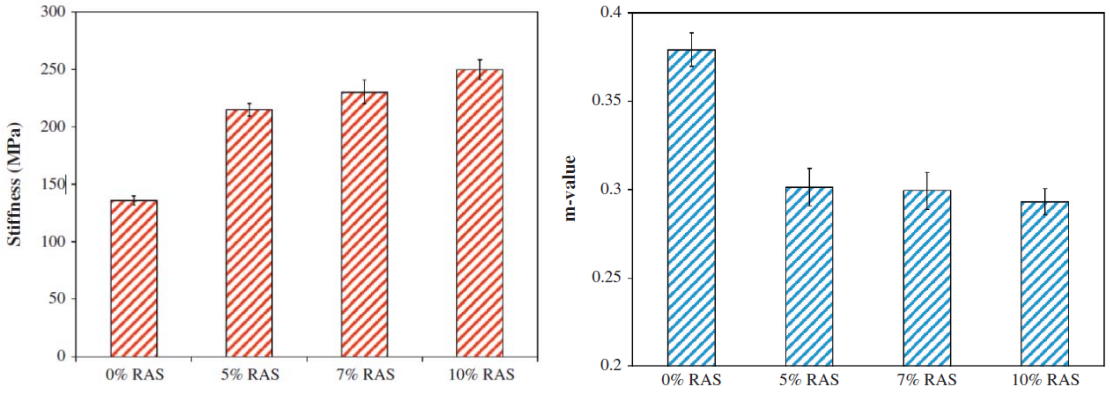

Figure A.6 BBR test results for PAV-aged binders at –18°C (Abbas et al. 2013).

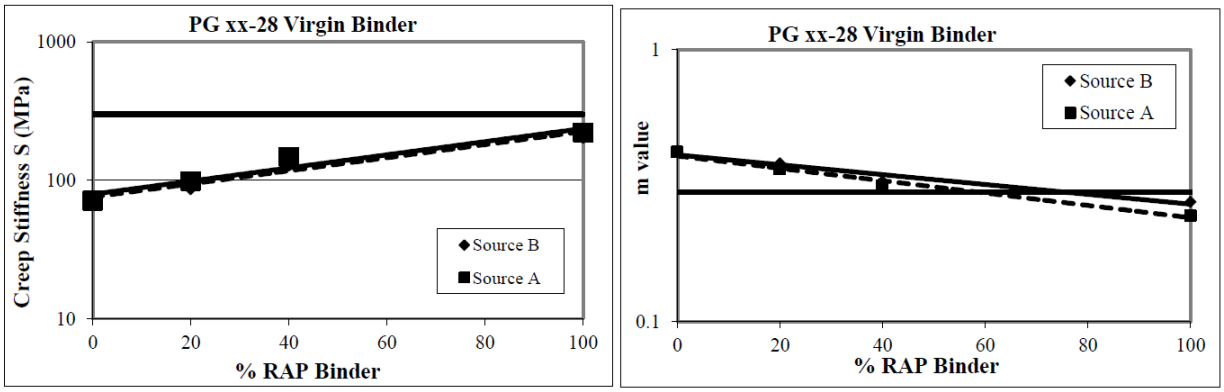

Figure A.7 Creep stiffness and m-value versus RAP content (Khosla et al. 2012).

Figure A.8 plots the both high and low Superpave grades versus RAP content. It shows that blending binder grades varied based on the base binder and types of RAP and that generally, both the high- and low-temperature grades increased with RAP content. Figure A.9 shows the same trends: that both the high-temperature and low-temperature grades increased with RAS content and slightly increased at a RAS content of less than 20% (Zhou et al. 2013).

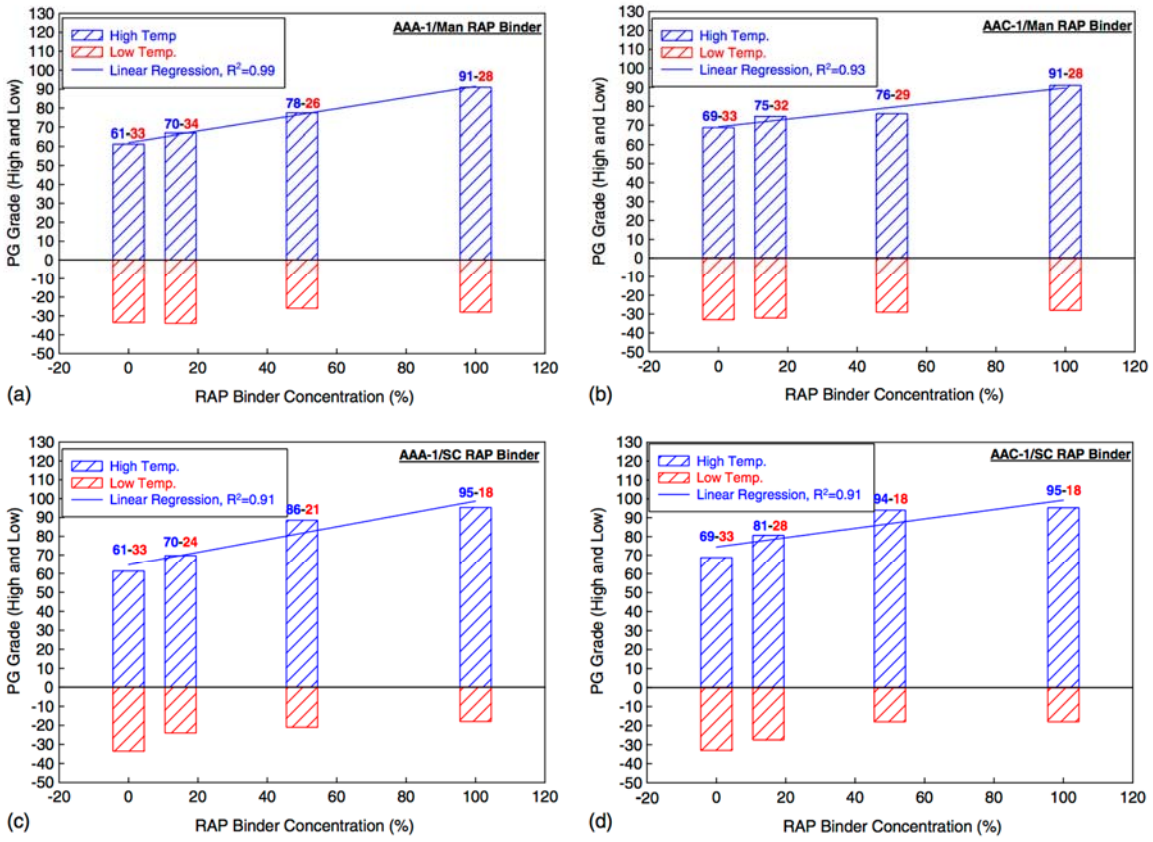

Figure A.8 Superpave asphalt binder performance grading (PG) of different blending results (Huang et al. 2014): SHRP asphalt AAA-1 and AAC-1, Man RAP (young RAP), and SC RAP (old RAP).

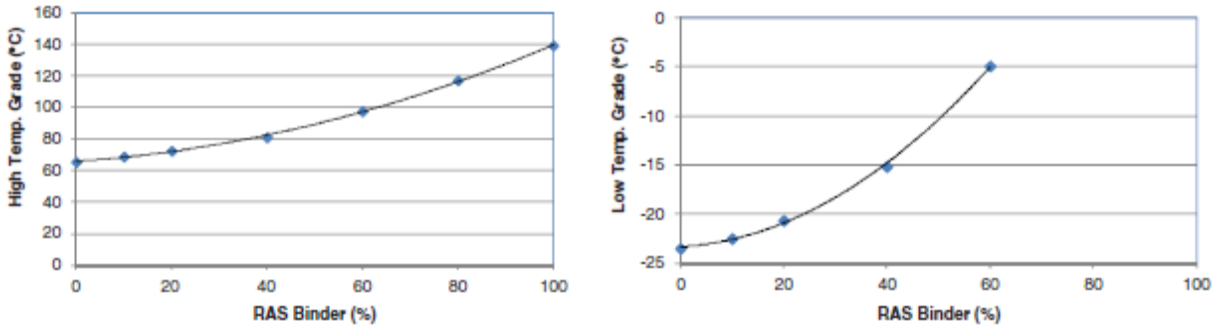

Figure A.9 Binder blending grades (Zhou et al. 2013).

As mentioned previously, some additional parameters were developed to predict the brittleness of the binder. Figure A.10 is an example plot of the Glover-Rowe (GR) parameter. The GR parameter plotted in a black space diagram (where the y-axis is the complex modulus and the x-axis is the phase angle) is a promising way to present the aging condition (Mogawer et al. 2016). Even though this study did not include any ABR binders, highly aged material properties were studied. Indeed, using recycled material in mixes can change the mixes to a pre-aged condition. As shown in Figure A.10, two types of binders (PG 76-22 and PG 64-22) were investigated, each with four aging conditions (RTFO, 20 hours PAV, 40 hours PAV, and 60 hours PAV). The two lines in the figure are the two criteria of the GR, and the same trend can be observed for each material as the aging condition is increased: the complex modulus is increased, the phase angle is decreased, and the points are moved to the fail side. This figure shows that the GR parameter combined with the black space diagram may be a good indicator of figure characterization.

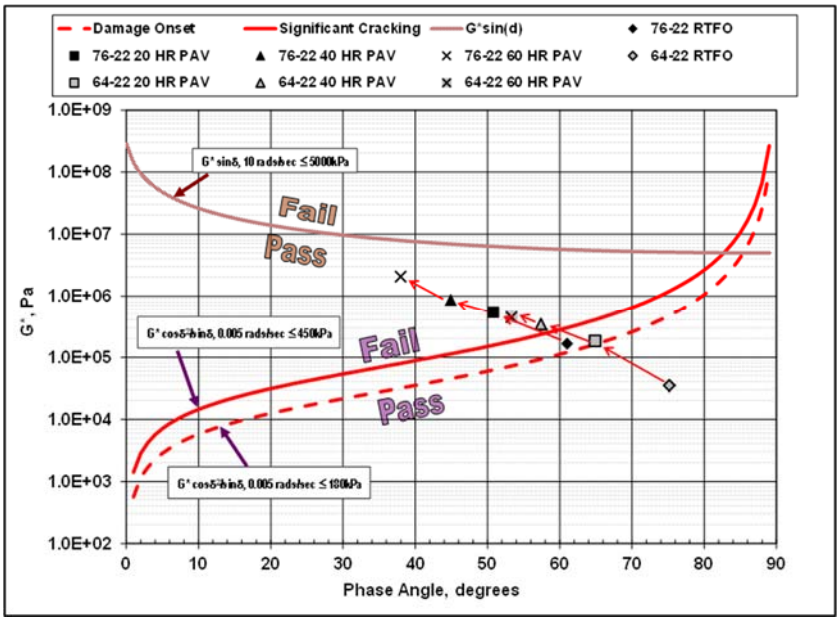

Figure A.10 PAV-aged binders passing through the Glover-Rowe damage zone (Mogawer et al. 2015).

A.2 CHEMISTRY

A.2.1 Fourier Transform Infrared Spectroscopy (FTIR)

FTIR is a technique used to obtain an infrared spectrum of absorption, emission, photoconductivity, or scattering of a material. FTIR is generally used for the following purposes: (1) to identify and quantify chemical groups, and (2) to evaluate the existence of SBS. Two functional groups, the carbonyls (C = O) and sulfoxides (S = O), are the most important indicators needed to evaluate binder aging. An increase in the carbonyls and sulfoxides increases the viscosity and hardens the binder. Liu et al. (2015) used three indices, ICO, ISO, and ISBS, for a qualitative study on the influence of recycling. The carbonyl peak appears at approximately 1700 cm^{-1} and the sulfoxides at approximately 1030 cm^{-1}. The existence of SBS in the binder was evaluated based on its two well-known absorbance peaks at 966 and 699 cm^{-1} (Figures A.11 and A.12).

The indices were defined as

$$\mathrm{ICO} = \frac{\text{Area around } 1700\ \mathrm{cm}^{-1}}{\text{Area around } 1460\ \mathrm{cm}^{-1} + \text{Area around } 1375\ \mathrm{cm}^{-1}}, \tag{A.1}$$

$$\mathrm{ISO} = \frac{\text{Area around } 1030\ \mathrm{cm}^{-1}}{\text{Area around } 1460\ \mathrm{cm}^{-1} + \text{Area around } 1375\ \mathrm{cm}^{-1}}, \tag{A.2}$$

$$\mathrm{ISBS} = \frac{\text{Area around } 966\ \mathrm{cm}^{-1} + \text{Area around } 699\ \mathrm{cm}^{-1}}{\text{Area around } 1460\ \mathrm{cm}^{-1} + \text{Area around } 1375\ \mathrm{cm}^{-1}}. \tag{A.3}$$

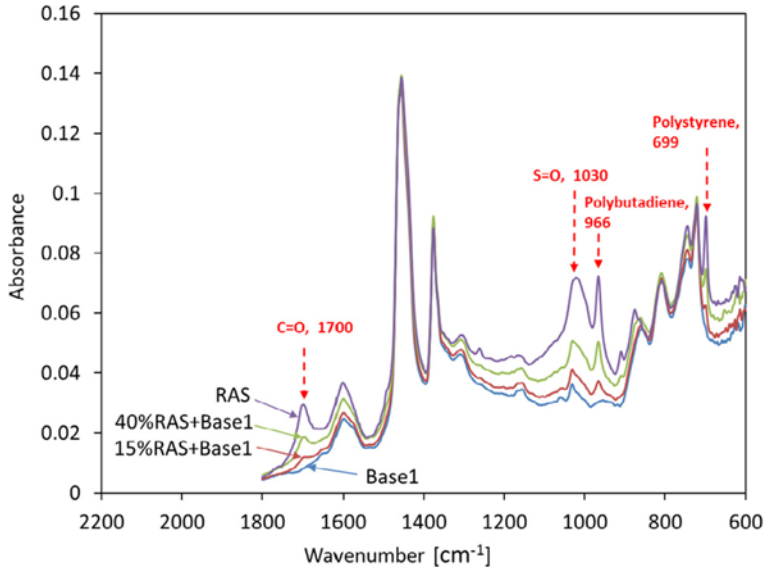

Figure A.11 FTIR curves for the RAS + Base 1 binder group (Liu et al. 2015).

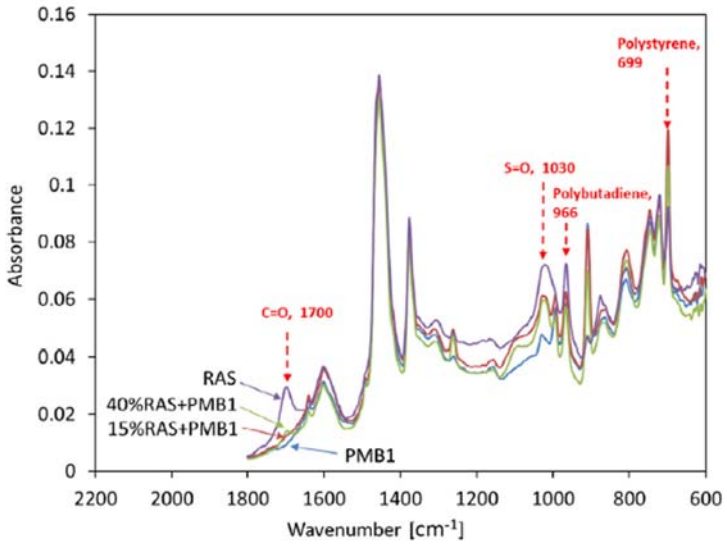

Figure A.12 FTIR curves for the RAS + PMB1 binder group (Liu et al. 2015).

Xiang et al. (2015) evaluated the effect of a change in the ICO and ISO on thermal aging of a matrix asphalt, crumb rubber (CR), a crumb rubber–modified asphalt (CRMA), an SBS-modified asphalt (SBSMA), and CR/SBSCMA. The CR/SBSCMA had excellent anti-aging performance, and the modifiers CR and SBS acted as anti-aging agents (thermal oxidative aging; Xiang et al. 2015).

Costa et al. (2010) monitored binder changes attributable to aging resulting from the formation of carbonyl and sulfoxide (Figure A.13). The results showed that C = O and S = O increased with aging. The application of RTFOT and PAV together caused a considerable increase in the ICO and ISO compared with the original and RTFOT-aged samples.

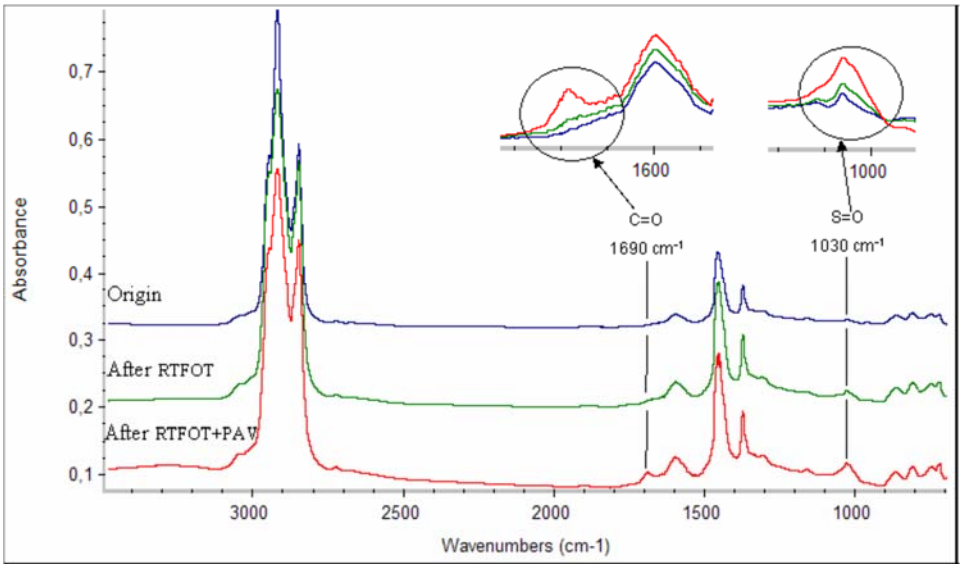

Figure A.13 Infrared spectra of the bitumen before and after aging tests (Costa et al. 2010).

Abbas et al. (2013) dissolved binder samples in chloroform at a 5 wt% concentration, applied the solution to potassium bromide (KBr) crystals to form a uniform thickness, and dried them with nitrogen. The KBr crystals were placed in the FTIR device and scanned at room temperature after the binder had dried. The test results are shown in Figures A.14 and A.15. The results showed that sulfoxide content did not increase with an increase in RAS percentage, whereas carbonyl content increased as the RAS percentage increased.

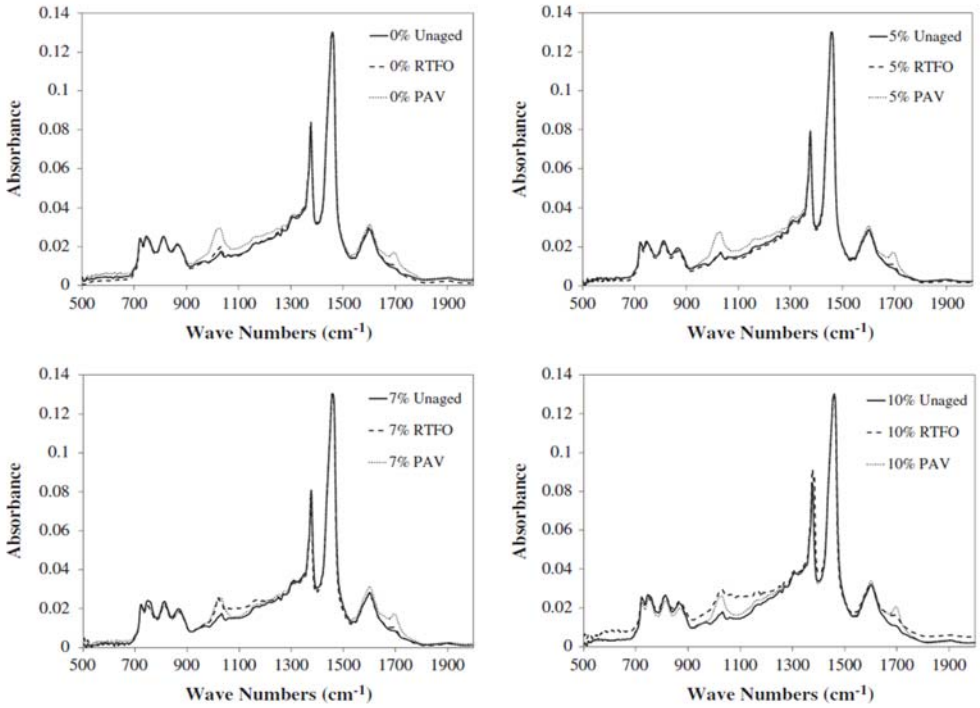

Figure A.14 FTIR spectra for RAS-containing asphalt binders (Abbas et al. 2013).

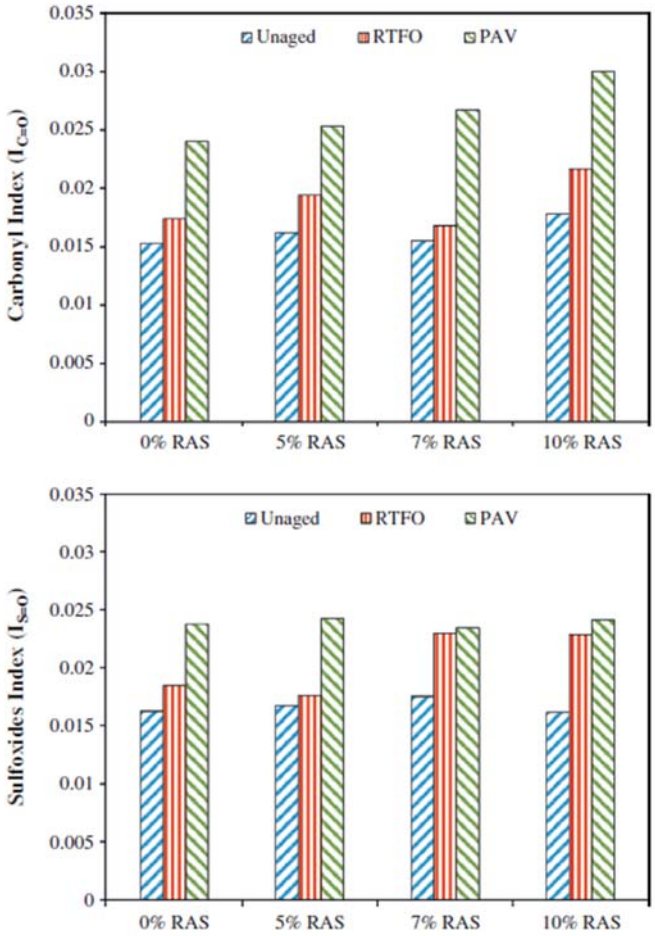

Figure A.15 Carbonyl and sulfoxide indices (ICO and ISO) for RAS-containing asphalt binders (Abbas et al. 2013).

To better evaluate the influence of aging on bituminous material properties, FTIR was applied to assess the amount of polymer in asphalt after the aging process (Stimilli et al. 2014). Figure A.16 shows the FTIR results of bituminous blends. Figure A.17 shows that the SBS polymer percentage varied with an increase in artificial reclaimed asphalt.

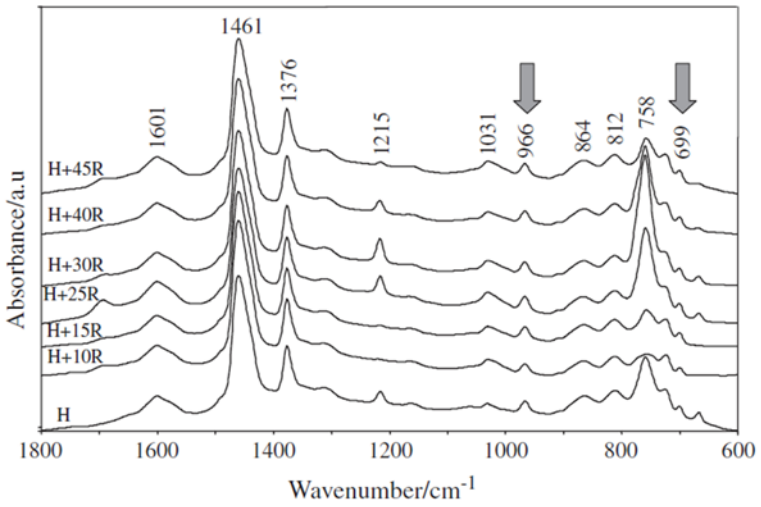

Figure A.16 Infrared spectrum for bituminous blends H + %R (Stimilli et al. 2014).

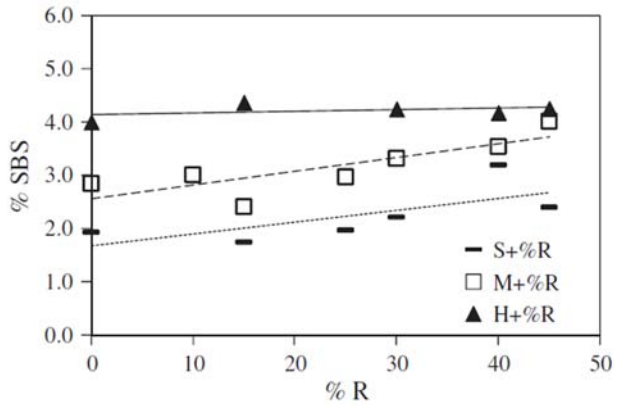

Figure A.17 Variation in SBS percentage with an increase in artificial reclaimed asphalt (Stimilli et al. 2014).

Sun et al. (2016) investigated the blending properties of bio-oil–modified asphalt binders by FTIR. The absence of any new peaks in addition to peaks for the bio-oil and asphalt binders indicated that the bio-oil and control asphalt were physically blended; thus, almost no chemical reactions between them were found. Gong et al. (2016) evaluated a virgin binder, an SBS-modified binder, and their respective aged binders and bio-oil–rejuvenated binders. The results showed an increase in ICO and ISO with aging. The addition of bio-oil did not change the ICO and ISO, which was attributed to larger ICO and ISO for both the bio-oil and aged binders. Decreases in ICO and ISO were observed in rejuvenated SBS-modified asphalt.

Poulikakos et al. (2014) investigated softer and harder virgin binders, aged binders, and virgin binders containing 0% and 40% RAP. The ICO and ISO increased more for binders extracted from the aged mixtures originally containing softer binders compared with mixtures containing harder binders because of the higher oxidation level. Specifically, higher oxidation levels were measured in samples that contained the softer binders with 0% and 40% RAP compared with samples that contained the

harder binders with 0% and 40% RAP. These results might have been due to the viscosity of the binder: as the viscosity increased, the mobility of the molecules in the binder decreased, so did the diffusion of oxygen; consequently, higher amounts of carbonyl and sulfoxide functional groups were produced for the binders with a lower viscosity after undergoing the aging process.

A.2.2 Elemental Analysis

Elemental analysis is a major analytical technique that can give the detailed elemental composition of asphalt binders. The elemental composition varies with aging and addition of RAS or RAP or other ABR materials. As mentioned above, the oxygen content increases with aging because the sample oxidizes. Therefore, elemental analysis can be used to study the aging of asphalt binders.

A.2.3 Thin-Layer Chromatography with Flame Ionization Detection (TLC-FID)—SARA Analysis

TLC-FID is generally used for the analysis of SARA fractions (saturates, aromatics, resins, and asphaltenes) in the asphalt. The SARA fractions vary with aging and from RAS or RAP binder addition to virgin binder.

Costa et al. (2010) studied the changes in molecular polarity in asphalt resulting from the oxidation process by fractionating the SARA fractions using an Iatroscan MK5 instrument. As shown in Table 1, aging induced changes in the cumulative contents of the SARA fractions. The fraction of saturates did not show a significant contribution during the aging process. A decrease in the aromatics content and an increase in the resin and asphaltene contents were shown as results of aging. The asphalt aging process seems to involve the displacement of components from the fraction of aromatics to resins, asphaltenes, or both.

Table A.1 Generic Fractions and Carbonyl and Sulfoxide Indices (ICO and ISO; Costa et al. 2010)

Bitumen	$I_{C=O}$	$I_{S=O}$	Saturates [%]	Aromatics [%]	Resins [%]	Asphaltenes [%]
Origin	-	0.030	1.8	67.1	19.9	11.2
After RTFOT	0.006	0.064	2.3	59.8	22.8	15.1
After RTFOT+PAV	0.040	0.120	2.6	50.5	30.9	16.1

Celauro et al. (2010) performed a SARA analysis of a 70/100 graded highly aromatic asphalt with an Iatroscan MK5 instrument. The colloidal index, I_c, was calculated based on the components of four SARA fractions:

$$I_c = \frac{(asphaltenes+saturates)}{aromatics+resins}. \quad \text{(A.4)}$$

The Iatroscan method was used to determine the SARA composition of asphalt (Stangl et al. 2006). Figure A.18 shows the chromatograms and the borderlines between different components. Table A.2 lists the fractions identified in the Iatroscan analysis. Figure A.19 graphically illustrates the information on B 50/70 from Table A.2.

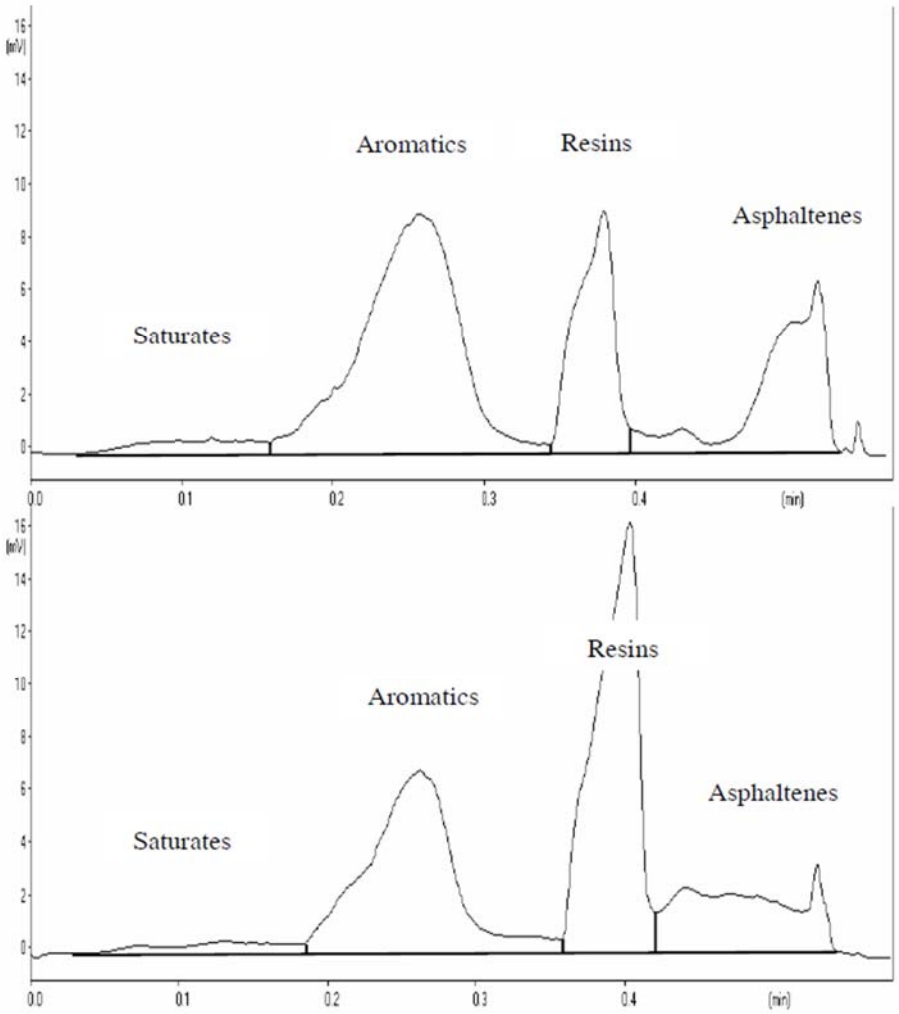

Figure A.18 Typical chromatograms of the original B 50/70 before (top) and after (bottom) RTFOT + PAV aging (Stangl et al. 2006).

Table A.2 Generic Fractions from Iatroscan Analysis of the Considered Asphalts (Stangl et al. 2006)

Bitumen	Generic fractions [%]			
	Saturates	**Aromatics**	**Resins**	**Asphaltenes**
B 50/70 - A	3.6	52.4	22.7	21.3
B 50/70 - B	2.7	44.5	30.5	22.2
B 50/70 - C	2.8	36.3	40.8	20.1
PmB 60/90 - A	4.1	37.5	38.4	20.0
PmB 60/90 - B	3.3	34.0	43.3	19.3
PmB 60/90 - C	4.2	30.3	49.5	16.0

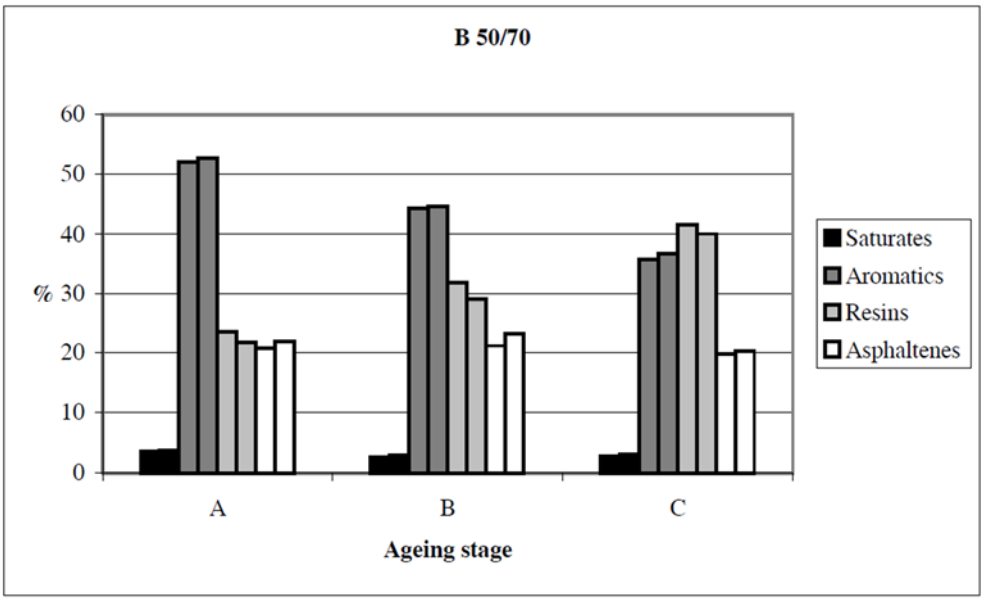

Figure A.19 Mean values of the generic fractions of B 50/70: unaged (A); after RFTOT aging (B); and after RTFOT + PAV aging (C). Left column: mean value for test series 1 (three samples); right column: mean value for test series 2 (three samples; Stangl et al. 2006).

Huang et al. (2014) separated SARA fractions (ASTM D4124-09) by dissolving isooctane-type maltenes in *n*-heptane and injecting the solution into a glass liquid chromatography column filled with approximately CG-20 chromatographic-grade activated alumina. Linear relationships were found between the asphaltene contents and RAP contents (Figure A.20), which indicated that the asphalt content for blend binders could be calculated proportionally from the properties of the virgin binder and RAP binder.

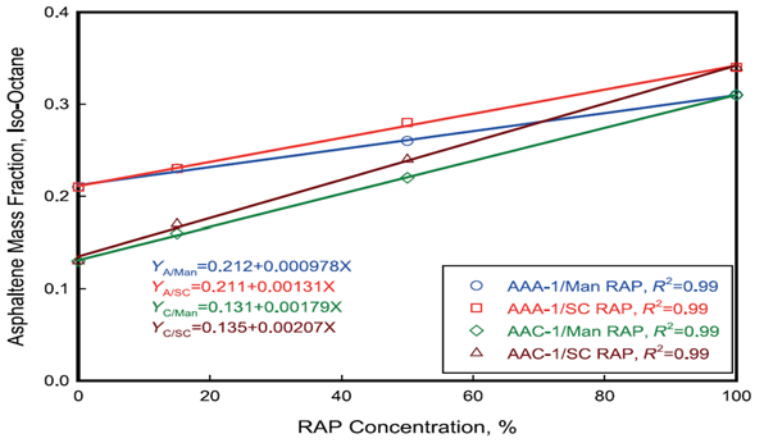

Figure A.20 Asphaltene contents versus RAP binder concentrations for two RTFO-aged asphalts and their RAP blends (Huang et al. 2014).

In the study by Yu et al. (2014), SARA fractionation was conducted based on ASTM standard D4124. Asphaltenes and maltenes were separated using isooctane. Maltene was separated into saturates, aromatics, and resins by injecting the solution into a glass liquid chromatography column with chromatographic-grade activated alumina. Figure A.21 shows the SARA fractions of different binders.

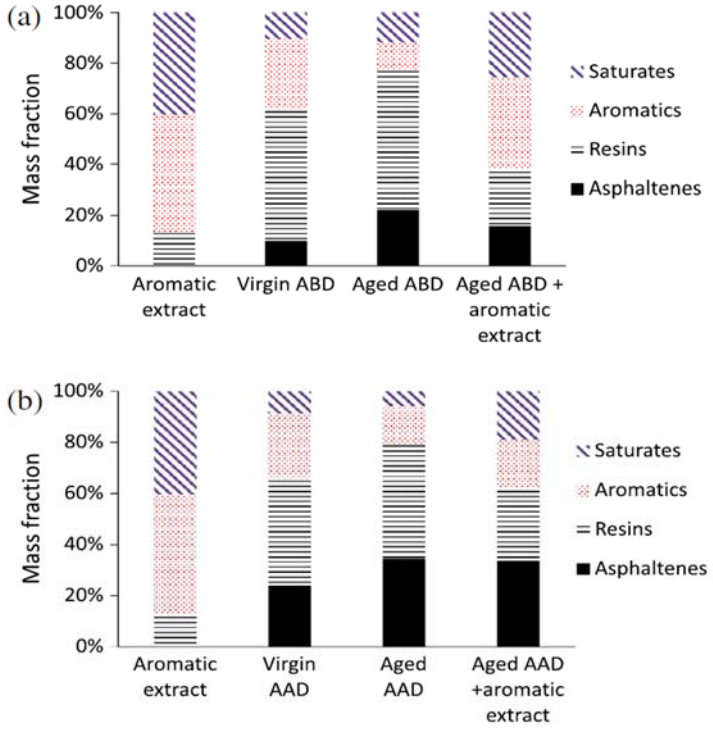

Figure A.21 SARA fractions of aromatic extract and virgin, aged, and aromatic extract-rejuvenated ABD (a) and AAD (b) (Yu et al. 2014).

Gong et al. (2016) evaluated a virgin binder, an SBS-modified binder, and their respective aged binders and bio-oil rejuvenated binders. Similar chromatograms were observed in aged asphalt and bio-oil–rejuvenated asphalt, indicating that no chemical reactions occurred during the rejuvenation. The alignment of the virgin binder was shifted away from the remaining binders, as shown in Figure A.22. This result may indicate that during the aging process, not only does the content of the fraction change but also that the chemical properties of each fraction are altered, which can be attributed to the oxidation reaction and volatilization. The oxidation reaction transformed aromatics into resins, as shown in the Figure A.22, in which the peak area of the resin is smaller in the virgin base binder compared with the aged and rejuvenated binders. Volatilization may increase the average molecular weight of saturates by volatilizing the light oil components. However, the asphaltene peaks aligned well with each other. This result was attributed to little or no change for the asphaltenes from virgin asphalt when exposed to thin-film oven test (TFOT) aging.

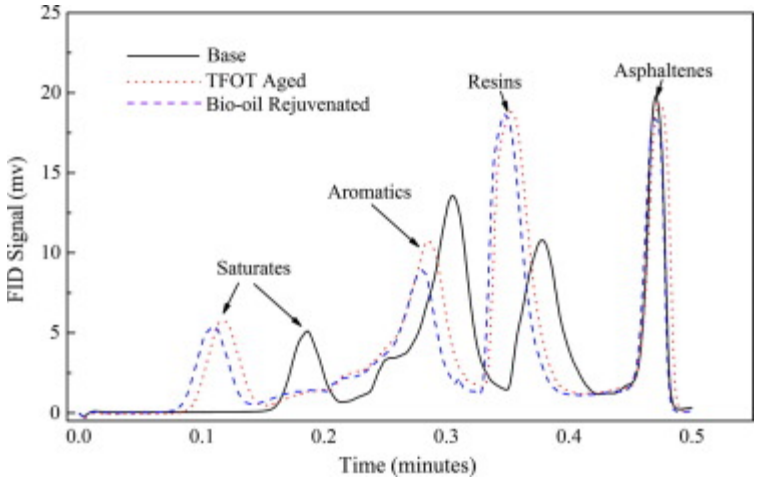

Figure A.22 Shift in alignment of the virgin binder, aged binder, and binder with rejuvenator.

A.2.4 Imaging with Atomic Force Microscopy (AFM)

AFM techniques are used to test the local mechanical response by micromechanical forces created by an atomic force microscope (Zhao et al. 2015). AFM is widely used to image information on structure and topology and to examine the local viscoelasticity, phase separation, and properties such as the adhesion and stiffness of thin materials (Zhao et al. 2015; Allen et al. 2014). The constant force tapping mode of an AFM with a soft cantilever can image and measure the elasticity of materials (Zhao et al. 2015). The tip of the cantilever taps the surface of a sample, and the oscillation amplitude changes with changing relative positions of a solution to the tip. The deflection of the cantilever is measured to calculate the elasticity of a sample (Wang et al. 2015). AFM can be used to identify microstructural differences between virgin and recycled binders. AFM is generally used for the following purposes: (1) to study microstructures, (2) to measure adhesion, (3) to determine physical properties (modulus), and (4) to evaluate blending.

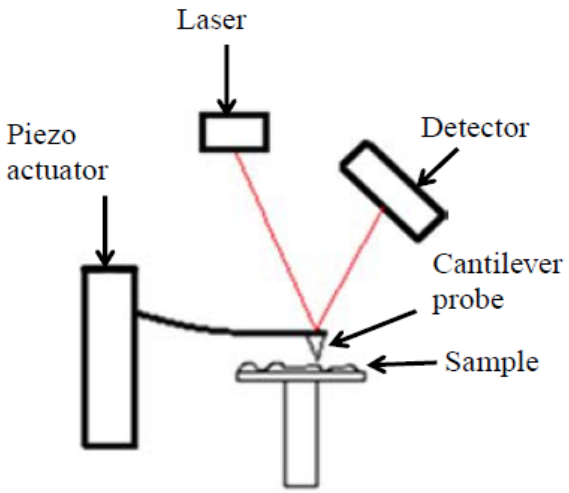

Figure A.23 Cantilever position detection technique (Allen et al. 2014).

Rippled microstructures several micrometers in diameter and tens of nanometers in height have been reported and nicknamed bumblebees because of their resemblance to the bee's black and yellow stripes; these are now commonly known as "bee-shaped" microstructures. These microstructures exhibit four phases: a catanaphase (bee structure), periphase (around the catanaphase), paraphase (solvent regions), and salphase (high phase contrast spots; Das et al. 2015). The number of bee structures increases greatly, together with a sharp reduction in size, after TFOT aging, and the bee structures from different asphalts evolve in different ways during aging and bio-oil rejuvenation processes (Gong 2016).

De Moraes et al. (2010) studied microstructure behavior as a function of temperature, and Wang et al. (2015) investigated the evolution of microstructures resulting from laboratory aging. Both research groups mentioned the possibility that the bee-shaped structuring might be related to paraffin wax crystallization. Schmets et al. (2010) found that when magnified, the bee structures resembled crystalline microstructures, and they concluded that the bee structure mainly consists of waxes.

Several groups have participated in studying binders using AFM and differential scanning calorimetry DSC techniques. These investigations showed that the key cause behind the formation of bee-shaped microstructures was the interaction between crystalline waxes and the remaining nonwax chemical components in the asphalt binder matrix (Das et al. 2015). Pauli et al. (2011) found bee structures in pure maltene (saturates, aromatics, and resins) but not dewaxed samples and concluded that the interaction between paraffin waxes and the remaining asphalt fractions, referred to as "wax-induced phase separation," was responsible for the bee structure. Therefore, the wax fraction did not correlate well with the observed percentage of bee structures. Moya-Aguiar et al. (2015) investigated bee structures by separating the components in binders using various solvents and investigating each component using AFM. Surprisingly, the results were contradictory compared with those obtained from other research; these researchers showed instead that the bee structure was due to the presence of aromatics.

Wang et al. (2015) investigated the interactions among saturates, aromatics, resins, and asphaltenes. Strong interactions between the dispersed phase and continuous phase generated a larger size and greater number of bee structures. Asphaltenes acted as a core, and long-chain paraffin acted as an inducer to affect the distribution of bee structures. Regarding the formation of bee-like structures, the results here revealed that asphaltenes were the main factor related to obtaining the bee structures but that long-chain alkanes acted as an inductive agent, prompting the distribution of these special structures. The measured fraction of long-chain alkanes did not correlate well with the observed percentage of bees, but the alkanes behaved as inducers to affect the bee structures. Therefore, binders with no saturates or no asphaltenes had an absence of bee structures.

Nahar et al. (2013) studied the effectiveness of RAP and virgin binder blending. The blend was made by melting a virgin binder and a RAP binder on a slide, which, upon melting, combined to form a blend. Their study showed that the virgin and RAP binders blended well and had a different topography from either the RAP or virgin binder individually.

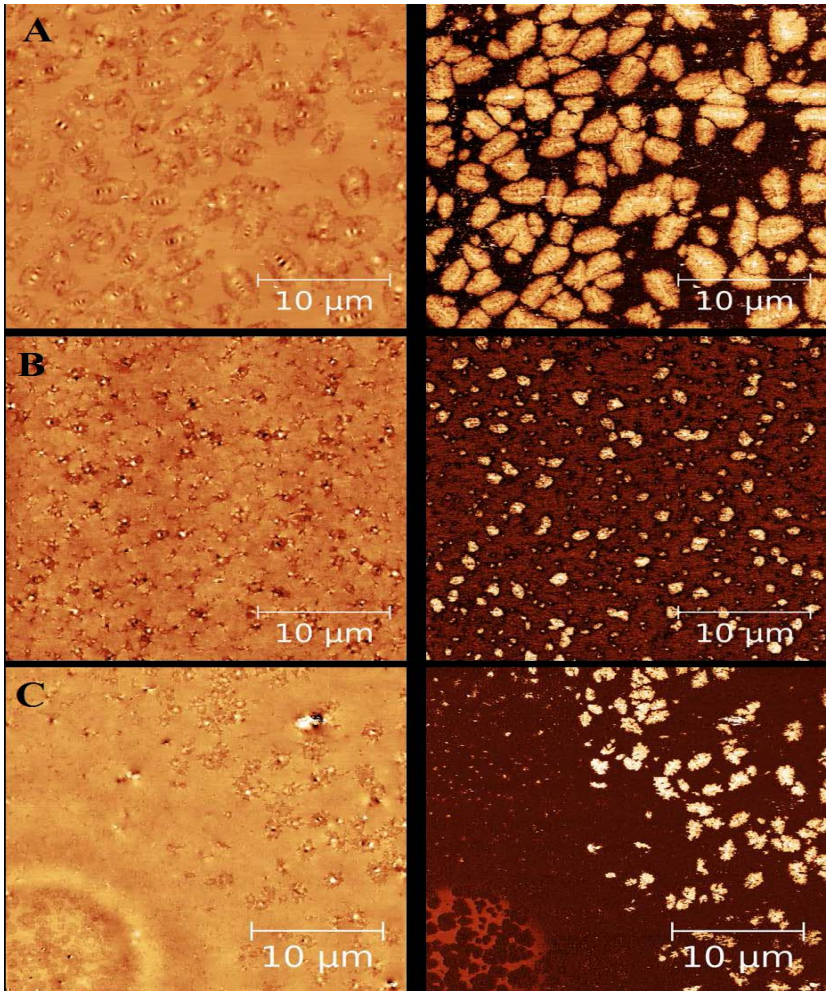

Figure A.24 AFM tapping mode topography (left) and phase (right): 30 × 30 µm scan size images revealing the microstructure morphology of the (a) virgin bitumen and (b) RAP binder, and (c) blending zone of the virgin and RAP binders.

Allen et al. (2014) studied the effect of SARA components in the binders. The virgin binder was doped with saturates, aromatics, resin, and asphaltenes. The aromatics and resin did not have an effect on the binder, whereas the bee structures increased and became more compact with the addition of asphaltenes. The bee structures became larger and less noticeable with the addition of aromatics, whereas with the addition of resin, only slight changes occurred in the bee structure.

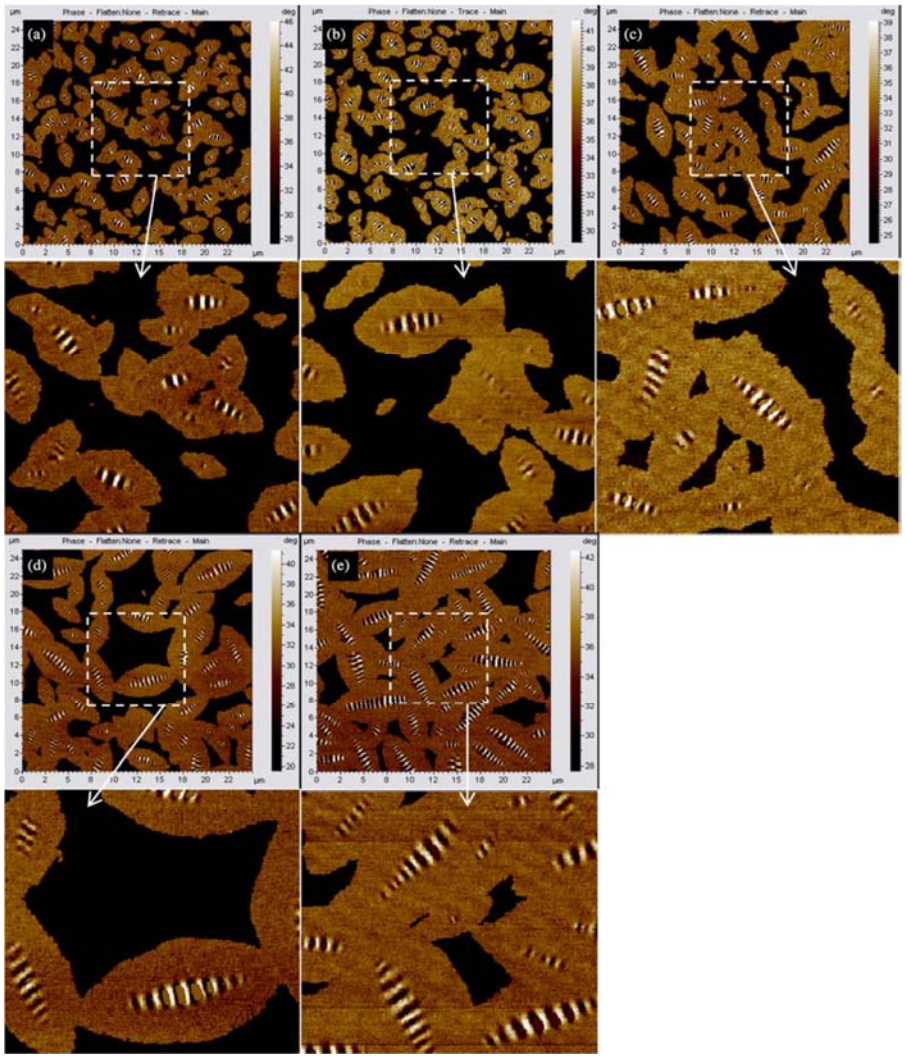

Figure A.25 AFM phase images of 25 × 25 mm of asphalt ARC BI0001 derivatives taken at room temperature (25.8°C): (a) control, (b) an asphaltene-doped blend, (c) a naphthenic aromatic-doped blend, (d) polar (resin)-doped blend, and (e) a saturate-doped blend (enlarged locations are 10 × 10 mm for each asphalt blend, respectively).

The properties and compositional changes of the binder upon aging were also studied by correlating micromechanical characteristics from AFM with rheological characteristics. The study by Wang et al. (2015) showed that oxidative aging generally increased the ratio between the dissipated energy and total work to deform the sample during the indentation process. It also increased the adhesive strength, cohesive strength, or both of the asphalt samples.

Poulikakos et al. (2016) studied the long-term and short-term aging of a binder by examining AFM topographic images. The results showed a change in topographic images of bitumen in aged samples compared with virgin binders. The aged and RAP samples were comparatively stiffer than the virgin samples. The phase signal in soft materials was sensitive to viscoelastic properties and adhesion forces and was an indication of the relative surface stiffness. This was because the phase was a

measure of the energy dissipation involved in the contact between the tip and the sample (Pauli et al. 2011). This result corroborates others presented in this paper, indicating that the addition of RAP results in a stiffening of the material.

A.2.5 Size Exclusion Chromatography (SEC)/Gel Permeation Chromatography (GPC)

GPC is a method used to separate solutions of mixtures based on the molecular size of the components (Robertson et al. 1991). The technique does not distinguish whether the size of molecules or molecule groups is being measured (Robertson et al. 1991). GPC is generally used for the following purposes: (1) to study the molecular weight distribution of binders before and after aging, or with different contents of reclaimed asphalt or polymers; (2) to develop statistical models to predict the physical properties of binders using GPC parameters; and (3) to investigate the changes in GPC profiles by adding rejuvenating agents to the aged binders.

Liu et al. (2015) conducted GPC experiments on three PMB (polymer-modified bitumens) containing binders extracted and recovered from three reclaimed asphalt pavement mixtures, one from Netherlands (RAN), another from Slovakia (RAS), and a third from Denmark (RAD) blended with soft virgin bitumens Base 1, PMB1, Base 2, or PMB2. Base 1 was a straight-run bitumen, PMB1 was a modified bitumen (10% SBS), Base 2 was produced by blending two different bitumen samples, and PMB2 was an SBS polymer-modified bitumen. Figures A.26 through A.28 show GPC chromatograms of all the binder groups. The areas of Fractions 1 and 2 in the GPC curves were calculated, and the ratio between them is shown in Figure A.29.

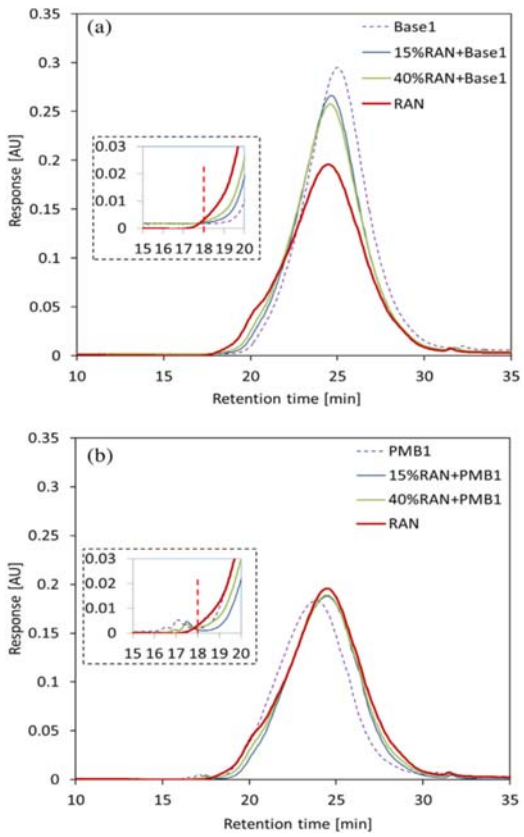

Figure A.26 Molecular weight distribution of (a) RAN + the Base 1 group and (b) RAN + the PMB1 group (Liu et al. 2015).

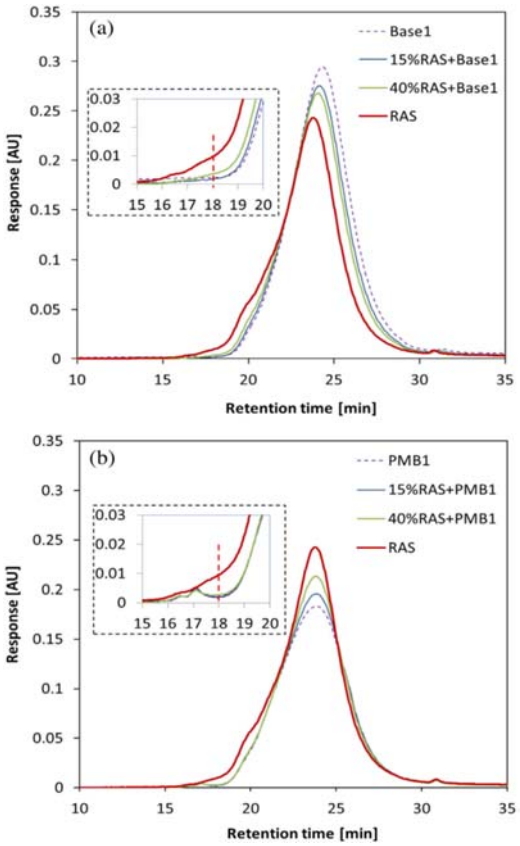

Figure A.27 Molecular weight distribution of (a) RAS + the Base 1 group and (b) RAS + the PMB1 group (Liu et al. 2015).

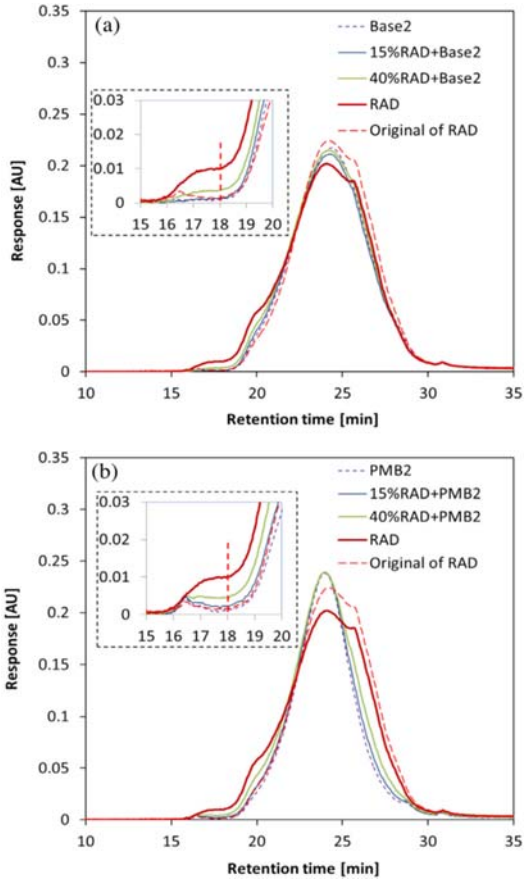

Figure A.28 Molecular weight distribution of (a) RAD + the Base 2 group and (b) RAD + the PMB2 group (Liu et al. 2015).

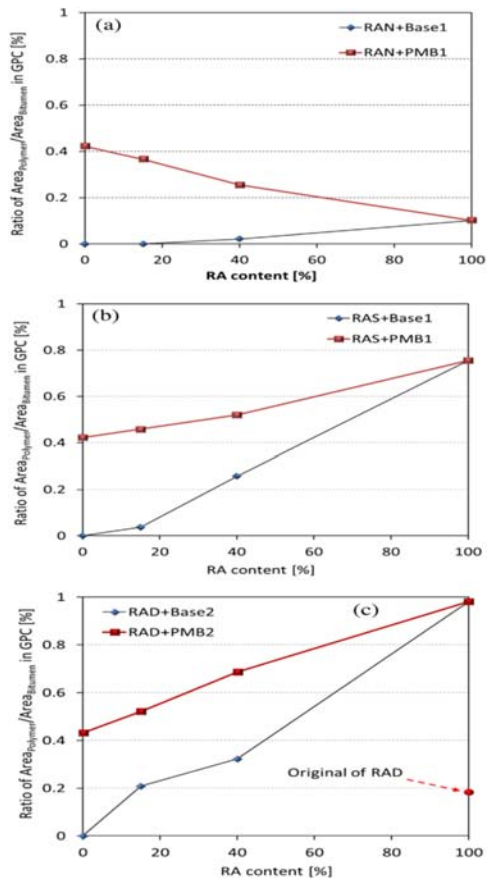

Figure A.29 Area ratio of the bitumen and polymer fractions in the GPC curve for (a) RAN-, (b) RAS-, and (c) RAD-containing binder groups (Liu et al. 2015).

The GPC technique was applied to study the molecular size distribution of RAS-containing asphalt binders (Abbas et al. 2013). Figure A.30 shows GPC chromatograms for the unaged and aged asphalt binders with different percentages of RAS, and Figure A.31 presents the molecular size distributions calculated from the GPC chromatograms.

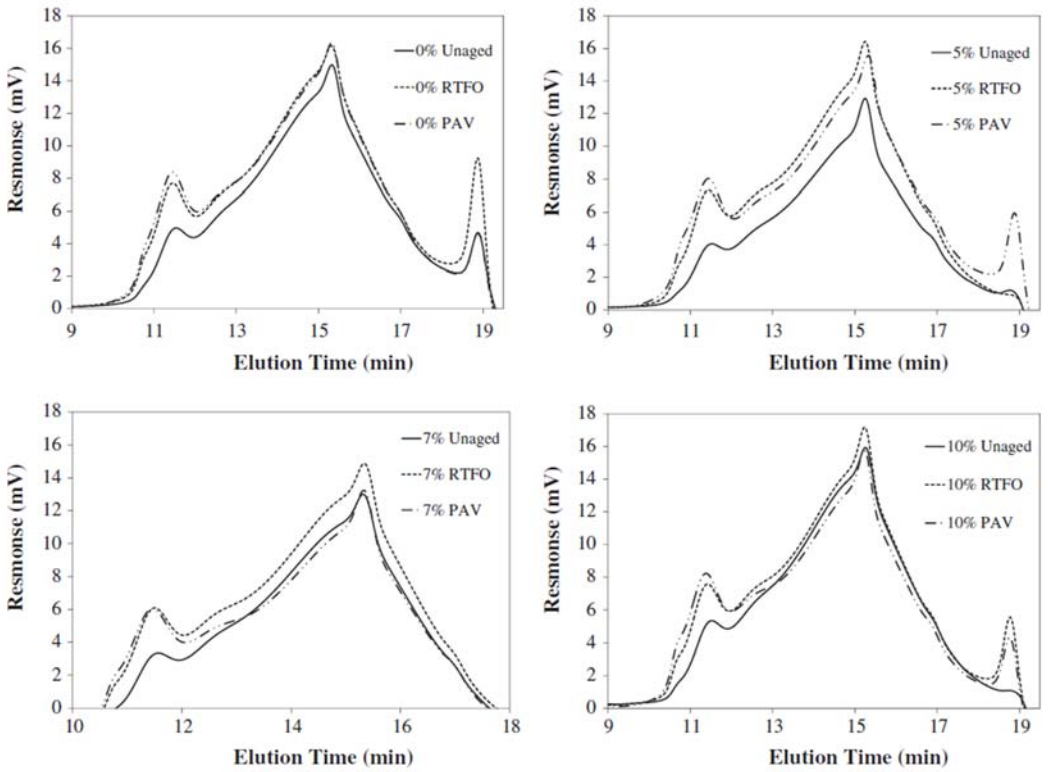

Figure A.30 GPC chromatograms for RAS-containing asphalt binders (Abbas et al. 2013).

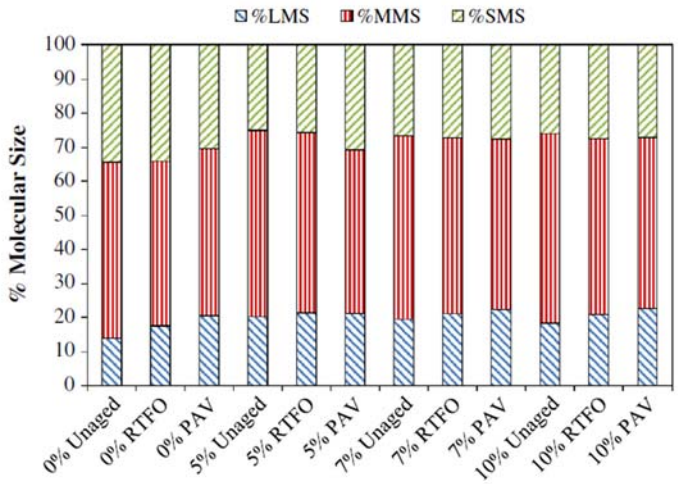

Figure A.31 Molecular size distribution for RAS-containing asphalt binders (Abbas et al. 2013).

Stangl et al. (2006) presented GPC results that illustrated the change in molecular composition caused by aging. Figures A.32 and A.33 show a decrease in molecules with a molecular weight of approximately 1000 g/mol and an increase in large molecules in the range of 10,000 g/mol.

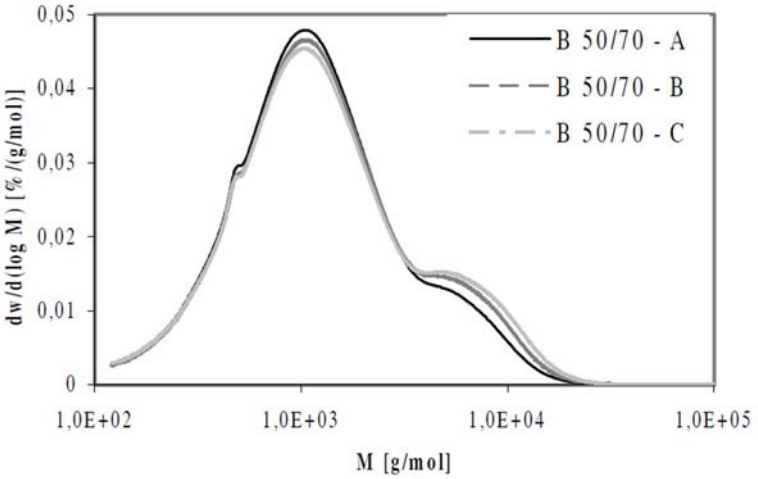

Figure A.32 Molecular weight distribution of B 50/70 in the original condition (A), after RFTOT aging (B), and after RTFOT + PAV aging (C) (Stangl et al. 2006)

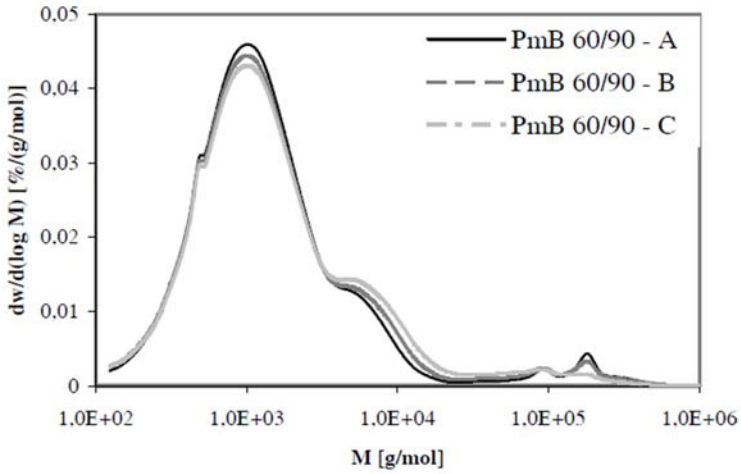

Figure A.33 Molecular weight distribution of PMB 60/90 in the original condition (A), after RFTOT aging (B), and after RTFOT + PAV aging (C) (Stangl et al. 2006)

Using experimental data, Chollar et al. (1985) predicted that a relationship exists between a larger molecular size in asphalt and thermal cracking properties of the pavement:

$$\text{LMS} = 2.355 - 0.000565\ \text{DUCT 77} - 2.203\ \text{SG} + 0.8817\ \text{ASPH},$$

where LMS is the larger molecular size, DUCT 77 is the ductility at 77°F (25°C), SG is the specific gravity, and ASPH is the asphaltene content (%). Shen et al. (2007) performed regression analyses to predict the viscosity and failure temperature based on LMS and SMS from GPC data. HP-GPC techniques were applied to study the compositional differences between rejuvenated aged crumb rubber-modified (CRM) binders and CRM binders. The authors presented the compositional changes in blends containing various percentages of either the rejuvenator or the softer binder. They found

that percentage changes in the composition of blends did not indicate any benefits of using rejuvenating agents. The rejuvenating agents had very high SMS percentages. When such a material is blended with an aged binder (with a higher LMS percentage), the overall SMS percentage will increase and the LMS percentage will decrease correspondingly compared with an aged binder without any chemical reaction. Only changes in the amounts—and not the LMS, SMS, and MMS percentages—will indicate whether the aged binder is truly modified, and if the rejuvenating agents in the blends are not stable, the blends will soon revert to their individual components before blending.

APPENDIX B: ADDITIONAL DATA ON MATERIALS USED IN THE STUDY

The types of materials used in the study are as follows:

- Different grades of virgin binders: virgin binders containing vegetable oil or ReOB supplied by IDOT
- Different grades of virgin binders either sampled from plants or distributed by the suppliers
- Laboratory-aged virgin binders
- Binders recovered from laboratory-produced asphalt mixtures developed in the ICT study R27-128 [32]
- Binders recovered from plant-produced asphalt mixtures used in the ICT study R27-128 [32]
- Binders recovered from field cores tested in the ICT study R27-128 [32]

Tables B.1 and B.2 provide a complete list of binders used in this study and their mixture characteristics if they were recovered from an asphalt mixture.

Table B.1 IDOT Asphalt Binders Used in This Study

Sample	RTFO-aged samples	PAV-aged samples
PG 58-28	PG 58-28 RTFO	PG 58-28 PAV
PG 58-22/58-28	PG 58-22/58-28 RTFO	PG 58-22/58-28 PAV
PG 58-28 ReOB 9% Safety Kleen	PG 58-28 RTFO ReOB 9% Safety Kleen	PG 58-28 PAV ReOB 9% Safety Kleen
PG 52-34 vegetable oil	PG 52-34 RTFO vegetable oil	PG 52-34 PAV vegetable oil
SBS 70-22 vegetable oil		
SBS 70-22/76-22		

Table B.2 ICT Asphalt Binders Used in This Study

1. Original binder					
Material ID	**Virgin binder**	**Aging condition**	**Original project information**		**Other remarks**
OB1	PG58-28	—	ICT R27-128 project used in N90 series		Used in N90-20, N90-30
OB2	PG58-28	RTFO			
OB3	PG58-28	PAV			
OB4	PG58-28	2PAV			
OB5	PG64-22	—	ICT R27-128 project used in N90 series		Used in N90-0 AS and N90-10
OB6	PG64-22	RTFO			
OB7	PG64-22	PAV			
OB8	PG64-22	2PAV			
OB9	PG70-22	—	ICT R27-128 project used in N90 series		Used in N90-0
OB10	PG70-22	RTFO			
OB11	PG70-22	PAV			
OB12	PG70-22	2PAV			
2. Extracted from mixture components					
Material ID	**Virgin binder**	**Aging condition**	**Original project information**		**Other remarks**
R1	RAS1	As extracted	ICT R27-128 project used in N90 series		Used in N90-10, N90-20, N90-30
R2	RAS2	As extracted	ICT R27-128 project used in N90 series		Used in N90-60 AS
R3	RAP1	As extracted	ICT R27-128 project used in N90 series		Used in N90-60 AS
R4	RAP2	As extracted	ICT R27-128 project used in N90 series		Used in N90-60 AS
3. Extracted from laboratory-produced mixtures					
Material ID	**Mix ID**	**Base binder**	**ABR content (%)**	**Aging condition**	**Other remarks**
MIX1	N90-0	PG70-22	0.0	As extracted	
MIX2	N90-0 AS	PG64-22	0.0	As extracted	
MIX3	N90-10	PG64-22	10.5	As extracted	2.5% RAS1
MIX4	N90-20	PG58-28	21.2	As extracted	5% RAS1
MIX5	N90-30	PG58-28	29.8	As extracted	7% RAS1
MIX6	N90-60 AS	PG52-34	60.8	As extracted	7% RAS2 + 20% RAP1 + 20% RAP2
MIX7	N90-0 AS PAV	PG64-22	0.0	PAV	
MIX8	N90-10 PAV	PG64-22	10.5	PAV	2.5% RAS1
MIX9	N90-20 PAV	PG58-28	21.2	PAV	5% RAS1
MIX10	N90-30 PAV	PG58-28	29.8	PAV	7% RAS1
MIX11	N90-60 AS PAV	PG52-34	60.8	PAV	7% RAS2 + 20% RAP1 + 20% RAP2

Table continues next page

Table B.2 ICT Asphalt Binders Used in This Study (continued)

4. Extracted from plant-produced mixtures					
Material ID	**Mix ID**	**Base binder**	**ABR content (%)**	**Aging condition**	**Other remarks**
TM1	TOL MIX 2	PG58-28	29.0	As extracted	27% RAP
TM2	TOL MIX 5	PG64-22	6.0	As extracted	10% RAP
TM3	TOL MIX 6	PG76-22	6.0	As extracted	10% RAP
TM4	TOL MIX 7	PG64-22	0.0	As extracted	—
5. Extracted from field cores					
Material ID	**Mix ID**	**Base binder**	**ABR content (%)**	**Aging condition**	**Other remarks**
FC1	Field core 6G2	—	8.50	As extracted	Good performance, year of construction 2013
FC2	Field core poor 22RT2	PG70-22	0	As extracted	Poor performance, year of construction 2003
FC3	Field core poor 22SRT2	PG58-18	0	As extracted	Poor performance, year of construction 2004
6. Virgin and aged binders containing ReOB					
	0% 0 DAYS	PG58-28	0	As extracted	
	0% 10 DAYS	PG58-28	0	As extracted	
	0% 0 DAYS PAV	PG58-28	0	As extracted	
	9% SK 0 DAYS	PG58-28	0	As extracted	
	9% SK 10 DAYS	PG58-28	0	As extracted	
	9% SK 0 DAYS PAV	PG58-28	0	As extracted	
	Unaged 9% CC	PG58-28	0		
	9% CC RTFO	PG58-28	0	RTFO	
	9% CC 20 PAV	PG58-28	0	PAV	
	9% CC 40 PAV	PG58-28	0	PAV	
	9% CC 60 PAV	PG58-28	0	PAV	
	Unaged 0% ReOB	PG58-28	0		
	0% ReOB RTFO	PG58-28	0	RTFO	
	0% ReOB 20 PAV	PG58-28	0	PAV	
	0% ReOB 40 PAV	PG58-28	0	PAV	
	0% ReOB 60 PAV	PG58-28	0	PAV	
	Unaged 9% SK	PG58-28	0		
	9% SK RTFO	PG58-28	0	RTFO	
	9% SK 20 PAV	PG58-28	0	PAV	
	9% SK 40 PAV	PG58-28	0	PAV	
	9% SK 60 PAV	PG58-28	0	PAV	

APPENDIX C: RHEOLOGY AND COMPOSITIONAL TEST DATA ON IDOT AND REOB BINDERS

C.1 RHEOLOGY

Table C.1 Superpave High-Temperature Grading Results

High-temperature grading	Replicate 1		Replicate 2		*Average of true grade*	*Graded as*
	Grade	*True grade*	*Grade*	*True grade*		
Virgin binder						
PG58-28	64	65	58	61.8	63.4	**58**
PG64-22	64	69.8	64	69.2	69.5	**64**
PG58-28 RTFO	64	64.4	64	66.2	65.3	**64**
PG64-22 RTFO	70	70.1	64	69.3	69.7	**64**
Extracted binder						
RAS1	88+	157.2	88+	156.2	156.7	**88+**
RAS2	88+	149.9	88+	150.3	150.1	**88+**
RAP1	88	89	88	91.1	90.1	**88**
RAP2	76	78	76	77.1	77.6	**76**
N90-0 AS	70	70.7	70	70.7	70.7	**70**
N90-10	64	69.4	64	70.0	69.7	**64**
N90-20	76	77.4	76	78.4	77.9	**76**
N90-30	76	79.1	76	79.4	79.3	**76**
N90-60 AS	88	88.2	88	88.2	88.2	**88**

Table C.2 Superpave Low-Temperature Grading Results

Low-temperature performance	Low grade	S (MPa)	m-value	Delta T	PG stiffness (Temp. in ºC)	PG m-value (Temp. in ºC)
PAV PG58-28	-28	220	0.310	0.39	-19.23	-19.62
2PAV PG58-28	-22	131	0.303	-7.73	-20.59	-12.86
PAV PG64-22	-22	239	0.301	-0.26	-13.83	-13.57
2PAV PG64-22	-16	114	0.310	-5.97	-13.00	-7.026
RAP1	-10	107	0.349	-5.37	-9.33	-3.96
RAP2	-22	159	0.316	-2.44	-16.83	-14.39
N90-0 AS	-22	126	0.392	2.22	-16.05	-18.27
PAV N90-0 AS	-22	219	0.302	-1.27	-13.56	-12.29
N90-10	-28	220	0.332	1.45	-19.34	-20.79
PAV N90-10	-16	90	0.350	-3.41	-14.39	-10.98
N90-20	-22	95	0.355	-4.12	-21.36	-17.24
PAV N90-20	-16	78	0.326	-17.71	-26.62	-8.91
N90-30	-22	206	0.318	0.35	-13.29	-13.64
PAV N90-30	-10	61	0.352	-8.37	-14.32	-5.95
N90-60 AS	-22	114	0.306	-8.69	-22.07	-13.38
PAV N90-60 AS	-10	53	0.303	-21.60	-22.23	-0.63

Table C.3 Detailed Superpave Low-Temperature Grading Results of RAS Using BBR

Detailed BBR results of RAP and RAS												
			Sample 1		Sample 2		Sample 3		Sample 4		Average	
ID	Grade	Temp. (ºC)	S(MPa)	m-value	S(MPa)	m-value	S(MPa)	m-value	S(MPa)	m-value	S(MPa)	m-value
RAS1		0	95.8	0.205			broken when demold		broken when demold			
		6	64.1	0.211								
		18	30.8	0.246	damage							
		24	damage									
RAS2		18	damage		damage							
		24					damage		damage			
RAP1	-10	0	109	0.349	107	0.347	104	0.35			107	0.349
		-6	226	0.271	240	0.277	227	0.277			231	0.275
RAP2	-22	-6	70.9	0.367	60.9	0.388	71.1	0.424	79.5	0.409	71	0.397
		-12	182	0.339	141	0.291	153	0.3	159	0.333	159	0.316
		-18	355	0.252	326	0.278	360	0.267	329	0.270	342	0.267

C.2 CHEMICAL TEST DATA

C.2.1 FTIR Analysis

The FTIR results showed that the virgin binders had ICO values between 0.01 and 0.04 and had ISO values between 0.06 and 0.12, as presented in Table C.4 for IDOT samples. Aged samples with PAV and RTFO were similarly analyzed using the FTIR technique (Figure C.1). Results showed that the oxidation of binders increased with aging. The virgin binders had a negligible oxygen content, whereas the binders aged using the long-term aging method (PAV) had the highest oxygen content. The ICO showed an increase in samples aged using the PAV method compared with those using the RTFO method. Similar trends were observed in the ISO. These results indicated that samples using the PAV aging method were more oxidized than were those using the RTFO method. However, the content of sulfoxide depended on the initial sulfur content in the sample. Although binders with vegetable oils would be expected to have higher ICO, but we observed that ICO indices for PG 52-34 with vegetable oil and its RTFO- and PAV-aged samples were less than 0.04, similar to virgin binders PG 58-28, PG 58-22/58-28, and PG 58-28 ReOB, and their RTFO-aged samples (Figures C.1). The ISO indices were higher for PG 52-34 with vegetable oil and its RTFO- and PAV-aged samples compared to other samples, which is due to initial higher ISO value for PG 52-34 with vegetable oil. Figure C.2 shows that the intensity of carbonyl and sulfoxide peaks were higher in PG samples with vegetable oil and ReOB because of the presence of oxygen.

Table C.4 Carbonyl and Sulfoxide Indices (ICO and ISO) Obtained from FTIR Spectra of IDOT Samples

Binder source	PG	ICO	ISO
Random samples collected from IDOT binders used in the ICT R27-128 study	46-34	0.04	0.07
	52-34	0.03	0.11
	70-28	0.03	0.10
	58-28	0.04	0.06
	58-22/58-28	0.03	0.08
	64-22	0.03	0.09
	58-28	0.01	0.10
	SBS 70-28/64-28	0.03	0.06
	SBS 70-22/76-22	0.03	0.08
	SBS 70-22	0.03	0.09
	SBS 76-22	0.04	0.12
	SBS 70-28	0.02	0.11
	PG 58-28 (ReOB)	0.03	0.06

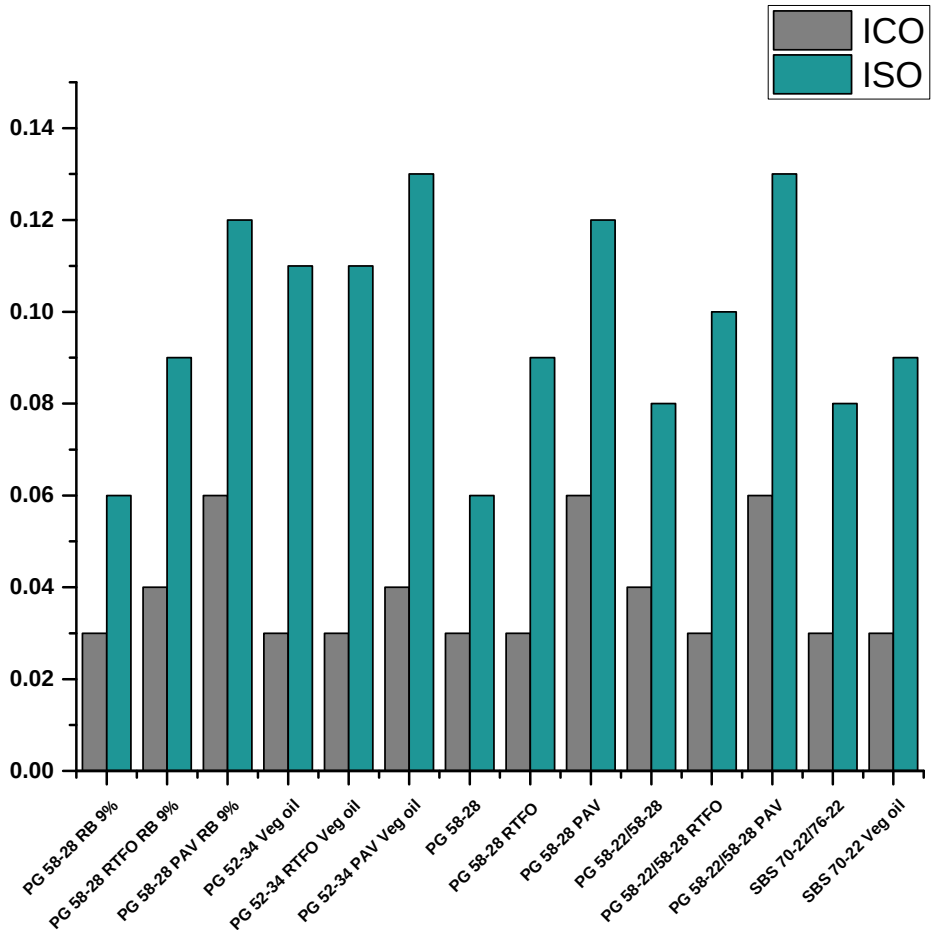

Figure C.1 Carbonyl and sulfoxide indices (ICO and ISO) calculated from FTIR spectra of samples obtained from IDOT.

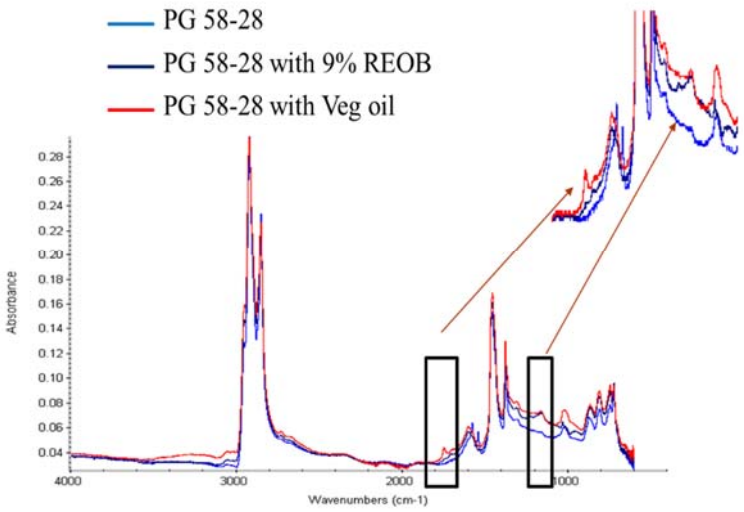

Figure C.2 FTIR spectra of virgin binders, virgin binders with vegetable oil, and virgin binders with ReOB. The intensity of carbonyl and sulfoxide peaks was higher in PG samples with vegetable oil and ReOB because of the presence of oxygen.

Similarly, the oxidation of extracted samples containing ReOB and their respective aged samples was studied. PAV-aged samples had higher carbonyl and sulfoxide values compared with unaged samples, and these values increased with aging time from 20 to 40 to 60 hours, as shown in Figure C.3. This result was as expected because a binder exposed to a changing environment will age faster with time because of oxidation. The ICO and ISO showed an enormous change as they changed from unaged to RTFO-aged samples and from RTFO to PAV samples. ICO for most virgin and RTFO-aged samples was less than 0.02, while for PAV samples, it was higher than 0.02. Similarly for most virgin and RTFO samples, ISO index was lower than 0.06, and for PAV samples, value was higher than 0.06. Although ICO index seems to be on increasing trend for PAV-aged samples at different lengths of time, but no major change in ISO index was observed.

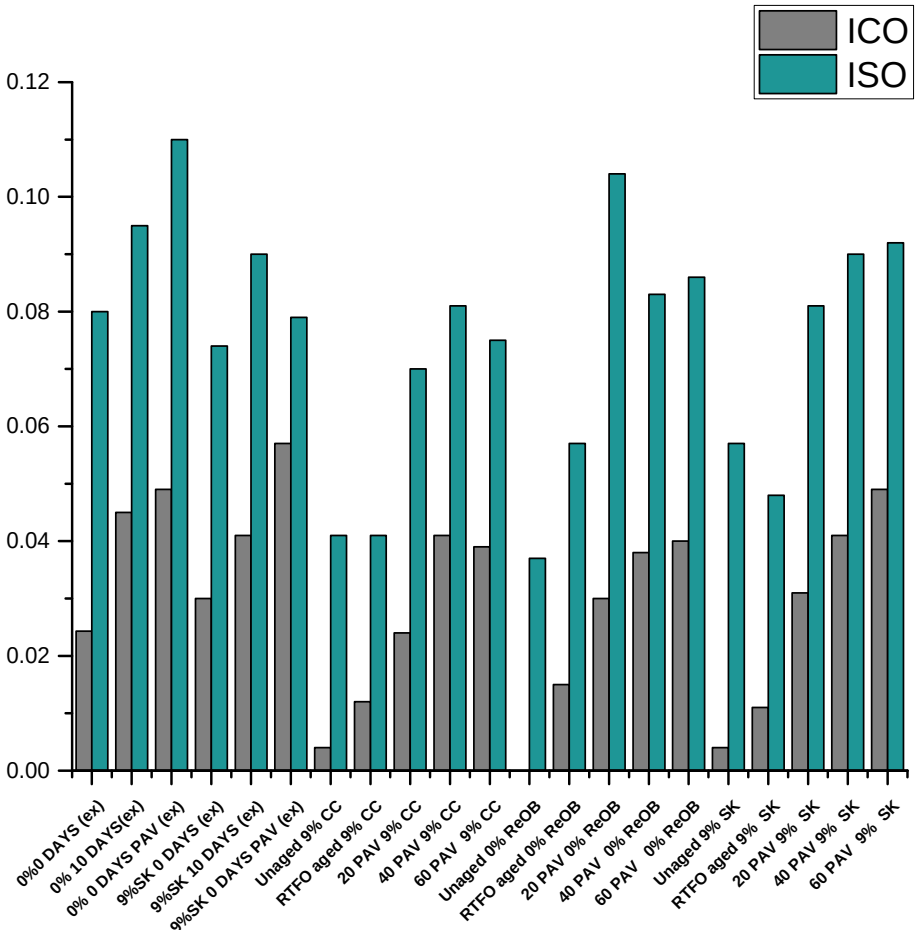

Figure C.3 Carbonyl and sulfoxide indices (ICO and ISO) of virgin binders and aged binders containing ReOB.

C.2.2 Elemental Analysis

The elemental composition of all the samples is shown in Table C.5. The oxygen content was higher in the samples with vegetable oil (>0.5%). The elemental composition report is in agreement with the FTIR results. The oxygen content increased with aging. Long-term-aged (PAV) samples had a higher oxygen content compared with RTFO-aged samples. Even though the trend of an increase in oxygen content from virgin binder to RTFO and then to PAV was observed in most of the samples, it should be noted that the virgin and aged samples did not all have the same origin; therefore, the trend of an increase in oxygen content from virgin to aged binder might not have been observed in all the samples.

Table C.5 Oxygen and Sulfur Contents in Binders Received from IDOT

Sample	S%	O%
PG 58-28	5.58	0.0
PG 58-28 RTFO	8.9	0.0
PG 58-28 PAV	4.9	1.0
PG 64-22	5.6	0.7
PG 64-22 RTFO	5.0	0.3
PG 64-22 PAV	4.9	1.1
PG 58-22/28	5.6	0.0
PG 58-22/28 RTFO	5.1	0.5
PG 58-22/28 PAV	5.0	1.1
PG 70-28	3.43	0.5
PG 70-28 RTFO	3.4	0.8
PG 70-28 PAV	2.8	1.7
PG 52-34 vegetable oil	5.1	0.02
PG 52-34 RTFO vegetable oil	4.9	0.03
PG 52-34 PAV vegetable oil	4.9	0.5
PG 64-28/70-28 RTFO vegetable oil	4.7	1.0
PG 64-28/70-28 PAV vegetable oil	2.5	2.7
PG 58-28 REOB	3.78	0.6
PG 58-28 RTFO w/ ReOB	4.7	0.4
PG 58-28 PAV w/ ReOB	4.6	1.1
SBS 70-28/64-28 vegetable oil	4.44	0.9
SBS 70-22 vegetable oil	4.82	0.7
SBS 76-22 vegetable oil	3.86	1.04
SBS 70-28 vegetable oil	4.62	0.49
PG 70-28	3.43	0.50
PG 58-28	5.60	0.0
PG 58-22/58-28	5.23	0.0
PG 64-22	5.06	0.72
SBS 70-22/76-22	4.65	0.11
PG 58-28	3.56	0.05
PG 46-34	3.98	0.53

In agreement with the FTIR results, the oxygen content of aged samples was higher than that of virgin samples, as shown in Figure C.4. The oxygen content was higher in samples that were aged using long-term aging (i.e., the PAV method) compared with short-term aging (i.e., the RTFO method). The sulfur content did not change as much with aging as expected. This result indicates that the sulfur content was similar to that in the virgin sample even after aging.

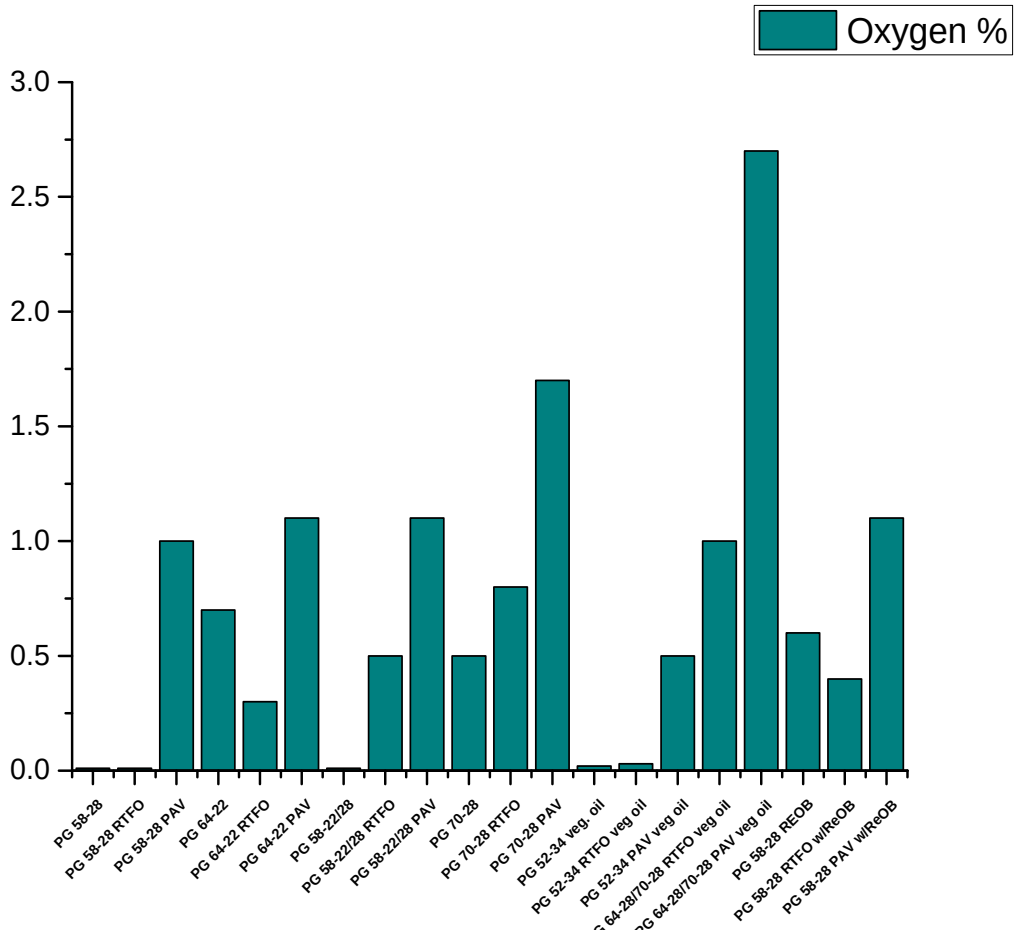

Figure C.4 Oxygen content in virgin and aged binders received from IDOT.

Similarly, oxygen and sulfur contents were evaluated in binders (PG 58-28) containing ReOB and their aged samples. The oxygen and sulfur contents were comparable to those in samples with no ReOB. However, the source of the PG 58-28 may have been different. The extracted samples had higher oxygen and sulfur contents compared with the virgin binder. The trend for the oxygen content to increase from unaged to RTFO-aged to PAV-aged at 20, 40, and 60 hours is shown in Table C.6. However, no significant increase in sulfur content was observed as the binder was aged.

Table C.6 Oxygen and Sulfur Contents in Binders Containing ReOB

Sample	S + O (%)
0% 0 DAYS (extracted)	6.4
0% 10 DAYS (extracted)	6.7
0% 0 DAYS PAV (extracted)	7.5
9% SK 0 DAYS (extracted)	7.5
9% SK 10 DAYS (extracted)	7.7
9% SK 0 DAYS PAV (extracted)	7.6
Unaged 9% CC	5.9
9% CC RTFO	11.0
9% CC 20 PAV	6.1
9% CC 40 PAV	6.3
9% CC 60 PAV	6.6
Unaged 0% ReOB	5.5
0% ReOB RTFO	5.5
0% ReOB 20 PAV	5.8
0% ReOB 40 PAV	6.3
0% ReOB 60 PAV	6.4
Unaged 9% SK	5.3
9% SK RTFO	5.5
9% SK 20 PAV	6.2
9% SK 40 PAV	6.0
9% SK 60 PAV	6.3

C.2.3 SARA Analysis

TLC-FID is a very good tool for investigating the SARA components in asphalt binders. All the virgin binders had higher aromatic contents, which decreased with aging. The resin content and the residue content increased with aging, as shown in Table C.7. As the binder aged, components in the binders formed various bonds, such as hydrogen, polar, and dispersive bonds, which caused a transition from aromatics to resins and then resins to asphaltenes to residue. Thus, higher molecular size components increased in the aged binders.

Table C.7 SARA Contents in Virgin Binders, Virgin Binders with Vegetable Oil, and Aged Binders Received from IDOT

Sample name	Saturates	Aromatics	Resins	Asphaltenes	Residue
PG 58-28 ReOB 9% Safety Kleen	14.73	34.5	44.6	6.1	7.47
PG 58-28 RTFO ReOB 9% Safety Kleen	12.03	36.9	44	7.06	5.8
PG 58-28 PAV ReOB 9% Safety Kleen	11.80	33.7	49.4	5.04	3.7
PG 52-34 vegetable oil	10.06	44.99	38.2	6.79	1.38
PG 52-34 RTFO vegetable oil					3.70
PG 52-34 PAV vegetable oil	8.05	37.67	48.34	5.94	3.72
PG 58-28	9.25	44.06	37.96	9.23	3.16
PG 58-28 RTFO	8.56	41.17	42.75	7.53	3.42
PG 58-28 PAV	8.09	36.45	51.20	4.26	4.38
PG 58-22/58-28	8.62	49.52	39.56	7.80	3.38
PG 58-22/58-28 RTFO	7.60	48.05	37.59	6.75	3.41
PG 58-22/58-28 PAV	8.81	45.94	42.01	7.64	4.94
SBS 70-22/76-22	13	28.40	51.2	7.4	4.23
SBS 70-22 vegetable oil	5.9	34.3	54.9	4.9	4.9
FIELD CORE					
Field core 6G2	8.2	30.6	51.2	10.0	6.3
Field core poor 22SRT2	7.7	23.3	62.9	6.1	22.6
Field core poor 22RT2	6.1	23.2	59.7	10.2	19.5

C.2.4 Molecular Size Analysis

GPC is a very good tool for investigating the molecular size distribution in asphalt binders. The SMS content was high in the virgin binders and decreased with aging in RTFO and PAV. RTFO and PAV aging increased either the LMS or MMS content in the binders and decreased the SMS content, as shown in Table C.8. These increases in MMS and LMS were attributed to the increase in resins contained in the binders with aging. Molecular distribution results of the binders complemented the SARA results, showing that the resin content increased with aging.

Table C.8 Larger, Medium, and Smaller Molecular Size (LMS, MMS, and SMS) Distributions of Virgin Binders, Virgin Binders with Vegetable Oil, and Aged Binders Received from IDOT

Sample name	LMS	MMS	SMS
PG 58-28 ReOB 9% Safety Kleen	0.40	0.50	0.10
PG 58-28 RTFO ReOB 9% Safety Kleen	0.42	0.53	0.05
PG 58-28 PAV ReOB 9% Safety Kleen	0.45	0.51	0.04
PG 52-34 vegetable oil	0.42	0.52	0.07
PG 52-34 RTFO vegetable oil	0.43	0.55	0.02
PG 52-34 PAV vegetable oil	0.45	0.49	0.06
PG 58-28	0.41	0.53	0.06
PG 58-28 RTFO	0.42	0.56	0.02
PG 58-28 PAV	0.46	0.52	0.02
PG 58-22/58-28	0.41	0.58	0.02
PG 58-22/58-28 RTFO	0.42	0.56	0.02
PG 58-22/58-28 PAV	0.45	0.54	0.01
SBS 70-22/76-22	0.43	0.55	0.02
SBS 70-22 vegetable oil	0.42	0.54	0.05

Similarly, the molecular size distribution was evaluated in binders (PG 58-28) containing ReOB and the aged samples. PAV-aged samples had higher LMS components and lower SMS components compared with the unaged sample. The LMS increased with aging time from 20 to 40 to 60 hours, whereas the SMS decreased respectively, as shown in Table C.9. This increase in LMS was attributed to an increase in resins contained in the binders with aging. The result was as expected: as the binder was aged, it tended to polymerize, forming LMS components. A substantial increase in LMS and decreases in MMS and SMS was observed as the binders changed from unaged to 60-hour PAV-aged binders.

Table C.9 Larger, Medium, and Smaller Molecular Size (LMS, MMS, and SMS) Distributions of Binders (PG 58-28) and the Aged Samples Containing ReOB

Sample	LMS	MMS	SMS
Virgin and aged			
0% 0 DAYS (extracted)	0.29	0.57	0.14
0% 10 DAYS (extracted)	0.29	0.58	0.14
0% 0 DAYS PAV (extracted)	0.31	0.57	0.12
9% SK 0 DAYS (extracted)	0.30	0.59	0.10
9% SK 10 DAYS (extracted)	0.34	0.57	0.09
9% SK 0 DAYS PAV (extracted)	0.34	0.56	0.10
Unaged 9% CC	0.27	0.61	0.11
9% CC RTFO	0.29	0.60	0.12
9% CC 20 PAV	0.32	0.58	0.09
9% CC 40 PAV	0.37	0.56	0.08
9% CC 60 PAV	0.38	0.55	0.07
Unaged 0% ReOB	0.29	0.62	0.10
0% ReOB RTFO	0.30	0.60	0.10
0% ReOB 20 PAV	0.32	0.57	0.11
0% ReOB 40 PAV	0.35	0.57	0.08
0% ReOB 60 PAV	0.38	0.55	0.07
Unaged 9% SK	0.27	0.61	0.12
9% SK RTFO	0.30	0.60	0.10
9% SK 20 PAV	0.33	0.58	0.09
9% SK 40 PAV	0.34	0.56	0.10
9% SK 60 PAV	0.36	0.55	0.10
FIELD CORE			
Field core 6G2	0.35	0.58	0.07
Field core poor 22SRT2	0.36	0.55	0.09
Field core poor 22RT2	0.35	0.57	0.07


Illinois Department
of Transportation


ILLINOIS
UNIVERSITY OF ILLINOIS AT URBANA-CHAMPAIGN